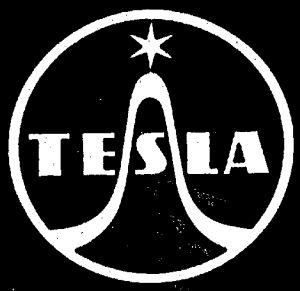

TESLA TECHNICAL REPORTS

DECEMBER 1949

TESLA TECHNICAL REPORTS

A DIGEST OF TECHNICAL ARTICLES ORIGINATED IN RESEARCH, DEVELOPMENT AND PRODUCTION DEPARTMENTS OF TESLA NATIONAL CORPORATION

Praha, Czechoslovakia *December, 1949*

LC Oscillators and their Frequency Stability

Jiří Vackář

UDC 621.396.615.12

The rapid development of quartz-crystal manufacture during the war somewhat reduced the use of tuneable LC oscillators and may even have given rise to the opinion that these oscillators have lost most of their importance. The experience of the four post-war years indicates that this conclusion was incorrect, that the stable LC oscillator retains its place beside the crystal in the first stages of broadcast transmitters, and that it is irreplaceable in wavemeters, signal-generators and receivers.

The demands placed on the stability of these types of oscillators increased as compared with pre-war times, especially for transmitters and oscillators for measuring instruments. Their design, which until now has been a question of trial and error, must therefore be put on a firm theoretical basis. During recent years a number of circuits have appeared solving the problem of stability by different means (Clapp, Lampkin, Seiler, etc.). These circuits, which have found popularity among amateurs, are, however, seldom used in industry, mainly because of the narrow range over which good tuning can be achieved. In addition, no general theory has yet been given which would permit an objective comparison with regard to the attainable stability, thereby enabling the selection of a suitable circuit for the purpose.

The aim of this article is to give the basic requirements for the design, and a general mathematical analysis, of oscillators with an eye to the frequency stability; to derive practical rules for the design and calculation of stable LC oscillators; to evaluate the existing circuits; and, lastly, to describe new circuits and their practical construction.

Those oscillators having a frequency ratio of 2 : 3 permit a precision of frequency adjustment of 0.002 % while their frequency stability is at least of the same order. Detailed results of the measurements are given below.

I. INDIVIDUAL CAUSES OF INSTABILITY. BASIC FACTS AND CONCEPTS

The frequency of a tuneable oscillator should be a single valued function of the tuning element (e. g. tuning condenser) setting. The frequency of normal oscillators is, of course, affected by a whole number of other factors, e. g. supply voltage, temperature, valve replacement, etc. Variations in these factors have to be reduced to a minimum for stable oscillators. The above assert themselves independently, and so an oscillator, which may be very stable as regards changes in the supply voltages can, on the other hand, be very unstable as regards changes in temperature. We must, therefore, pay special attention to each of these questions, for thereby we can obtain rules for the proper design. The table below is a summary of causes of frequency changes and the necessary preventive steps.

A more detailed account of design principles especially in regard to the design of coils and condensers, follows.

frequency change		change df/f	
Mechanical vibration	tuning coil and condenser	up to a few $^0/_0$	mechanical stability, suitable design of coil and condenser, temperature compensation, etc.
Change in temperature.....	tuning coil and condenser	up to $1^0/_{00}$ C	
Change in atmospheric pressure	air condensers	up to $3 \cdot 10^{-5}$ mm Hg	hermetically sealed tuning circuits
Change in humidity		up to $1 \cdot 10^{-6}$ $1^0/_0$ humidity	
Change in CO_2 of air.....		up to $2 \cdot 10^{-6}$ $1^0/_0$ CO_2	
Ageing of materials.....	tuning coil and condenser	up to a few $^0/_0$	do not use organic insulating materials
Change of valves.....	valves	up to a few $^0/_0$	suitable circuits and or stabilised power supplies
Change of supply voltages		up to a few $^0/_{00}$	
Valve vibrations		up to a few $^0/_{00}$	

2. MECHANICAL DESIGN OF TUNING CIRCUIT

The coils of a stable oscillator must have a stable mechanical design and their inductance should be as possible independent of temperature and ageing of materials. From an electrical point of view, the Q should be the highest possible, while the self-capacity does not have to be kept low. Perhaps the best of all existing designs are those utilising ceramic formers with deposited silver windings. Nearly equally good results can be obtained by winding bare solid copper wire at a temperature of 80° to 90° C (e. g. over a suitable heating element) into grooves on a ceramic former, which, after fastening the ends, can be left to cool. On cooling, the wire contracts and is strained, thereby following only the thermal expansion of the ceramic former which for the normal temperatures is very small. In this way we obtain coils with a cyclic thermal coefficient $\frac{dL}{dt} = 0$ to $8 \cdot 10^{-6}$, i. e. after repeated heating and cooling there is no change of inductance. The high Q is obtained by making the coil short and with a relatively large diameter ($0.3 < l/D < 0.6$) and by choosing the diameter of the wire to be approx. 0.6 ... 0.7 of the winding pitch leaving a comparatively small distance between wires. The shield has to be of rigid design and its diameter at least twice that of the coil.

The tuning condenser requires the same attention as the coil but the constructional requirements depend on the frequency ratio needed. In the extreme case when a ratio of 2 : 3 was required without switching, with a precision of adjustment of one part in 50.000, it was necessary to design a condenser with axial and radial play less than 0.001 mm and a ground worm gear of 1 to 100 to permit accurate adjustment. Generally, however, this sort of solution is not economical and we try to do with less expensive parts. For example, better quality variable condensers with large air gaps have a stability of the order of one part in a thousand, i. e. chance variation of capacity over longer periods is less that one thousandth of their maximum capacity. Normal tuning condensers used in broadcast receivers have a stability of one part in 500.

If we want to use such a condenser (e. g. stability of one part in 500) to tune an oscillator with a frequency stability of $5 \cdot 10^{-5}$ then we have to use such a circuit that the tuning range $f_{min} : f_{max}$ covered by the said condenser will be only 1 : 1,025, i. e. the overall relative frequency change $\frac{\Delta f}{f} = \frac{1}{1000}$. The tuning condenser error of 1 500 is then reduced to $1 : 500 \cdot 10 = 5 \cdot 10^{-5}$. This we achieve by adding fixed condensers or by connecting the tuning condenser to a tap on the coil. For larger frequency ratios than 1 : 1.025 we either switch the coil taps or the padding condensers. The fixed condensers are best chosen from among the larger ceramic types (test voltage 2 to 3 kV).

Very exacting requirements are put on the coil tap or fixed condenser switch. As in the interest of short leads and mechanical rigidity, this switch is generally placed near the coil, it is important that the points of contact should be well defined and that the whole switch should be electrically and mechanically stable. These requirements are best satisfied by a cam-operated switch with ceramic insulation or a robust ceramic wafer-switch. Here too, we try to avoid organic insulating materials (bakelite, bakelite bonded paper, styrene, etc.) which over longer periods change their degree of polymerisation and therefore their dielectric constant, power factor and even dimensions.

The coils, condensers and switch are the most important parts which affect the frequency stability regardless of the circuit used. As a rule we place these parts in a common shield. It is very advantage-

one to cover this shield with a thermal insulating material (felt or cork 5 to 10 mm thick), thereby protecting the tuning elements from sudden changes in temperature. This is especially important when using thermal compensation, which fulfils its purpose only when all temperature changes occur at the same time and throughout the whole tuning circuit.

The above paragraphs describe the conditions of design of stable tuning circuits. The second part discusses the causes of frequency instability which originate in the valve. The valve used in the oscillators is connected to the tuning circuit and its internal capacity, lead inductance, and internal resistance are, therefore, part of that circuit thereby affecting the frequency. The grid-cathode capacity, for example, varies with the space charge as much as $\pm 10\%$ depending on variations in the supply voltages, causing an indirect influence on the frequency. Likewise the other internal capacities vary from valve to valve up to $\pm 10\%$. The effect of these variations on the frequency has to be minimised by a proper choice of external circuit.

3. CIRCUIT OF OSCILLATOR

To get an objective measure for different oscillator circuits, we have to get a common starting point in the form of an equivalent circuit valid for all types of oscillator circuits. If we limit ourselves to oscillators with negligible transit time effects, then we can use the equivalent circuit shown in Fig. 1. This circuit is satisfactory for all usual feed-back oscillators and even for cases like the dynatron and the cathode-follower oscillator, where the input and output terminals of each four-pole in Fig. 1 are joined, thereby changing the four-pole into a two-pole with equivalent properties.

The equivalent circuit shown in Fig. 1 is an oscillator represented by interconnecting two four-poles, the upper one being the active network, representing the valve, while the lower is passive and represents the tuned circuit.

Let us introduce the following notation:

- Z_1 input impedance of valve (mainly grid-cathode capacity)
- Z_2 output impedance of valve (mainly anode-cathode capacity)
- G_m mutual conductance
- I_1 input current into grid of valve
- E_1 input voltage at grid of valve
- I_{2s} short circuit output current of valve
- E_{20} open circuit output voltage of valve
- I_2 output current of valve in load Z_2'
- E_2 output voltage of valve across load Z_2'
- Z_1' input impedance of tuned circuit (on grid side)
- Z_1' output impedance of tuned circuit (on grid side)
- Z_M mutual impedance of tuned circuit (see below)
- E_{10} open circuit output voltage of tuned circuit (on grid side)
- I_{1s} short circuit output current of tuned circuit
- R_0 parallel impedance of tuned circuit at resonance
- E_0 voltage on tuned circuit.

All the above quantities (except R_0) are regarded as complex.

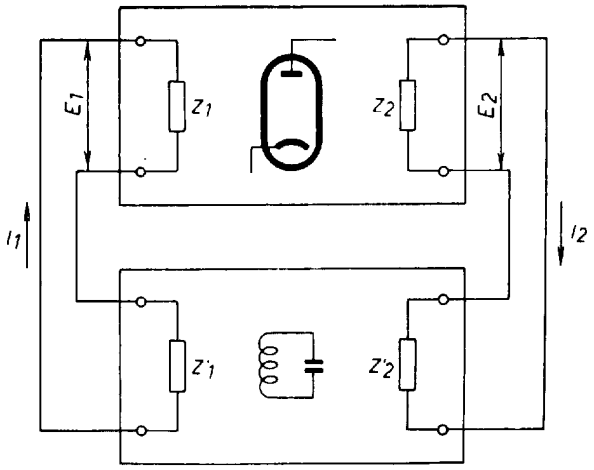

Fig. 1

We can now describe the properties of the two four-poles by the following relations:

$$Z_1 \quad \frac{E_1}{I_1}. \tag{1}$$

$$Z_2 \quad \frac{E_{20}}{I_{2s}}. \tag{2}$$

$$G_m \quad \frac{I_{2s}}{E_1}, \tag{3}$$

$$G_m \quad ae^{jx} \tag{4}$$

Equation (4) is a general way of writing the mutual conductance where x is the phase-angle by which the anode current lags behind the grid voltage as a result of the finite transit time of the electrons in the valve.

In a similar way we define the properties of the second four-pole. If we assume that all the losses of the circuit are concentrated in the parallel resistance R_0, and that the transformations from the anode to the tuned circuit and from the tuned circuit are loss-less, a condition met in practice, then the well-known impedance transformations are valid:

$$E_0 \quad E_2 \left| \frac{R_0}{Z_2'} \right. \tag{5}$$

$$E_{10} \quad E_0 \left| \frac{Z_1'}{R_0} \right. \tag{6}$$

from which it follows that

$$E_{10} \quad E_2 \left| \frac{Z_1'}{Z_2'} \right. \tag{7}$$

and since

$$E_2 \quad I_2 Z_2' \tag{8}$$

we obtain by substituting (8) into (7)

$$E_{10} \quad I_2 \left| Z_1' Z_2' \right. \tag{9}$$

The geometric mean of the impedances Z_1' and Z_2' we can call the mutual impedance Z_M and write symbolically:

$$Z_M \quad Z_1' Z_2' \quad be^{i\beta} \tag{10}$$

where b represents the magnitude and β the phase-angle of the impedance.

For the passage from the first to the second four-pole the following relations hold:

$$I_2 \quad I_{2s} \frac{Z_2}{Z_2 + Z_2'} \tag{11}$$

where the fraction can be expressed symbolically by:

$$\frac{Z_2}{Z_2 + Z_2'} \quad ce^{i\gamma} \tag{12}$$

and finally

$$E_1 \quad E_{10} \frac{Z_1}{Z_1 + Z_1'} \tag{13}$$

$$\frac{Z_1}{Z_1 + Z_1'} \quad de^{i\delta}. \tag{14}$$

The quantities E_1, I_{2s}, I_2, E_{10}, E_1 are, therefore, cyclically inter-connected by equations (3), (11), (9), (13), their mutual substitution furnishing conditions for oscillation:

$$abcd \quad 1, \tag{15}$$

$$\alpha + \beta + \gamma + \delta \quad 0^\circ. \tag{16}$$

This general criterion of oscillation may be simplified in practice as the following relations generally hold:

$$Z_1' \quad Z_1, \tag{17}$$

$$Z_2' \quad Z_2 \tag{18}$$

and therefore

$$I_2 \quad I_{2s}, \tag{19}$$

$$E_1 \quad E_{10}, \tag{20}$$

$$c \quad d \quad 1, \tag{21}$$

$$\gamma \quad \delta \quad 0^\circ. \tag{22}$$

The criterion of oscillation then is:

$$ab \quad 1. \tag{23}$$

yields

$$\left| Z_1' Z_2' \right. \quad \frac{1}{G_m} \tag{24}$$

Let us now examine the change of frequency caused by a change of internal capacity of the valve. This we shall do on the basis that by resonant transformations the ohmic and reactive impedances are transformed equally. A change, ΔC_1, in the input capacity connected to the impedance Z_1' manifests itself in a detuning caused by an equivalent capacity ΔC_0 in the tuned circuit of dynamic resistance R_0 so that:

$$\frac{\Delta C_1}{\Delta C_0} \quad \frac{R_0}{Z_1'} \tag{25}$$

if the tuning condenser is C_0 then

$$\frac{\Delta f}{f} \quad \frac{\Delta C_0}{2 C_0} \tag{26}$$

which after substituting for ΔC_0 from (25) yields

$$\frac{\Delta f}{f} \quad \frac{\Delta C_1 Z_1'}{2 C_0 R_0}. \tag{27}$$

The greater the impedance Z_1', the greater is the change of frequency. The same considerations hold for changes in capacity ΔC_2 and impedance Z_2'. For minimum frequency changes caused by changes in the capacities C_1 and C_2, when $Z_1' Z_2'$ is given in (24), the optimal solution is:

$$Z_1' \quad Z_2' \quad Z_M \quad \frac{1}{G_m}. \tag{28}$$

From the above and further from equations (5) and (6) we get

$$E_1 \quad E_2, \tag{29}$$

i. e. the grid voltage is equal to the anode voltage. This results in the valve working with a low efficiency, which in low-power stable oscillators is of little importance.

An oscillator with impedances designed according to equations (28) has, therefore, the highest possible stability with regard to changes in internal capacities of the valves. We shall now estimate the frequency change caused by a change of 1 pF in either internal capacity, the highest value likely to be met with in usual valves. Starting from equation (27)

$$\frac{\Delta f}{f} \quad \frac{\Delta C_1 Z_1'}{2 C_0 R_0} \tag{27}$$

substituting for Z_1' from (28) and the well-known value for R_0

$$R_0 \quad \frac{Q}{\omega C_0} \tag{30}$$

we get

$$\frac{\Delta f}{f} \quad \frac{\Delta C_1 \omega}{2 G_m Q}. \tag{31}$$

The relative change of frequency is smaller, with higher circuit Q and with higher mutual conductance of the valve, and for a given ΔC_1 it is proportional to the frequency.

We therefore work with high slope valves and try to obtain a Q as high as possible. Another important point demonstrated by equation (31) is that the stability is independent of $\frac{L}{C}$ of the tuned circuit. We can therefore choose $\frac{L}{C}$ so as to obtain a simple mechanical design.

If we re-write equation (31) so as to be able to substitute practical units, we get after putting $\Delta C_1 = 1$ pF

$$\frac{\Delta f}{f} = \frac{1}{\lambda Q G_m}, \qquad (32)$$

where λ is wavelength in metres and G_m the mutual conductance in mA/V (millimhos). For example, when using a valve with $G_m = 5$ mA/V and a tuned circuit of $Q = 100$ we get for $\lambda = 1000$ m

$$\frac{\Delta f}{f} = 2 \times 10^{-6}.$$

4. A CRITICAL REVIEW OF EXISTING CIRCUITS

Criterion (28) derived above means that the highest possible stability regarding the internal capacities of the valves can be achieved by connecting the anode and grid to points of the tuned circuit of as low an impedance as will still maintain oscillation. This criterion, independently discovered by a number of authors, was realised in different ways as shown in the diagrams. The oscillator of Gouriet which has been in operation at the B.B.C. since 1938 (as stated by E. K. Sandeman in his "*Radio Engineering*", 1947), was not published before this date and was re-discovered by J. K. Clapp in 1946 (see Fig. 2). The circuits by Seiler (QST 1941) and Lampkin (Proc. IRE 1939) follow the same idea. It seems, therefore, that if we keep, with their designs, to the rules contained in equations (5), (6) and (28) we must arrive at the same results as regards stability.

This reasoning is correct with regard to a single-frequency for which the calculation is carried out. But if the frequency is varied, conditions change abruptly and different oscillators give very different results. We shall try, by an example, to follow these conditions in the circuit of Gouriet-Clapp (Fig. 2). Let C_0 be the tuning condenser, C_a and C_g the anode-cathode and grid-cathode capacities, respectively. Further, let us assume that the Q is nearly constant over the tuned frequency range and that $C_a = C_g$; we can then write

$$R_0 = \frac{Q}{\omega C_0}, \qquad (30)$$

$$Z_1' = Z_2' = R_0 \left(\frac{C_0}{C_a}\right)^2. \qquad (33)$$

$$G_m = \frac{\omega C_a C_a}{Q C_0} \qquad (34)$$

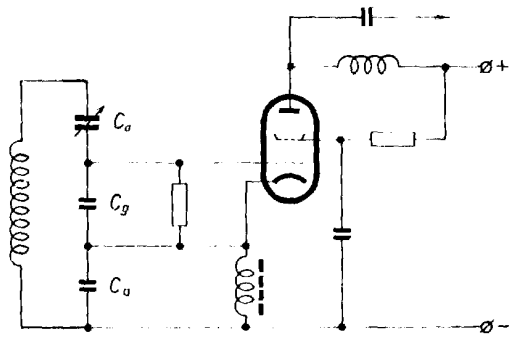

Fig. 2

and because

$$C_0 = \frac{k}{\omega^2} \qquad (35)$$

we can substitute into (34) and write

$$G_m = \text{const.}\,\omega^3. \qquad (34a)$$

We see that the mutual conductance necessary to maintain oscillations in the Clapp oscillator is proportional to the third power of the frequency. The consequence is that the mutual conductance necessary to maintain oscillations when tuning the oscillator towards longer waves decreases: for constant mutual conductance the amplitude, and therefore also the grid bias, increases until the valve operates in class "C" and the dynamic conductance decreases to the needed value. When tuning towards shorter waves the necessary conductance rises and the amplitude decreases until oscillations stop. Even though Clapp's circuit has the advantage of simplicity, it can only be used for operation on fixed frequencies

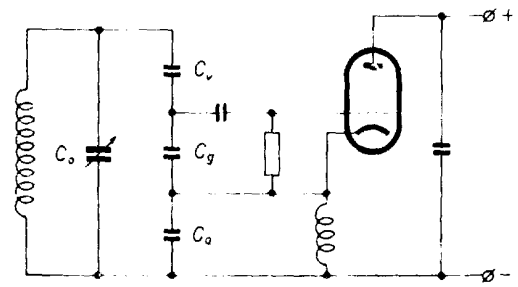

Fig. 3

1 : 1.2).

The circuits due to Lampkin (Fig. 4) and Seiler (Fig. 3) behave quite differently. The two circuits are equivalent, the only difference being that Seiler uses a capacitive and Lampkin an inductive voltage divider (the tuning coil) for impedance transforma-

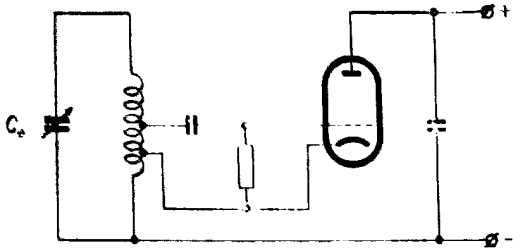

Fig. 4

tion. Let us calculate the dependence of mutual conductance on the frequency for the circuit due to Seiler which has, moreover, the advantage that when operating in class "C" or "B" its capacitive divider effectively short-circuits higher harmonics to ground. Let C_0 again be the tuning condenser, C_a and C_g the anode-cathode and grid-cathode capacities respectively and let C_v be the condenser from the grid to the "live" side of the tuned circuit. If we assume that $C_0 \gg C_v$ and $C_a + C_g \gg C_v$ we can write:

$$R_0 = \frac{Q}{\omega C_0}, \tag{30}$$

$$Z_1' = Z_2' = R_0 \left(\frac{C_v}{C_a}\right)^2, \tag{30}$$

$$G_m = \frac{\text{const}}{\omega}. \tag{30a}$$

It can be seen that the mutual conductance is inversely proportional to the first power of the frequency. The amplitude dependence on frequency is reversed to that of Clapp's circuit but the change in amplitude is much less pronounced. This circuit can therefore be used for larger frequency ranges up to approx. 1 : 1.8.

The next circuit, known as the cathode follower oscillator, in short CFO (see Fig. 7), can also achieve a comparatively high stability when connected to the tuned circuit at a point of lowest possible impedance. For its operation the following relations hold. If:

R_k common cathode resistor

G_m mutual conductance, equal for both triodes

E_{v1}, E_{v2} AC voltage on grid of first and anode of second triode

E_k AC voltage on common cathode

and if

$$G_m R_k \gg 1,$$

$$E_k = \tfrac{1}{2} E_{v2},$$

$$I_{a2} = \tfrac{1}{2} E_{v1} G_m$$

and for this current to produce the voltage E_{v1} (condition of oscillation) the impedance at the point of connection of the valve

$$Z = \frac{E_{v1}}{I_{a2}} = \frac{2}{G_m}.$$

The impedance is obviously twice that calculated for the previous cases and the same as if we had used valves with halved mutual conductances. Because the condition of stability equation (28) is valid for this case too

$$\frac{df}{f} = \frac{1}{\lambda Q G_m}, \tag{28}$$

we get for equal mutual conductance half the stability as in the previous oscillator. Its advantage, of course, is a certain simplicity in design of the tuned circuit. When tuning this oscillator over larger frequency ranges, the amplitude will change similarly as in the oscillator due to Seiler, because of the constant transformation of dynamic resistance. The amplitude, therefore, rises proportionately with the frequency.

The development of stable oscillators in Czechoslovakia progressed independently and without technical information about developments in the West. In 1945, the firm Radioslavia developed a stable oscillator which successfully combined the

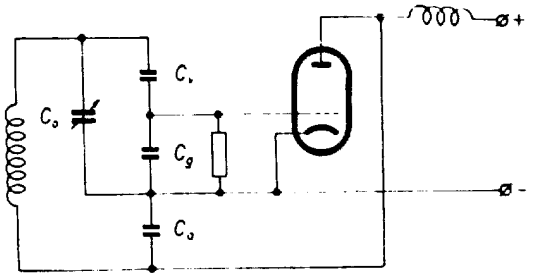

Fig. 5

properties of the two above-mentioned circuits and maintained a comparatively constant amplitude over a wide frequency range. This circuit (Fig. 5) has been in practical operation since 1946 in code transmitters of the Czechoslovak Post Office and has an operating frequency stability of $5 \cdot 10^{-5}$, although oscillating on a relatively short wave (130 – 180 m).

was discovered independently and described just a year ago by the Italian O. Landini in the journal Radio Rivista. The latter, however, worked only experimentally and to the extent that he gives theoretical calculations at all, he starts from false premises. We shall therefore give an outline of the calculations.

Let us assume the same symbols C_a, C_g, C_c, and C_0 as in the previous example and further let $C_c \gg C_{gc}$, $C_g \gg C_{gc}$ and $C_a \gg C_0$; we can then write

$$G_m = \frac{1}{|Z_1' Z_2'|} \tag{24}$$

$$Z_1' = R_0 \left(\frac{C_c}{C_g}\right)^2, \tag{37}$$

$$Z_2' = R_0 \left(\frac{C_0}{C_a}\right)^2, \tag{38}$$

$$R_0 = \frac{Q}{\omega C_0} \tag{30}$$

substituting into (24) we get

$$G_m = \frac{\omega}{Q} \frac{C_c}{C_g C_a}. \tag{39}$$

Since, with the coil used, the Q increased moderately with frequency, the necessary mutual conductance, and thus also the amplitude, is constant.

The values of the condensers C_c, C_g and C_a have to be determined so that equation (28) will be satisfied for centre frequency of the range, i. e.

$$\frac{1}{G_m} = \frac{Q}{\omega_c C_{gc}} \cdot \left(\frac{C_{gc}}{C_a}\right)^2 = \frac{Q}{\omega_c C_0} \left(\frac{C_c}{C_g}\right)^2 \tag{40}$$

When actually designing this oscillator we proceed in the following manner:

Let us say the oscillator has to have a frequency range of 1700 — 2000 kc/s and a stability of 10^{-4}; we first decide on the tuning condenser. We can either use a specially designed condenser which of course would be considerably laborious and expensive but which would, without switching, tune the whole range with sufficient precision or we can use a condenser of normal production. Then, of course, it is necessary to sub-divide the frequency range and use a switch to obtain the required precision; e. g., to use a 100 pF circular plate condenser (when tuning such a narrow range logarithmic plates are of no advantage) with an estimated stability of one part in 500, then its maximum tuning range to get a resultant stability of 10^{-4} will be:

$$\frac{f_{max}}{f_{min}} = 1 + \frac{500}{10000} = 1.05.$$

If we want to cover the range of 1700 — 2000 kc/s, i. e. 1 : 1.17, we can sub-divide it into four bands e. g. 1690 — 1775 kc, 1770 — 1860 kc, 1850 — 1940 kc and 1930 — 2020 kc.

To a tuning range of $f_{max} : f_{min} = 1.05$ corresponds a tuning condenser with

$$\frac{C_0 \max}{C_0 \min} = \left(\frac{f \max}{f \min}\right)^2 = 1.1,$$

i. e. the tuning capacity has a variation $C \pm \Delta C = 1.1 C_0$ min. The difference $\Delta C = 0.1 C_0$ min. corresponds to the tuning condenser capacity of 100 pF, the fixed minimum condenser then is

$$C_0 \min = 10 \cdot \Delta C = 1000 \text{ pF}$$

and is best made of Calit or Tempa S. part of which can be of Condensa and can serve as thermal compensation. The inductance we calculate from $C_0 \min = 1000$ pF and the maximum frequency 2020 kc/s.

$$L = \frac{25{,}300}{C f^2} = 6.2\ \mu\text{H}.$$

for which we can use our normal ceramic form of 45 mm diameter and pitch of 1 mm. According to the known formula we find $\frac{l}{D} = 0.21$, i. e. 9.5 turns. The coil is wound with a wire of 0.7 of the pitch, that is, a diameter of 0.7 mm according to the method given above. The other three ranges are covered by switching further 100 pF condensers into the circuit.

The parallel impedance of the circuit of a centre frequency of 1850 kc/s will be

$$R_0 = \frac{Q}{\omega C_0}. \tag{30}$$

If we assume the Q to be 100 and with a capacity $C_0 = 1200$ pF, we get

$$R_0 = 7200\ \Omega.$$

To fulfil the optimum condition of stability (28) with an EF 50 of 5 mA/V operating conductance we have:

$$Z_1' = Z_2' = \frac{1}{G_m} = 200\ \Omega.$$

The impedance transformation ratio is, therefore, $R_0 : Z_{12}' = 36 : 1$, by which the voltage transformation ratio is fixed and also the ratio of condensers which is $\sqrt{36 : 1} = 6 : 1$.

We therefore get:

$$\frac{C_a}{C_0} = \frac{C_g}{C_c} = 6 : 1,$$

$$C_a = 6\, C_0 = 7200 \text{ pF},$$

and by choosing $C_c = 100$ pF we get $C_g = 600$ pF.

One must not forget, of course, that because of the necessary assumptions (e. g. Q) these results will

only be approximate, and in practice it will be necessary to adjust these values according to exact measurements.

The stability with respect to internal capacity changes will be, according to (32),

$$\frac{df}{f} \quad \frac{1}{2Q\,G_m} \quad 1.25 \times 10^{-3},$$

i. e. for a change of internal capacity of 1 pF we get a change of frequency

$$1.85 \times 10^6 \times 1.25 \times 10^{-5} \quad 23 \text{ cps}.$$

The next circuit shown in Fig. 6 is similar to the previous one, the only difference being that the condenser C_g is divided into C_{g1} and C_{g2} between which the tuning condenser is connected. This circuit is a compromise between the previous circuit and that due to Seiler, and permits a constant amplitude in a still greater frequency range (up to

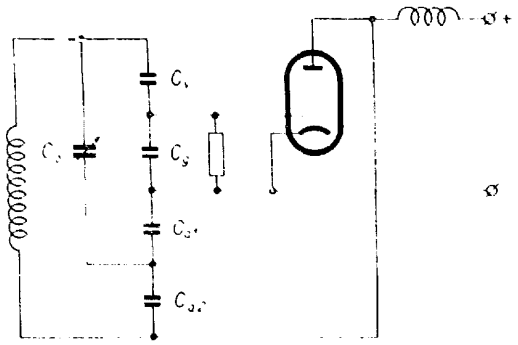

Fig. 6

1 : 2.5) which is of importance for wave meters and communication receivers. Its calculation is, of course, more involved, as we have to take into account the frequency dependence in the given frequency range of the Q of the coil used. The best method, therefore, is one of trial and error: choosing as a starting point these values of circuit parameters: C_1 $0.1C_0$, C_g C_{g1} we calculate in the same way as above, C_{g2} $10C_0$, C_{g1} is adjusted finally so as to keep the amplitude of oscillation practically constant over the whole tuning range. Should the amplitude be too small, or should the circuit not oscillate at all, then we have to decrease both C_1 and C_g, and the reverse. The amplitude of oscillation should be adjusted to such a value that the anode current when oscillating is 60% of the quiescent current, which is the case only if there is no cathode bias resistor.

This bias should not be used, but rather the screen or anode voltage should be lowered so as not to endanger the valve when oscillation stops. The best valve for this purpose is, as was shown, a valve with a high mutual conductance. As the anode load impedance Z_2 is small (of the order of 100 300 Ω), the internal resistance is of no significance and it is all the same whether we use a triode or a pentode; only a high mutual conductance is of importance. It is further of advantage for the valve to have this high

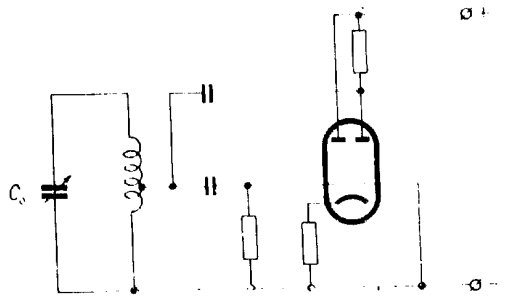

Fig. 7

conductance with a low anode current, for in this case the power delivered by the valve to the tuned circuit is only of the order of a few milliwatts, which does not cause the well-known "creeping" of frequency after switching on. This calls for using high-slope H.F. pentodes, e. g. EF50, EF14, etc. Good results can also be obtained by using the usual output valves EL12, EBL21, etc. with reduced screen grid voltage (100 140 V). These facts are, of course, valid for all types of oscillators described here.

The last circuit (shown in Fig. 8) uses a variable inductance which can be tuned, either by moving an iron core or a short-circuited turn, by a micrometric screw instead of a variable condenser. The frequency

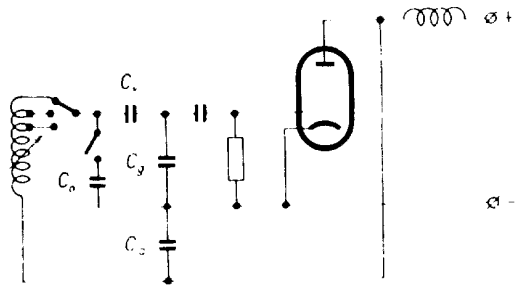

Fig. 8

range obtainable with an iron core is 1 : 1.1, that with a short-circuited turn is, because of the losses and hence necessarily looser coupling used, max. 1 : 1.05. By fixing the iron core to a micrometric screw we obtain great precision; in a concrete case, e. g., with a total travel of the core of 20 mm and a pitch of the micrometric screw of 1 mm, one division of the hundred division circular dial corresponds to a change in frequency of one part in 20,000. This component is, of course, considerably simpler

and cheaper than a special tuning condenser designed to satisfy the same specifications.

When a greater tuning range than 1 : 1.1 is needed, we provide the coil with taps, switch condensers, or even both. In Fig. 8 the switched condenser is connected similarly to the tuning condenser in Fig. 5 which ensures a constant amplitude when switching this condenser into the circuit. The condensers C_v, C_a and C_g are dimensionally equal to those used in Fig. 5.

CONCLUSION

In the above article a survey has been made of the factors affecting the frequency stability of oscillators; mechanical and electrical conditions have been derived for the design and construction of oscillators with high frequency stability; a method of calculating the general oscillator with regard to its frequency stability has been given; causes of instability have been separated and defined; and a formula has been derived for the direct evaluation of electrical stability (defined as the relative change of frequency caused by a change of 1 pF in the internal capacitance of a valve).

A survey has also been made of existing circuits of modern stable low impedance oscillators, i. e. the impedances seen by the valve are as low as possible, their evaluation as regards attainable frequency stability; and amplitude versus frequency dependence when they are tuned over a given frequency band. When optimal frequency and amplitude stability is required, new circuits have been proposed which have been tested in practice and which are used in the construction of oscillators for broadcast transmitters at TESLA. The evaluation of these circuits and practical results are given.

Thanks are due for many valuable hints and suggestions given by Mr. Vilém Klika and for the devoted collaboration of all our colleagues in workshop, design department and laboratories.

BIBLIOGRAPHY

[1] *F. B. Lewellyn: Constant Freq. Oscillators. Proc. IRE. Dec. 1931.*
[2] *Janusz Groszkowski: Problem of Constant Freq. Oscillators. Proc. IRE 1931.*
[3] *W. L. B. Roberts: The Limits of Inherent Freq. Stability. RCA Rev. April 1940.*
[4] *G. F. Lampkin: An Improvement in Constant Freq. Osc., Proc. IRE, March 1939.*
[5] *E. O. Seiler: Var. Freq. Oscillator, QST Nov. 1941.*
[6] *J. K. Clapp: An Inductance-Capacitance Oscillator. Proc. IRE. March 1948.*
[7] *E. K. Sandeman: Radio Engineering, Chapman-Hall, London 1947.*
[8] *O. Landini: Radio Rivista, November 1948.*

Rotatable Directional Antenna

Josef Bříza

UDC 621.396.677.2

SUMMARY

Advantages and disadvantages of short-wave directional antennas. Description of a new rotatable directional antenna.

The present antenna is basically a sloping rhombic antenna, suspended on a single mast so that it can be rotated and attached to three cars which in turn run on rails around the mast; shifting the cars controls three parameters: direction of transmission or reception; apex angle of the rhombus; the angle between the plane of the antenna and the ground plane. This permits favorable horizontal and vertical transmitting and receiving directional patterns for each frequency used and with respect to the electrical properties of the ground; the effectiveness of the antenna is improved; the frequency range of the antenna is increased and its dimensions are reduced. Lower investment costs are involved for installation of an antenna for transmission or reception in various directions and on various frequencies.

Determining the intensity of the electromagnetic field of the transmitting antenna according to the proposal. Determining the azimuthal and vertical radiation patterns. Consideration of the optimum apex angles of the rhombus, and favorable elevation angles for the maximum vertical directivity.

Description and results of measurement of the azimuthal and vertical radiation pattern on a scale model of the antenna.

Editor's note: The apex angle here considered is twice the complement of the "tilt" angle used by some other authors.

1. SHORT WAVE DIRECTIONAL ANTENNAS

11. Advantages and Disadvantages of Directional Antennas

One of the characteristic properties of short waves, which are usually used for radioelectrical communication over long distances, is the possibility of effective concentration of the transmitted electromagnetic energy in a direction towards the receiver by means of directional transmitting antennas. Such concentration has many advantages. Above all, the intensity of the electromagnetic field of the transmitter at the place of reception is increased, other conditions being equal. This means: lower operating costs for the transmitter and also lower cost of installation, assuming the system of directional antennas and transmission lines is not too expensive; increased ratio of signal strength to noise level in the receiver; such an excess of energy received that the influence of fading on reception is more easily compensated; reduction of mutual interference of transmitters; reduction of reception in undesired places; reduction of the disturbance of reception by signals which go in opposite directions around the earth, etc.

For similar reasons, directional receiving antennas are used as well, mainly for communication between fixed stations.

The more sharply the transmitted energy has to be concentrated in a desired direction, the greater must be the dimensions of the directional antenna in relation to the wavelength used. Generally, these dimensions are of the order of several wavelengths. On short waves, with these dimensions, it is practically necessary to suspend the antenna on masts several tens of meters in height. With such fixed constructions, the directional antenna can be used only for transmission in some particular direction. Therefore, for each direction desired, a special directional transmitting antenna has to be installed.

Due to the periodic and irregular changes in the state of the ionosphere, it is constantly necessary to change wavelength, for communication between given locations, over very wide limits. Even for transmission to various distances in the same direction, it is necessary to use different wavelengths.

Directional transmitting antennas usually are systems of conductors, which maintain electrical standing waves. Impedance and directional properties of such antennas are very sensitive to change of wavelength of the transmitted energy; antennas practically lose their favorable directional properties when the wavelength is changed – even a small per cent – from the wavelength for which they have been constructed. Some directional antennas with non-resonant current distributions such as the so-called series-phase antennas, have similar properties. A special antenna is necessary not only for each direction of transmission, but also for each wavelength used in each direction. This is especially disadvantageous for short-wave broadcasting stations, which usually send out several relatively brief programs to places in different directions and at different distances every day, and at different hours.

This is why forests of antenna masts with many antennas hanging from them, have grown up on extensive grounds around such transmitters. Such antenna systems with their respective transmission lines used to be very expensive and uneconomical.

12. Rotatable Antennas

In order to do away with the necessity of having special antennas for each direction of transmission or reception, different systems of short-wave rotatable directional antennas have been designed. Usually they are arrays of horizontal or vertical dipoles mounted on one or two rotating towers [1]. Should the desired concentration of energy transmitted or received be very sharp, such arrays must be complicated, heavy, and expensive. If the length of the dipoles is not adjustable, they can be used for only one wavelength. If adjustable, such arrays are mechanically and electrically even more complicated, and at the same time usable only within a relatively narrow band of wavelengths.

13. Aperiodic Antennas

The disadvantages resulting from the necessity of constructing a special resonant antenna for each wavelength used are eliminated by aperiodic antennas, whose impedance and directivity change but little within a fairly broad frequency range. The best known of these is the *rhombic antenna* [2]. It consists of four horizontal conductors forming a rhombus, suspended from four fixed masts. The rhombus is connected to the transmitter or receiver by a line going to a corner with an acute angle, while to the opposite corner a terminating impedance is connected, which is equal to the characteristic impedance of the line and antenna, so that a non-resonant current distribution is obtained. The main radiation of the rhombic antenna is along the long diagonal of the rhombus, in the direction from the transmission line towards the terminating impedance. The radiation diagram depends on the ratio of the length of the rhombus legs to the wavelength, on the apex angle of the rhombus, on the height of the conductors above ground, and on the electrical properties of the earth below the antenna. The dimensions of the antenna, the angles of the rhombus, and the height of the antenna above ground are such that the antenna has optimum directional properties for one wavelength. On other wavelengths the directional properties deteriorate because with a conductor of a given length, different apex angles, and a different height of the antenna above ground would be necessary. This deterioration is not serious within a fairly wide band about the wavelength for which the antenna has been constructed. Thus, for example, a fixed rhombic antenna with fixed apex angle is usually used within a band of wavelength which is between one-half to one-sixth of the length of one leg of the rhombus.

14. Advantages and Disadvantages of the Rhombic Antenna

Besides the above-mentioned advantages, common to all directional antennas, the rhombic antenna has in addition chiefly these two: simplicity of construction and high input impedance which enables the antenna to be directly connected to a symmetrical transmission line. Horizontal polarization of the waves in the direction of the main lobe makes the shape of the directional pattern less dependent upon the electrical properties of the ground near the antenna. This is because at elevations less than 30°, the ground reflection coefficient of the horizontally polarized wave component depends much less on ground conductivity than does the ground reflection coefficient of the vertically polarized wave component.

Furthermore the elevation angle of the main lobe diminishes with the wavelength. This is advantageous because shorter waves are used for communication over longer distances and they require greater angles of incidence at the ionosphere. Of course, these elevation angles depend to some extent on the properties of the ground near the antenna.

The greatest disadvantage of the rhombic transmitting antenna is the loss of a great part of the power supplied by the transmitter in the terminating impedance. This loss can be reduced by connecting two or more rhombic antennas in series, so that each additional antenna radiates a part of the energy not radiated by the preceding one [3]. There are designs according to which it would be possible to feed the unradiated energy from the terminating point back to the feeder point of the antenna [4].

An additional disadvantage is the above-mentioned deterioration of the directional effect of the antenna at the extreme limits of the usable range of wavelength. In order to eliminate this disadvantage a horizontal rhombic antenna hung on four masts has been described, which provides for changing the apex angles of the rhombus when changing the wavelength [5]. This, at the same time, results in broadening the band of wavelengths for which the antenna can be used, but at the cost of complicating the mechanical construction.

Another disadvantage is the fact that the directional properties of the antenna, especially the vertical

radiation pattern, as well as the angle of elevation of maximum radiation, depend to some extent upon the electrical properties of the ground near the antenna, i. e. upon the weather conditions. In order to eliminate this disadvantage it has been proposed to change the height of the antenna above ground when the ground properties change [6]; this, of course, means again complications in mechanical construction.

With a standard horizontal rhombic antenna, having a useful band of wavelength of 1:3, hung at a height approximately one half of the longest usable wavelength, the elevation of the main lobe is too great (15° to 30°). Hence a considerable part of the radiated energy goes through the ionosphere.

A very considerable disadvantage is that the antenna can be used for one direction of transmission or reception only. It is therefore necessary to erect a special antenna for each particular direction, which results in higher construction and maintenance costs and, of course, requires a greater land area as the longer diagonal of the antenna is almost four times the longest usable wavelength. Installation of the antenna requires four masts, usually higher than 20 meters.

In the following part of this paper a proposal for a rotatable directional antenna is given, which eliminates or diminishes most of the mentioned disadvantages of directional antennas, and of the rhombic antenna in particular, and brings some very substantial advantages. A transmitting antenna will be described, but the same construction may be used for the receiving antenna as well.

2. A ROTATABLE DIRECTIONAL ANTENNA

21. Description

A schematic diagram of the main features of the proposed rotatable directional antenna [7] is given in Fig. 1. The antenna consists of conductors of the same length, *31*, *31*, *32*, *32*, symmetrically arranged to form a rhombus. The higher ends of conductors *31* are attached by means of insulating members to the rotating head of a wooden mast *1*. Their lower ends are conductively connected to the conductors *32*, the far ends of which are insulated, attached to the cable drum of the car *20* by means of a hempen rope *50*, and loaded by the weight *60*. The remaining two apexes of the rhombus, at the junctions of conductors *31* and *32*, are attached by means of the sectioned cables *4*, *4* to the cars *21*, *21*, the positions of which are symmetrical to the car *20*. The length of the insulated sections of the cables *4* is about $\frac{1}{3}$ of the shortest wavelength to be used. Cars *20*, *21*, *21*, run on a circular track, the center of which is at the mast *1*. In the picture only a section of the track has been drawn.

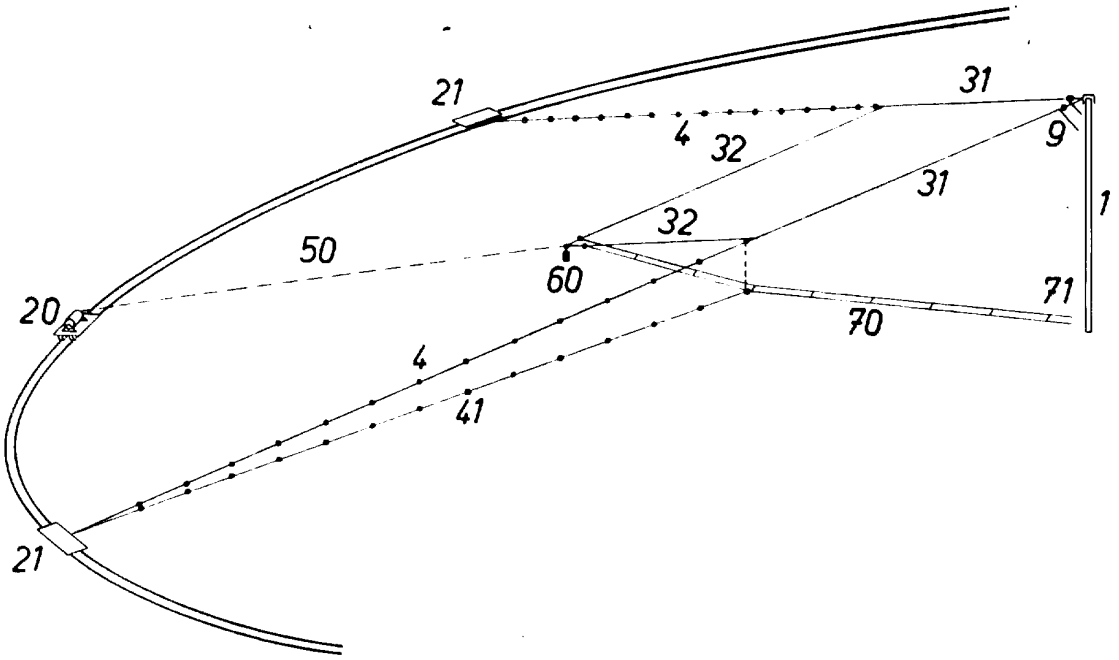

Fig. 1

The far ends of conductors *32* are fed by means of the twin line *70*, connected at the point *71* to a transformer located at the bottom of the mast *1*. The

primary of this transformer is connected to the transmitter by means of a pipe feeder or coaxial cable.

The twin line *70* is attached to the car *21* by means of a sectioned cable *41* and, at the point of attachment hung under the junction of conductors *31* and *32* of the rhombus by an insulating member. The upper ends of conductors *31* are connected by means of the twin line *9*, led along the mast to a terminating impedance equal to the characteristic impedance of the feeder *70* and the input impedance of the antenna. The connection of the twin line *70* at point *71* to the feeder and of the twin line *9* to the terminating impedance is constructed in such a way that it permits rotation of the antenna and its feeding and termination at different positions of the cars. This is achieved e. g. by use of coupling transformers coaxial to the mast, one winding of which is fixed around the mast, while the other, coaxial to the first, may rotate around it. (Should the antenna be used for reception, the terminating resistor will be hung at the point *9*).

Though no anchoring system is shown in the picture, the mast *1* has to be anchored. This can be done by sectioned cables connected to an extension of the mast above the rotatable top head, so that the antenna, as well as the cables *4* can rotate under the anchors. Another way of anchoring the mast would be by sectioned cables fixed to the rotary mast head on one side and on the other to two anchoring cars which run on a circular track.

The whole antenna system can be rotated by simultaneously moving all three cars to such positions that the radius between the car *20* and the mast *1* coincides with the direction of transmission or reception. The motors of all cars (as well as the cable drum motor of the car *20*) can be switched on from the operating room. Their switching off according to the desired direction of transmission can be done automatically, e. g. by sets of three particular stops for each direction in question, which can be controlled from the operating room as well. Then the apex angle of the rhombus is set in order to secure optimum directional properties of the antenna on each frequency used.

This setting of the apex angle of the rhombus is carried out by symmetrically driving cars 21 nearer to or away from the car 20. This again occurs by distant switching on the motors: they are switched off by preset stoppers or from the operating room, after they have reached the correct positions for the frequency in use. Before moving the cars *21* away from each other, the rope *50* has to be loosened by turning the cable drum on car *20*. Finally, conductors *32* and *31* are aligned in the same plane by taking up the slack in the rope *50*, combined with the effect of the counterweight *60*.

Feeder *70* may be constructed so that it will lie in the vertical plane of symmetry of the antenna; at one point between the connection to the antenna at the counterweight *60* and the point *71*, the feeder will be supported by a non-conducting rope, running freely through a pulley fastened to the rotary mast head and stretched along the mast by a counterweight hanging on a free pulley. However, this kind of construction does not provide for setting the apex angle of the rhombus within such broad limits as the construction pictured in Fig. 1.

In order to avoid an eventual influence of the rails on the directional patterns of the antenna the rails have to be grounded at many points and, if necessary, electrically divided into sections isolated one from another.

22. Adjusting the Antenna

Fig. 2 represents a schematic diagram of the proposed rotatable directional antenna for short-wave broadcasting purposes in a waveband from roughly 11 to 50 meters. It is assumed that the length of the antenna conductors is 50 meters, height of the mast about 35 meters, radius of the track 150 meters and the height of the feed point of the rhombus about 13 meters. The ground-plan in the lower part of the picture shows positions of the antenna conductors and the three cars at different settings for five short-wave broadcast bands. Only the lower part of the ground-plan is drawn, the upper half being symmetrical to the lower. The antenna conductors are drawn in full lines, while the sectioned suspension cables connecting the side apexes of the rhombus to the cars *21* are drawn in broken lines. The rope connecting the bottom apex of the rhombus to the cable drum of the middle car *0* is drawn in dotted line at the setting of the antenna for the 11 meter wave, being partially drawn for the other extreme setting of the antenna, i. e. at 50 meters as well. The optimum apex angle is given by curve δ'_m, shown in Fig. 6. For wavelengths about 50, 31, 25, 17 and 11 meters, when the respective ratios of the length of the antenna legs to wavelengths are approximately 1, 1·5, 2, 3 and 4·5, the side car shown will move on the rail to positions 1, 1·5, 2, 3 and 4·5. For these apex angles, δ'_m, the radiated field will attain its maximum values. In the cross section along the vertical plane of symmetry, sketched in the upper part of Fig. 2, different planes of the antenna can be seen; these respective planes are determined by the antenna conductors, drawn in full line, and by the suspension cables (drawn in broken line), which tie

the antenna to the side cars. Sketched planes belong to the same positions of the side cars as mentioned above, marked again 1, 1·5, 2, 3 and 4·5, and their elevation angles are about 20°, 16½°, 15½°, 14° and 13⅛° respectively. In the antenna position for the 11 meter waveband (cars being in the position 4·5), a dotted line represents the hempen suspension rope connecting the feed point of the antenna conductors with the cable drum of the center car 0, while in the antenna position for the 50 meter waveband (side cars in position 1) only a part of this rope nearest to the ends of the conductors is drawn.

The adjustment of the apex angles of the rhombus by moving the side cars is automatically connected with the setting of the elevation angle of the plane of rhombus. In the lower right-hand corner of Fig. 2, a graphical representation is shown of the dependence of the elevation angle ϑ upon the value of the angle δ (i. e. half the apex angle of the rhombus at the mast), expressed, with the antenna of dimensions stated above, by the equation

$$\vartheta = \arcsin \frac{0{\cdot}22}{\cos\delta}.$$

The apex angle at the mast being diminished by moving the side cars towards each other, the inclination angle of the antenna plane, as well as the angular elevation of the maximum radiation pattern of

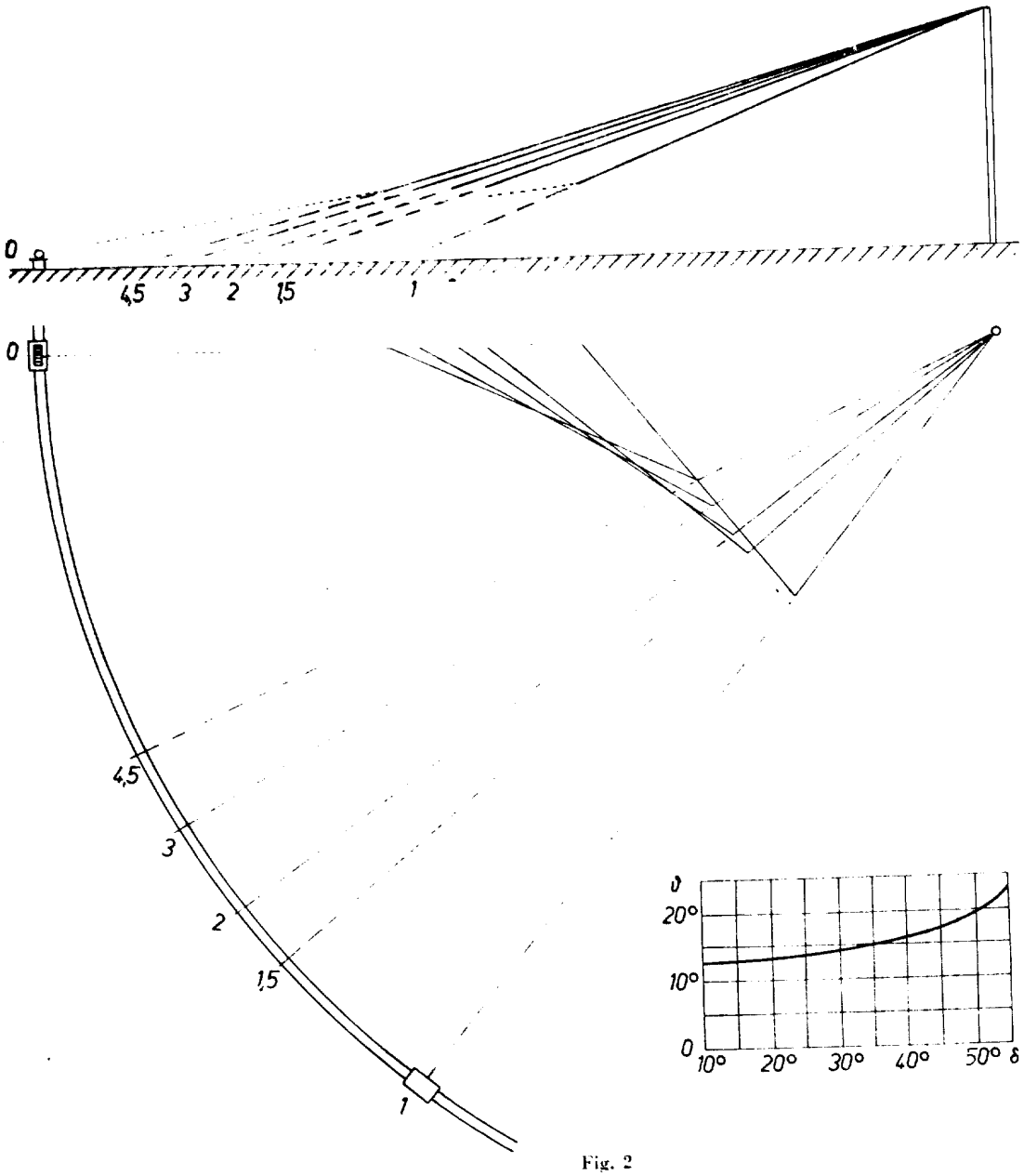

Fig. 2

the antenna become smaller. This automatic setting of the apex angle with the inclination angle is very favorable, because it is advantageous to diminish the apex angle and to lower the angle of elevation of the maximum radiation with shorter waves.

By diminishing the height of the antenna mast and the radius of the rails, the angular elevation of the maximum radiation becomes somewhat greater, as can be seen by comparison of the upper part of Fig. 18 (height of the mast 23 meters, radius of the rails 100 meters) with the full line diagram of Fig. 7 (height of the mast 35 meters, radius of the rails 150 meters). Both diagrams are valid for rhombus legs of 50 meters and at a wavelength of 50 meters. The field strength in the direction of maximum radiation will become lower at the same time.

23. *Advantages and Disadvantages of Rotatable Directional Antenna*

A great advantage of the proposed antenna is that it enables us to rotate the beam of concentrated radiation to any direction without rotating an entire complicated construction, by simply moving three cars. Instead of the four masts necessary with ordinary rhombic antennas, this antenna has one fixed mast only.

In addition, the present antenna is aperiodic within far greater limits than the rhombic antenna. This extension of the usable band is made possible by resetting the appropriate apex angles of the rhombus for each wavelength. In contrast to a fixed rhombic antenna of the same dimensions, the proposed antenna can be used even on a wavelength twice as long as the longest usable wavelength of the fixed antenna. Going towards the shorter wavelengths, the usable waveband is limited only by the length of the insulated sections of the anchoring guy wires. These sections being short enough, say 2 meters, the useful range of the antenna can comprise the entire short-wave broadcasting spectrum; moreover, the antenna will have the best possible directivity on each used wavelength.

Owing to its rotatability and wideband aperiodicity the proposed antenna will replace a complicated system of many directional antennas. It means reduction of construction and maintenance costs as well as savings in the necessary ground space. When an unexpected change of beam direction becomes necessary, a few small adaptations, such as resetting the car stoppers, etc., will do the trick; there is no need to construct an entirely new antenna.

The apex angles of the rhombus are set by the same mechanical means which rotate the antenna. This resetting of the angles for each wavelength brings, as against the fixed rhombic antenna, the following additional advantages: the transmission becomes more effective by obtaining optimum concentration of radiation, the shape of the radiation pattern can easily be set according to actual need, and the dimensions of the antenna systems can be diminished by nearly one half.

The dependence of the field strength in the direction of maximum radiation upon the electrical properties of the ground under the antenna and consequently upon the weather is diminished by the slanting suspension of the antenna, because the field strength of the wave reflected by the ground in the direction of maximum radiation is substantially lower than the field strength of the direct radiation in that direction. It is true that this results in a slightly lower total field strength in that direction, but this loss is more than equalized by the gain from greater effectiveness in consequence of the control over the apex angles of the rhombus and of lower angular elevations of the main lobe. The angular elevation of the maximum radiation of an ordinary fixed rhombic antenna (legs from two to six wavelengths) is usually from 30° to 15°, whereas with the proposed antenna of the dimensions mentioned above and at the same wavelengths the angle of the maximum radiation will be from about 15° to nearly 4°, as can be seen from the curve $90° - \Theta_m$ in Fig. 6. This lowering of the angular elevation of the maximum radiation results in two consequences: 1. The phase difference between the fields of the wave reflected from the ground and of the direct radiation will be lowered and, therefore, the overall field strength will be higher; 2. the radiation in the direction of great angles, which goes through the ionosphere, will be reduced. The lowering of the overall field strength resulting from the slanting suspension of the antenna is of no practical consequence, because due to the changes of the angular elevation of maximum radiation in consequence of the changes of ground properties through weather, the fixed rhombic antenna will not put the maximum field in the desired direction anyway.

A further advantage of the proposed antenna is the dependence which exists between the setting of the apex angles of the rhombus and the setting of the slope of the antenna and the consequent automatic resetting of one when the other is being set. This aids in lowering the angle of elevation of the vertical radiation pattern when the wavelength decreases.

The proposed antenna is very elastic in traffic. Direction, wave angle and the shape of the radiation patterns may be directed quickly and from a distant operating room according to the traffic conditions,

e. g. when the electrical properties of the ground change due to different weather conditions.

The proposed antenna is particularly suitable for communication with mobile stations, and for short-wave broadcast transmitters which put out a great number of quickly changing program schedules destined for different countries. Two such antennas, which happens to be switched off, would have to be considered.

The proposed antenna has the disadvantage of all rhombic antennas, i. e. that it will radiate only about half the supplied power. These losses may be reduced by using the same steps as with an ordinary rhombic antenna: e. g. a second identical antenna

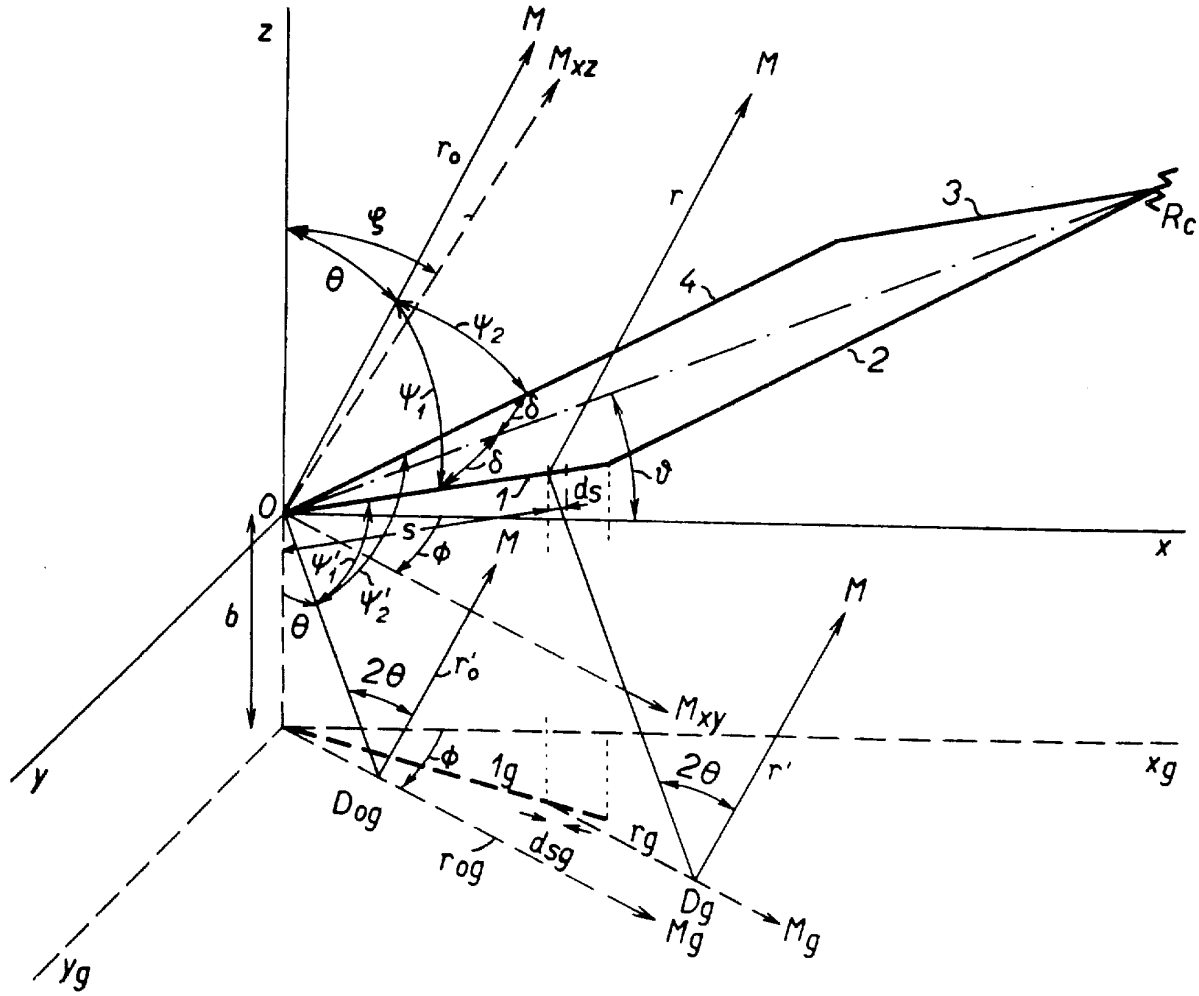

Fig. 3

set for somewhat differing directions, and perhaps suspended on a common mast, could probably be used for leading a mobile station to a target, applying the method of two alternating directional patterns.

With this system, the direction of landing and the sharpness of its indication could be changed according to the position of the mobile station or other circumstances (wind direction, etc.), by turning or sharpening the directional patterns. Should the two antennas be suspended on a common mast, problems of mutual influence of both antennas, as well as of the possible resonance of the antenna connected in series could be rotated to another favorable direction. This direction, as well as the concentration of radiation could then be chosen according to the actual need.

The above-mentioned disadvantage resulting from the partial lowering of the overall field strength due to the sloping suspension is more than amply compensated by the control over the apex angles of the rhombus as well as by setting and stabilising the angular elevations of the maximum radiation.

Even when the maintenance of the control mechanisms must be considered, the maintenance of the proposed antenna will, in all probability, be simpler

than would be the maintenance of the whole system of antennas which the proposed antenna will replace.

Should the supporting mast be anchored by further cars, some measure for ensuring a sychronized motion and constant distances between the center car and both the anchoring cars would be necessary.

3. COMPUTATION OF THE DIRECTIONAL PATTERNS

31. *Electromagnetic Field of the Radiating Conductor*

A linear conductor in space, having a negligible diameter when compared with the length l, carries high frequency current and radiates electromagnetic waves. In the element ds of the conductor, the distance of which from the start of the conductor is s, at time t there is a current i and a charge q. The electromagnetic field at the point M (co-ordinates x, y, z of the left-hand rectangular system as in Fig. 3), the distance of which from ds is r, and at time t is given by the electric field $\mathbf{e}$ and the magnetic field $\mathbf{h}$ at that point and time, expressed in electromagnetic cgs units [8]:

$$\mathbf{e}(x, y, z, t) = -\frac{\partial}{\partial t}[\mathbf{a}(x, y, z, t)] - \nabla q(x, y, z, t), \quad (1)$$

$$\mathbf{h}(x, y, z, t) = \nabla \times \mathbf{a}(x, y, z, t), \quad (2)$$

where the retarded scalar potential q and the retarded vector potential $\mathbf{a}$ at M and t are given by

$$q(x, y, z, t) = c^2 \int_s^l \frac{q\left(s, t - \frac{r}{c}\right)}{r}\, ds, \quad (3)$$

$$\mathbf{a}(x, y, z, t) = \int_s^l \frac{\mathbf{i}\left(s, t - \frac{r}{c}\right)}{r}\, ds. \quad (4)$$

32. *The Sloping Rhombic Antenna*

Fig. 3 is a diagram of a sloping rhombic antenna, the conductors *1* and *4* of which are fed at the origin *0* of co-ordinates, with a phase difference of 180°, by the currents $\pm Ie^{j\omega t}$. The conductors *2* and *3* are terminated by the resistance R_c equal to the real part of the characteristic impedance of the conductors. The positive direction of the conductors is from 0 to R_c. The length of each conductor is l. The angles δ between the conductors and the axis OR_c is always positive. The plane of the antenna, is inclined to the ground plane (xy) at an angle ϑ; the height of the driving point O above the ground $(x_g y_g)$ is b. The distance from O to M, a distant point, is given by r_0, forming the angles ψ_1 and ψ_2 with conductors *1* and *4* respectively and the angle Θ with the axis z. The projection of r_0 on the plane (xy) is inclined to the axis x at an angle Φ, which is positive from $+x$ to $+y$ and negative from $+x$ to $-y$. The projection of r_0 on the vertical plane (xz) is inclined to the axis z at an angle ζ, which is positive from $+z$ to $+x$ and negative from $+z$ towards $-x$. At point M direct radiation from ds is received in the direction of r while energy reflected from the ground, with angle of reflection Θ, at point D_g reaches M in the direction r'. The ray r_0', radiated from O towards the point of reflection D_{og} is inclined to the conductors *1* and *4* at angles ψ_1' and ψ_2' respectively. M is sufficiently far that the angle of incidence and reflection at D_{og} is equal to that at D_g.

The following computation of the field strength of the electromagnetic radiation from a transmitting rhombic antenna suspended aslant above an imperfectly conductive ground has been worked out under the usual assumptions, viz. that the damping along the conductors and the mutual impedance of the conductors and between them and ground have been neglected. Consequently the characteristic impedance of the conductors is real (R_c) and the current in the element ds of the conductor at time t is

$$i = I_a e^{j\omega\left(t - \frac{s}{c}\right)}, \quad (5)$$

where $I_a e^{j\alpha}$ is the current at the starting point of the conductor.

33. *Direct Radiation*

The currents in elements ds of the conductors, the distance of which from the starts of the conductors is s, are according to (5):

$$\begin{aligned} i_1 &= I_{01} e^{j\omega\left(t - \frac{s}{c}\right)}, \\ i_2 &= I_{02} e^{j\omega\left(t - \frac{l}{c} - \frac{s}{c}\right)}, \\ i_3 &= -I_{03} e^{j\omega\left(t - \frac{l}{c} - \frac{s}{c}\right)}, \\ i_4 &= -I_{04} e^{j\omega\left(t - \frac{s}{c}\right)}, \end{aligned} \quad (6)$$

where the vectors $I_{01}\ldots$ have the magnitudes I_0 in the positive directions of conductors *1* ... The amplitude I_0 is held constant when the wavelength or the form of the antenna is changed.

The direction cosines of the antenna conductors are:

$$\begin{aligned} \cos(1x) &= \cos\delta \cos\vartheta = \cos(4x), \\ \cos(1y) &= \sin\delta = -\cos(4y), \\ \cos(1z) &= \cos\delta \sin\vartheta = \cos(4z). \end{aligned} \quad (7)$$

The direction cosines of the ray r_0 are:

$$\begin{aligned} \cos(\widehat{r_0x}) &\quad \sin\Theta\cos\Phi, \\ \cos(\widehat{r_0y}) &\quad \sin\Theta\sin\Phi, \\ \cos(\widehat{r_0z}) &\quad \cos\Theta. \end{aligned} \tag{8}$$

When (7) and (8) used, the angles between r_0 and the conductors are

$$\begin{aligned} \cos\psi_1 &\quad \cos(\widehat{r_0x})\cos(\widehat{lx}) + \cos(\widehat{r_0y})\cos(\widehat{ly}) + \\ &+ \cos(\widehat{r_0z})\cos(\widehat{lz}) \quad m + n + p, \\ \cos\psi_2 &\quad \cos(\widehat{r_0x})\cos(\widehat{4x}) + \cos(\widehat{r_0y})\cos(\widehat{4y}) + \\ &+ \cos(\widehat{r_0z})\cos(\widehat{4z}) \quad m - n + p, \end{aligned} \tag{9}$$

where

$$\begin{aligned} m &\quad \cos\Phi\sin\Theta\cos\delta\cos\vartheta, \\ n &\quad -\sin\Phi\sin\Theta\sin\delta, \\ p &\quad \cos\Theta\cos\delta\sin\vartheta. \end{aligned}$$

The distance between the point M and the antenna is great, compared with the dimensions of the antenna.

The components (produced by currents in the respective conductors) of the retarded vector potential at point M, the distance of which from the points ds on the conductors is r and from the point 0 is r_0, at time t will be computed from (4) by substituting from (6) and by using the following relations for distances of M from ds at $r_0 \gg l$:

conductor 1 ..... $r = r_0 - s\cos\psi_1$
conductor 2 ..... $r = r_0 - l\cos\psi_1 - s\cos\psi_2$
conductor 3 ..... $r = r_0 - l\cos\psi_2 - s\cos\psi_1$
conductor 4 ..... $r = r_0 - s\cos\psi_2$.

The influence of the difference $r_0 - r$ at $r_0 \gg l \geq \lambda$ on the amplitudes is only a small one, but it is very substantial upon the phase angles of $\boldsymbol{a}$. After integration and rearranging according to (12), the result in the first approximation will be

$$\begin{aligned} \boldsymbol{a}_1 &= \frac{l}{r_0} I_{01} e^{j\omega\left(t-\frac{r_0}{c}\right)} e^{-ju} \frac{\sin u}{u}, \\ \boldsymbol{a}_2 &= \frac{l}{r_0} I_{02} e^{j\omega\left(t-\frac{r_0}{c}\right)} e^{-j2u} e^{-jv} \frac{\sin v}{v}, \\ \boldsymbol{a}_3 &= -\frac{l}{r_0} I_{03} e^{j\omega\left(t-\frac{r_0}{c}\right)} e^{-j2v} e^{-ju} \frac{\sin u}{u}, \\ \boldsymbol{a}_4 &= -\frac{l}{r_0} I_{01} e^{j\omega\left(t-\frac{r_0}{c}\right)} e^{-jv} \frac{\sin v}{v}. \end{aligned} \tag{10}$$

where after substituting from (9):

$$\begin{aligned} u &= \omega\frac{l}{2c}(1-\cos\psi_1) \quad \pi\frac{l}{\lambda}(1-m-n-p) \\ v &= \omega\frac{l}{2c}(1-\cos\psi_2) = \pi\frac{l}{\lambda}(1-m+n-p) \end{aligned} \tag{11}$$

and

$$1 - e^{-j2u} = 2je^{-ju}\sin u. \tag{12}$$

A vertical plane, including the point M, ray r and the element ds of the radiating conductor is the plane of incidence .1, because it includes the ray r' from ds to the ground and reflected at D_g from the ground to M as well (see Fig. 3). When $r_0 \gg l$, the planes of incidence comprising various elements ds and the identical point M are nearly parallel to each other and to the vertical plane which includes 0, M and the ray r_0. It is necessary to divide the electric field of the radiation falling on the ground at the antenna into a component with a vector perpendicular to the plane of incidence and a component with a vector included in the plane of incidence; to each of these belongs a different coefficient of reflection from the ground. We therefore divide the direct radiation into these two components as well, and, furthermore, decompose the component with the vector in the plane of incidence into the radial component (with the vector in the direction of the ray) and the tangential component (with a vector perpendicular to the ray).

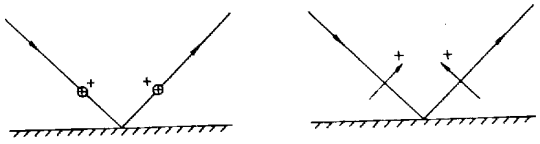

Fig. 4

The normal n to the plane of incidence has a positive direction according to the left part of Fig. 4 (i. e. into the paper) and direction cosines:

$$\begin{aligned} \cos(\widehat{nx}) &= -\sin\Phi, \\ \cos(\widehat{ny}) &= -\cos\Phi, \\ \cos(\widehat{nz}) &= 0. \end{aligned} \tag{13}$$

The line t perpendicular to r_0 and lying in .1 has a positive direction according to the right part of Fig. 4, and direction cosines:

$$\begin{aligned} \cos(\widehat{tx}) &= -\cos\Phi\cos\Theta, \\ \cos(\widehat{ty}) &= -\sin\Phi\cos\Theta, \\ \cos(\widehat{tz}) &= \sin\Theta. \end{aligned} \tag{14}$$

The component $\boldsymbol{a}_n$ of the retarded vector potential at M and t, perpendicular to .1, is the sum of projections of the components of the individual conductors from (10) on the normal n. The result of using (7), (13) and of rearrangement with the use of (12) will be:

$$\begin{aligned} \boldsymbol{a}_n &\quad (\boldsymbol{a}_1 + \boldsymbol{a}_3)[\cos(\widehat{nx})\cos(\widehat{lx}) + \cos(\widehat{ny}) \cdot \\ &\cdot \cos(\widehat{ly}) + \cos(\widehat{nz})\cos(\widehat{lz})] + (\boldsymbol{a}_2 + \\ &+ \boldsymbol{a}_4)[\cos(\widehat{nx})\cos(\widehat{4x}) + \cos(\widehat{ny})\cos(\widehat{4y}) + \\ &+ \cos(\widehat{nz})\cos(\widehat{4z})] = \boldsymbol{A}e^{j\omega t}\alpha l\sin\delta\left[\begin{matrix} m \\ \cos\Phi \end{matrix}\right. \cdot \\ &+ \cos\Phi(p-1)\Big] \end{aligned} \tag{15}$$

where

$$\boldsymbol{A} = j\frac{2l}{r_0} I_0 \frac{\sin u}{u}\frac{\sin v}{v} e^{-j\left(\omega\frac{r_0}{c} + u + v\right)} \qquad (16)$$
$$\alpha = 2\pi/\lambda.$$

The radial component $\boldsymbol{a}_r$ is the sum of projections on r_0 of components given by (10). By using (9) and rearranging with (12) we get:

$$\boldsymbol{a}_r = (\boldsymbol{a}_1 + \boldsymbol{a}_3)\cos\psi_1 + (\boldsymbol{a}_2 + \boldsymbol{a}_4)\cdot \cos\psi_2 = \boldsymbol{A}e^{j\omega t}\alpha l n. \qquad (17)$$

The tangential component $\boldsymbol{a}_t$ is the sum of projections of components according to (10) on t. By using (7), (14) and rearranging according to (12) we get:

$$\begin{aligned}\boldsymbol{a}_t = {} & (\boldsymbol{a}_1 + \boldsymbol{a}_3)[\cos(\widehat{tx})\cos(\widehat{1x}) + \cos(\widehat{ty})\cdot \\ & \cdot \cos(\widehat{1y}) + \cos(\widehat{tz})\cos(\widehat{1z})] + (\boldsymbol{a}_2 + \\ & + \boldsymbol{a}_4)[\cos(\widehat{tx})\cos(\widehat{4x}) + \cos(\widehat{ty})\cdot \\ & \cdot \cos(\widehat{4y}) + \cos(\widehat{tz})\cos(\widehat{4z})] = \boldsymbol{A}e^{j\omega t}\alpha l \cdot \\ & \cdot \frac{n}{\sin\Theta}\left(\frac{p}{\cos\Theta} - \cos\Theta\right)\end{aligned} \qquad (18)$$

The three respective components of the intensity of the electric field $\mathbf{e}$ at M and t of the direct radiation at $r_0 \gg l \geq \lambda$, will be determined from (1) by using (15), (17) and (18). After omitting the members occurring with higher than the first power of r_0, we get the following values of the vectors of components of the electric field:

$$\boldsymbol{E}_n = E_n j^{\prime n} = j\omega\boldsymbol{A}\alpha l \cdot \sin\delta[\cos\Phi(1-p) - \sin\Theta\cos\delta\cos\vartheta], \qquad (19)$$

$$\boldsymbol{E}_\Delta = E_\Delta e^{j\gamma_\Delta} = \boldsymbol{E}_t = j\omega\boldsymbol{A}\alpha l \cdot \sin\delta\sin\Phi(\cos\Theta - \cos\delta\sin\vartheta). \qquad (20)$$

where $\boldsymbol{A}$ is given by (16), $\boldsymbol{E}_r = 0$.

The component $\boldsymbol{E}_n$ of the field, perpendicular to Δ, has positive direction according to the left part of Fig. 4, the component $\boldsymbol{E}_\Delta$ in Δ has positive direction according to the right part of Fig. 4. Both components are in phase: the directly radiated wave is polarised linearly. The value of the total electric field at M and t of the direct radiation results from (19) and (20) after rearranging with the use of (9) and (11):

$$E = \sqrt{E_n^2 + E_\Delta^2} = \omega A\alpha l \cdot \sqrt{r^2\sin^2\psi_1 + u^2\sin^2\psi_2 + 2ur(\cos\psi_1\cos\psi_2 - \cos 2\delta)}. \qquad (21)$$

The magnetic field of the direct radiation would be determined by a similar process. It is polarised linearly, and in phase with the electric field; its vector is perpendicular to the vector of the electric field, and its value is $H = E/c$ [9].

34. Radiation Reflected by the Ground

Besides the electric field $\mathbf{e}$ at M and t from the direct radiation of the antenna, there is the field $\mathbf{e}'$ of the radiation reflected from the ground. From the element ds of the antenna conductor (e. g. conductor 1, Fig. 3), the very distant point M will be reached not only by the ray r radiated into the space in the direction inclined to the axis z at angle Θ, but also by the ray r' radiated towards the ground at the angle of incidence Θ and reflected towards M at the same angle Θ. When $r_0 \gg l$, the rays r' are nearly parallel to the ray $r_0' = OD_0 + D_0M$.

The direction cosines of the ray OD_0 are

$$\begin{aligned}\cos(\widehat{OD_0x}) &= \sin\Theta\cos\Phi, \\ \cos(\widehat{OD_0y}) &= \sin\Theta\sin\Phi, \\ \cos(\widehat{OD_0z}) &= -\cos\Theta.\end{aligned} \qquad (22)$$

The angle ψ_1' between the positive direction of the conductor 1 and the ray OD_0, and the angle ψ_2' between the positive direction of the conductor 4 and the ray OD_0 are given according to (7) and (22) and by comparison with (9):

$$\begin{aligned}\cos\psi_1' &= m + n - p = \cos\psi_1 - 2p, \\ \cos\psi_2' &= m - n - p = \cos\psi_2 - 2p.\end{aligned} \qquad (23)$$

The components of the retarded vector potential from the individual conductors of the antenna at time t and at the points of incidence D of the rays r' on the ground at distances $d' = \overline{DM}$, but prior to the reflection of the wave from the ground, are, according to (4) and after substituting from (6):

$$\begin{aligned}\boldsymbol{a}_{1d}' &= \int_{s=0}^{l}\frac{I_{01}}{d'}e^{j\omega\left(t-\frac{s}{c}-\frac{d'}{c}\right)}\,\mathrm{ds}, \\ \boldsymbol{a}_{2d}' &= \int_{s=0}^{l}\frac{I_{02}}{d'}e^{j\omega\left(t-\frac{l}{c}-\frac{s}{c}-\frac{d'}{c}\right)}\,\mathrm{ds}, \\ \boldsymbol{a}_{3d}' &= -\int_{s=0}^{l}\frac{I_{03}}{d'}e^{j\omega\left(t-\frac{l}{c}-\frac{s}{c}-\frac{d'}{c}\right)}\,\mathrm{ds}, \\ \boldsymbol{a}_{4d}' &= -\int_{s=0}^{l}\frac{I_{04}}{d'}e^{j\omega\left(t-\frac{s}{c}-\frac{d'}{c}\right)}\,\mathrm{ds}.\end{aligned} \qquad (24)$$

The component $\boldsymbol{a}_{nd}'$ of the retarded vector potential prior to the reflection from the ground, perpendicular to Δ, will be determined from (24) similarly as in the equation (15), the direction cosines of the normal to Δ being given by (13) and the direction cosines of the conductors by the equations (7). Similarly as in (17) will be determined the radial component $\boldsymbol{a}_{rd}'$ with the use of (23) and the tangential component $\boldsymbol{a}_{td}'$, which has positive direction as in the right part of Fig. 4 prior to reflection; the direction cosines:

$$\cos(\widehat{a_{td}'x}) = \cos\Phi\cos\Theta,$$

$$\cos(\widehat{a'_{td}x}) = \sin\Phi\cos\Theta, \qquad (25)$$
$$\cos(\widehat{a'_{td}z}) \quad \sin\Theta,$$

$\mathbf{a}'_{td}$ will be determined similarly as in equation (18) with the use of (7) and (25).

The three respective components of electric field intensity e'_d at D and t prior to reflection will be determined by substituting $\mathbf{a}'_{nd}$, $\mathbf{a}'_{rd}$ and $\mathbf{a}'_{td}$ in (1).

The complex coefficient of reflection of the electromagnetic wave from the ground is the ratio between the complex vector of the field of the reflected wave and the complex vector of the field of the incident wave. The coefficient of reflection of the wave component with the electric vector perpendicular to the plane of incidence is $\mathbf{K}_n \quad K_n e^{ix_n}$, the coefficient of reflection of the component with the electric vector in the plane of incidence is $\mathbf{K}_1 = K_1 e^{ix_1}$. Consequently, the components of the electric field at points D after reflection of the waves from the ground are

$$\mathbf{e}'_n \quad \mathbf{K}_n \mathbf{e}'_{nd}, \quad \mathbf{e}'_r \quad \mathbf{K}_1 \mathbf{e}'_{rd}, \quad \mathbf{e}'_t \quad \mathbf{K}_1 \mathbf{e}'_{td}. \qquad (26)$$

When computing the field of the wave reflected from the ground to the distant point M and at the time t, the components of the retarded vector potential of the reflected wave produced by the individual conductors at M and t will be determined by substituting $r' \quad \mathrm{d}s\overline{D} + \overline{DM}$ for d' into (24). When using (23), the values are:

conductor *1*

$$r' = \frac{b + s\cos\delta\sin\vartheta}{\cos\Theta}(1 + \cos 2\Theta) + r_0 - s\cos\psi_1$$
$$= r_0' - s\cos\psi'_1,$$

conductor *2*

$$r' = r_0' - l\cos\psi_1' - s\cos\psi_2',$$

conductor *3*

$$r' = r_0' - l\cos\psi_2' - s\cos\psi_1',$$

conductor *4*

$$r' = r_0' - s\cos\psi_2',$$

where: $r_0' \quad r_0 + 2b\cos\Theta$.

When $r_0 \gg l \geq \lambda$, the influence of the differences $r_0' - r'$ and $r_0' - r_0$ respectively will be small upon the amplitudes, but considerable upon the phase angles of $\mathbf{a}'$. After integration and rearrangement according to (12), a first approximation results in:

$$\mathbf{a}_1' = \frac{l}{r_0} I_{01} e^{j\omega\left(t - \frac{r_0}{c} - \frac{2b}{c}\cos\Theta\right)} e^{\quad jx'} \frac{\sin u'}{u'},$$
$$\mathbf{a}_2' = \frac{l}{r_0} I_{02} e^{j\omega\left(t - \frac{r_0}{c} - \frac{2b}{c}\cos\Theta\right)} e^{\quad i2x'} e^{\quad jx'} \frac{\sin v'}{v'},$$
$$\mathbf{a}_3' \quad \frac{l}{r_0} I_{03} e^{j\omega\left(t - \frac{r_0}{c} - \frac{2b}{c}\cos\Theta\right)} e^{\quad jx'} e^{\quad i2x'} \frac{\sin u'}{u'},$$
$$\mathbf{a}_4' \quad \frac{l}{r_0} I_{04} e^{j\omega\left(t - \frac{r_0}{c} - \frac{2b}{c}\cos\Theta\right)} e^{\quad jx'} \frac{\sin v'}{v'}, \qquad (27)$$

where with the use of (23), (9):

$$u' \quad \omega\frac{l}{2c}(1 \quad \cos\psi_1') \quad \pi\frac{l}{\lambda}(1 \quad m \quad n + p),$$
$$v' \quad \omega\frac{l}{2c}(1 \quad \cos\psi_2') \quad \pi\frac{l}{\lambda}(1 \quad m + n + p). \qquad (28)$$

Components $\mathbf{a}_n'$, $\mathbf{a}_r'$, $\mathbf{a}_t'$ of the reflected wave at M and t will be determined from (27) similarly as in (15), (17), (18), with the use of (7), (13), (23), (25), (28). Rearrangement with the use of (12) results in

$$\mathbf{a}_n' \quad \mathbf{A}' e^{j\omega t}\alpha l\sin\delta\left[\frac{m}{\cos\Phi} \quad \cos\Phi(p + 1)\right],$$
$$\mathbf{a}_r' \quad \mathbf{A}' e^{j\omega t}\alpha l n, \qquad (29)$$
$$\mathbf{a}_t' \quad \mathbf{A}' e^{j\omega t}\alpha l\frac{n}{\sin\Theta}\left(\cos\Theta + \frac{p}{\cos\Theta}\right),$$

where

$$\mathbf{A}' \quad j\frac{2l}{r_0} I_0 \frac{\sin u'}{u'}\frac{\sin v'}{v'} e^{-j\left(\omega\frac{r_0}{c} - \omega\frac{2b}{c}\cos\Theta + u' + v'\right)} \qquad (30)$$

The three respective components of the electric field $\mathbf{e}'$ at M and t of the wave reflected by the ground at $r_0' \gg l \geq \lambda$ will be determined from (1) by substitution from (29) with use of (26). After omitting the members occurring with a higher than first power of r_0', we get the following vector values of the components of the electric field of the reflected wave:

$$\mathbf{E}_n' \quad \mathbf{E}_n' e^{jx_n'} \quad \mathbf{K}_n j\omega\mathbf{A}'\alpha l \cdot$$
$$\cdot \sin\delta[\cos\Phi(1 + p) - \sin\Theta\cos\delta\cos\vartheta]. \qquad (31)$$

$$\mathbf{E}_1' \quad E_1' e^{jx_1'} \quad \mathbf{E}_t' \quad -\mathbf{K}_1 j\omega\mathbf{A}'\alpha l \cdot$$
$$\cdot \sin\delta\sin\Phi(\cos\Theta + \cos\delta\sin\vartheta), \qquad (32)$$

where $\mathbf{A}'$ is given by (30), $\mathbf{E}_r' = 0$.

Both field components of waves reflected from the ground generally have a different phase angle; this wave is elliptically polarised.

35. *The Total Radiation*

The complex vector $\mathbf{E}_{nc} \quad E_{nc}e^{j\xi_n}$ of the component of the total electric field at M and t, both direct and reflected radiation, perpendicular to the plane of incidence, will be determined as the sum of the vectors $\mathbf{E}_n$ and $\mathbf{E}_n'$ from equations (19), (31):

$$E_{nc} \quad \sqrt{E_n^2 + E_n'^2 + 2E_nE_n'\cos(x_n - x_n')},$$
$$\tan\xi_n \quad \frac{E_n\sin x_n + E_n'\sin x_n'}{E_n\cos x_n + E_n'\cos x_n'} \qquad (33)$$

The complex vector $\mathbf{E}_{\Delta c} = E_{\Delta c} e^{j\xi_\Delta}$ of the total field component at M and t, both direct and reflected radiation, lying in Δ, will be determined from (20), (32):

$$E_{\Delta c} = \sqrt{E_\Delta^2 + E_\Delta'^2 + 2E_\Delta E_\Delta' \cos(\nu_\Delta - \nu_\Delta')},$$
$$\tan\xi_\Delta = \frac{E_\Delta \sin\nu_\Delta + E_\Delta' \sin\nu_\Delta'}{E_\Delta \cos\nu_\Delta + E_\Delta' \cos\nu_\Delta'} \quad (34)$$

The vectors $\mathbf{E}_{nc}, \mathbf{E}_{\Delta c}$ are perpendicular to each other in space and generally have a different value and phase angle. The resulting electric field $\mathbf{e}_c$ is elliptically polarised; the end of the space vector $\mathbf{e}_c$ describes an ellipse with average angular frequency ω, but with periodically varying angular velocity. The plane of the ellipse is perpendicular to the ray and therefore to Δ.

The value e_c of the vector $\mathbf{e}_c$ is:

$$\varepsilon_c = [E_{nc}^2 \cos^2\omega t + E_{\Delta c}^2 \cos^2(\omega t + \xi)]^{\frac{1}{2}}, \quad (35)$$

where

$$\xi = \xi_\Delta - \xi_n. \quad (36)$$

The electric angle ωt_m, when $\mathbf{e}_c$ is at its maximum (i. e. in the position of the greater semi-axis of the polarisation ellipse) will be determined by taking

$$\frac{\partial \varepsilon_c}{\partial(\omega t)} = 0.$$

Wherefrom, after rearrangement:

$$\cos^2\omega t_m = \frac{1}{2}\left[\frac{E_{nc}^2 + E_{\Delta c}^2 - \cos 2\xi}{(E_{nc}^4 + E_{\Delta c}^4 + 2E_{nc}^2 E_{\Delta c}^2 \cos 2\xi)^{\frac{1}{2}}} + 1\right], \quad (37)$$

and

$$\cos^2(\omega t_m + \xi) = \frac{1}{2}\left[\frac{E_{nc}^2 \cos 2\xi + 2E_{\Delta c}^2}{(E_{nc}^4 + E_{\Delta c}^4 + 2E_{nc}^2 E_{\Delta c}^2 \cos 2\xi)^{\frac{1}{2}}} + 1\right]. \quad (38)$$

By putting (37), (38) into (35) we get the maximum value of the intensity of the resulting electric field at point M and at time t:

$$E_{c\max} = \sqrt{\tfrac{1}{2}\left(E_{nc}^4 + E_{\Delta c}^4 + 2E_{nc}^2 E_{\Delta c}^2 \cos 2\xi + E_{nc}^2 + E_{\Delta c}^2\right)}. \quad (39)$$

36. Directional Field Patterns

In short-wave long distance radio communication at a given state of the ionosphere, we get the best reception at a location lying in a certain direction and at a certain distance from the transmitting location by using a suitable carrier frequency. This selected frequency determines also the angle of elevation of the transmitted energy for reception at a given distance after reflection from the ionosphere. It is economical to concentrate the radiation from the transmitting antenna at this angular elevation and direction towards the receiver. It is, of course, impracticable continually to change the frequency and angular elevation according to the ionosphere changes. But at a chosen compromise frequency, it is necessary to respect the changes of the angle of elevation at least by the fact that the concentration of the radiated wave around the compromise angular elevation is not too sharp and that it includes all the changing directions of the optimum elevation. The dependence of the strength of reception, at a given linear performance of the receiving apparatus (without AVC, non-linear detection, etc.), upon the intensity of the electromagnetic field is approximately linear. It is therefore possible to judge the effect of the concentration of the radiated wave upon the strength of reception by studying the following two directional patterns of the transmitting antenna field:

1. *Vertical field pattern* in vertical plane including the transmitting and receiving locations; this pattern shows the dependence of the field strength at a constant distance upon the angular elevation.

2. *Azimuthal field pattern* at a constant elevation; this pattern indicates the dependance of the field strength at a constant distance and at a constant angular elevation upon the direction of transmission.

37. The Vertical Pattern

It is necessary that the maximum field or the maximum of the main lobe be in the direction of the required angular elevation; that the radiation be concentrated in a definite sector about the optimum angular elevation; and that the secondary lobes in other directions be small. In order to concentrate the maximum radiation in the direction towards the receiver, the sloping rhombic antenna is to be adjusted so that the vertical plane of symmetry of the antenna contains the direction towards the receiver and is, therefore, the plane of incidence Δ. In that plane $\Phi = 0$ or π.

From (11), (28) substituting ζ instead of $\pm\Theta$:

$$u = v = \pi\frac{l}{\lambda}[1 - \cos\delta\sin(\zeta + \vartheta)], \quad (40)$$

$$u' = v' = \pi\frac{l}{\lambda}[1 - \cos\delta\sin(\zeta - \vartheta)]. \quad (41)$$

From (19), (20), (31), (32), the result is:

$$\mathbf{E}_n = +\frac{8\pi c}{r_0} I_0 \frac{l}{\lambda}\sin\delta\frac{\sin^2 u}{u} e^{-j\left(\omega\frac{r_n}{c} + 2u\right)}, \quad (42)$$

$$\mathbf{E}_n' = +K_n\frac{8\pi c}{r_0} I_0 \frac{l}{\lambda}\sin\delta\frac{\sin^2 u'}{u'} e^{-j\left(\omega\frac{r_n}{c} + \omega\frac{2b}{c}\cos\zeta + 2u'\right)}, \quad (43)$$

$$\mathbf{E}_\Delta = 0, \quad \mathbf{E}'_\Delta = 0,$$

where the upper sign is valid for Φ 0, the lower for Φ π.

The total field vector $\mathbf{E}_{nc}$ will be determined by putting (42), (43) into (33) or by graphical addition of vectors $\mathbf{E}_n$, $\mathbf{E}'_n$. The direction of polarisation is perpendicular to A. The vertical pattern is made by indicating the amplitudes E_{nc} on the respective rays ζ.

By setting (42) equal to zero we get the equation for the direction of nulls of the vertical field pattern of the direct radiation:

$$\sin(\zeta + \vartheta) \quad \frac{1 - k\lambda/l}{\cos\delta}, \tag{44}$$

where k 1, 2, ...

There is a null in the direction of ζ $-\vartheta$ for integral values of l/λ.

The directions of lobes of this pattern will be determined by equating the first derivative to zero:

$$\frac{dE_n}{d\zeta} = 0.$$

From this we get the following conditions for the directions of the maxima:

1. $\tan u = 2u$,

2. $\zeta = \frac{\pi}{2} - \vartheta$.

The following equation results from the first condition:

$$\sin(\zeta + \vartheta) \quad \frac{1 - k'\lambda/l}{\cos\delta}, \tag{45}$$

where k' 0·371, 1·466, 2·48, etc. for the first (greatest), second, third, etc. lobes of the pattern [10], [11].

The direction of the diagonal of the rhombus (from the feeding point to the terminating point), given by the second condition, is generally the minimum. Both maxima of the main lobe unite in the direction of the diagonal, when:

$$\cos\delta = 1 - 0{\cdot}371\lambda/l. \tag{46}$$

The angle at which the maximum of the vertical field pattern of the direct radiation is in the direction of the diagonal, for variable l/λ is shown in broken line in Fig. 6.

This maximum, however, is not the greatest which the field of direct radiation in the direction of the diagonal can attain by varying δ at the given l/λ. Computation of the angle δ_m, at which setting the field in the direction of the diagonal reaches its maximum, is given in paragraph 42. The angle δ_m (Fig. 6) is to some extent greater than the angle resulting from equation (46), at which the vertical field pattern of the direct radiation is at its maximum in the diagonal. For δ_m the direction of this maximum will be a little deviated from the diagonal.

The nulls of the vertical field pattern of the reflected wave will be similarly determined by setting (43) equal to zero:

$$\sin(\zeta - \vartheta) \quad \frac{1 - k\lambda/l}{\cos\delta}. \tag{47}$$

Directions of the maxima of this pattern will be found by equating the first derivative to zero:

$$\frac{dE_n'}{d\zeta} \quad 0,$$

$$1.\ \sin(\zeta - \vartheta) \quad \frac{1 - k'\lambda/l}{\cos\delta}, \tag{48}$$

$$2.\ \zeta = \vartheta - \frac{\pi}{2}$$

where k' has the same values as in (45).

38. *Azimuthal Field Pattern at Constant Angular Elevation*

The azimuthal field pattern at constant angular elevation for the antenna of Fig. 1 is given by the absolute value of the electric field, $E_{c\max}$, as a function of Φ, with r_0, I_0 constant. The supplement Θ of the constant angular elevation above ground is constant as well. $E_{c\max}$ is given by equation (39) where the amplitude E_{nc} and the phase angle ξ_n of the component of the total electric field with the vector perpendicular to the vertical plane of incidence (which includes O and M) will be determined by addition of complex vectors $E_n e^{j\nu_n}$ and $E'_n e^{j\nu'_n}$, graphically or with the use of (33). Amplitude E_{1c} and phase angle ξ_1 will be determined by adding, graphically or with the use of (34), the complex vectors $E_1 e^{j\nu_1}$ and $E_1' e^{j\nu'_1}$; ξ is given by (36).

The amplitude E_n and phase angle ν_n of the component of the direct radiation field with the vector perpendicular to A and the amplitude E_1, as well as the phase angle ν_1 of the field component of direct radiation with the vector in A, are given by equations (19), (20), where A, χ are given by (16), u and v by relations (11).

The amplitude E'_n as well as the phase angle ν'_n of the field component of the wave reflected by the ground and having the vector perpendicular to A, and the amplitude E'_1 as well as the phase angle ν'_1 of the field component of the wave reflected by the ground and having the vector in A are determined by equations (31), (32); A' is given by (30), u' and v' by (28).

The polarisation of the field is elliptical with the exception of the case Φ 0, π, when it is linear with the vector perpendicular to A.

By equating (19) to zero we determine the directions of nulls of the direct radiation azimuthal field pattern with the vector perpendicular to Δ:

$$u = k\pi, \quad k = 1, 2, \ldots \tag{49}$$

$$v = k\pi, \tag{50}$$

$$\cos\Phi = \frac{\sin\Theta \cos\delta \cos\vartheta}{1 - \cos\Theta \cos\delta \sin\vartheta}. \tag{51}$$

Setting (20) equal to zero results in determination of nulls of the azimuthal radiation field with the vector in Δ. The first two conditions are the same as in (49), (50): the third condition is:

$$\Phi = 0, \pi.$$

The directions of nulls of the reflected wave field pattern with the vector perpendicular to Δ results from setting (31) equal to zero:

$$u' = k\pi, \tag{52}$$

$$v' = k\pi, \tag{53}$$

$$\cos\Phi = \frac{\sin\Theta \cos\delta \cos\vartheta}{1 + \cos\Theta \cos\delta \sin\vartheta}. \tag{54}$$

By equating (32) to zero we finally get the directions of nulls of the field of the reflected wave with the vector in Δ. The first two conditions correspond to (52), (53). and the third is:

$$\Phi = 0, \pi.$$

4. OPTIMUM ANGLES

41. Ground Reflection Coefficients

The reflection coefficients K_n and K_Δ are given graphically in Fig. 5. Fig. 5 presents as functions of the angle of incidence Θ: magnitudes K_n and K_Δ at the top; phase angles $\varkappa_n$ (right scale) and $\varkappa_\Delta$ (left scale) for different parameters σ/f (within the limits 1...50), where σ is the ground conductivity in electrostatic cgs units and f the transmitted frequency. Graphs on the left side are valid for ground dielectric constant $k_g = 20$ esu (which is possible with a well conducting ground); graphs in the center for $k_g = 10$ esu, and the ones on the right side are good for $k_g = 5$ esu (which occurs with poor ground conductivity).

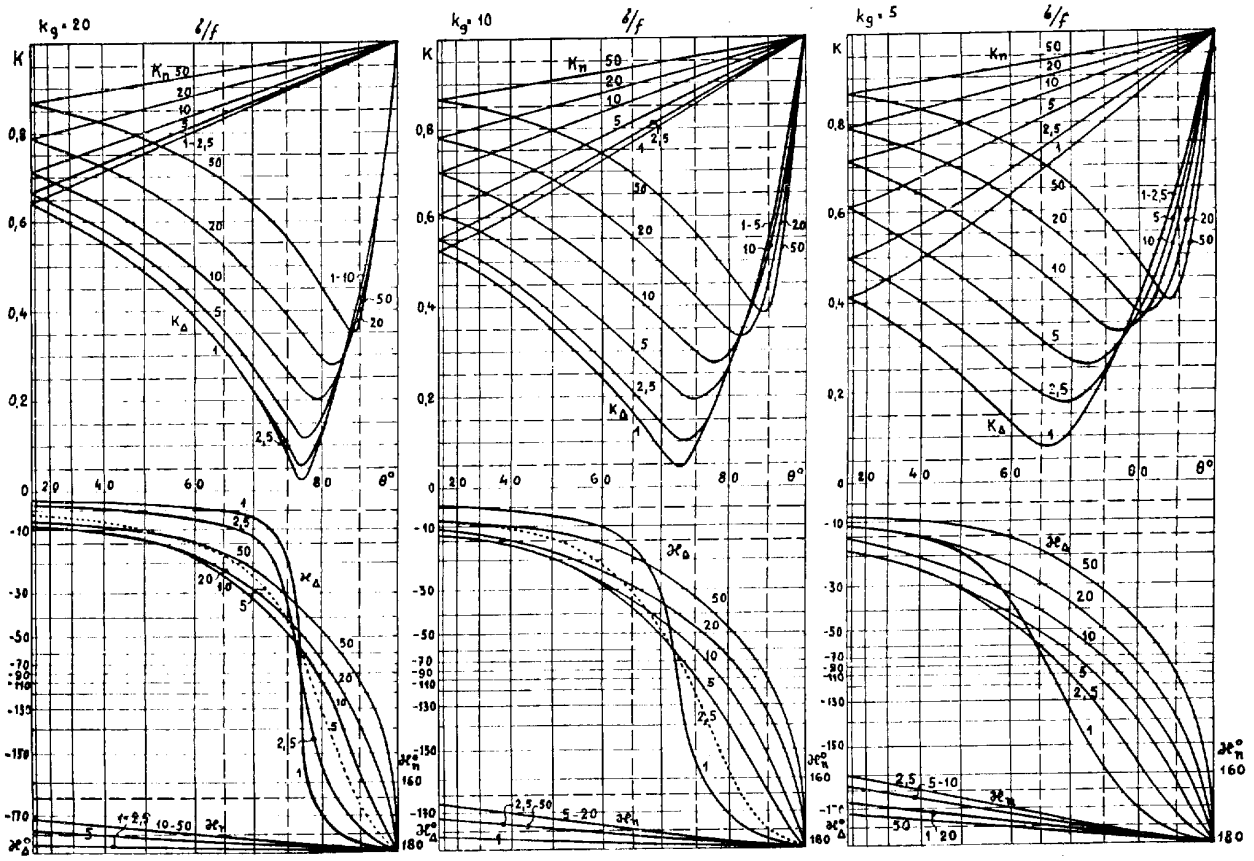

Fig. 5

The curves of Fig. 5 are based upon the fourteen graphs published in the paper by McPetrie [12], representing (in the complex plane) the real as well as the imaginary components of K_n, K_Δ for parameters Θ, σ/f, k_g. The curves of Fig. 5 within the

limits Θ 80°, ..., 90°, not included in McPetrie's graphs, have been computed with the use of modified Fresnel functions [12].

The electrical properties of the ground change with its geological structure as well as with its humidity and temperature; they are a function of frequency as well. According to measurements of ground samples to a depth of up to 3 meters, carried out by Smith-Rose [13], the conductivity at 10 Mc s was σ = (0·007, ..., 13). 10^8 esu, and the dielectric constant k_y 5, ..., 65. With humidity changes of 5 to 20%, σ becomes ten times, k_y five times higher. The humidity of the ground at its surface annually changes from 4% to 40%, approximately, while at a depth of 0·3 meters it generally does not fall under 16%. Short waves can only penetrate into the ground a few meters. With rising temperature, the increase in conductivity is 2, ..., 2·5% per 1° C. At the freezing point, the conductivity falls to one tenth, k_y to one third. The conductivity slowly rises from 1 to 10 Mc s and more quickly above 10 Mc s, while the dielectric constant falls slowly to 10 Mc s and remains almost constant above that frequency.

Fig. 5 shows clearly how great is the influence of ground conductivity with usual angular elevations, i. e. from 3° to 30° approximately, upon the amplitude and phase angle of the reflection coefficient of the wave component, polarized in the vertical plane of incidence. With the horizontally polarized component, i. e. in the direction of the concentrated radiation, such variations are considerably lower, but at 30° differences in the amplitude $K_{\perp}$ may be some tens of per cents, even in this case. Such variations usually result mainly from the changes of the humidity of the ground and from frost.

At low angular elevations and low σf, the vertically polarized component undergoes a phenomenon resembling Brewster's wave incidence on a boundary of two perfect dielectrics ($\sigma = 0$). Brewster's incidence occurs at the angle of incidence Θ_B given by the relation

$$\tan\Theta_B = n$$

where n is the index of refraction. In that case, the component polarized in the plane of incidence is annulled. In the case of ground with low conductivity the index of refraction is nearly n $\sqrt{k_y}$; with k_y 20 or 5, and σf 1, an incidence could occur, similar to Brewster's at Θ'_B 77° or 66° respectively, showing minima of $K_{\perp}$ (see Fig. 5). At the same time in such incidences $\varkappa_{\perp} = \pi$ 2 with inversion of the phase angle of the reflection coefficient the more rapid, the smaller is σf and the greater k_y. It can be clearly seen from Fig. 5 how advantageous is horizontal polarization of the transmitted wave.

As changes of σ depend upon weather, it is advantageous to concentrate the radiation at low elevations above the ground in order to minimize the magnitude changes of the reflection coefficient of the horizontally polarized waves. The value of the ground reflection factor, especially at high σf and k_y, approaches the extreme value $K_{\perp}$ 1 at the same time.

42. Optimum Angles of the Rhombus

The value of the field strength of direct, as well as of reflected waves in the direction of the main lobe, and the angular elevation of that direction depend, for given length of the antenna conductors and given wavelength upon the values of the angles of the rhombus; height of the feeding point above the ground; slant of the antenna with respect to ground; and partially upon the electrical properties of the ground near the antenna. The sloping plane of the antenna results in lower angular elevation of the main lobe and, consequently, in lower influence of the height of the feeding point upon the difference in phase angle of the direct and reflected waves in the direction of the main lobe; furthermore it results in lowering the influence of the ground properties. Finally, the contribution of the reflected waves in that direction will be reduced. For these reasons it is roughly possible to suppose the setting of the apex angles of the rhombus to be the main factor influencing the value and the elevation of the maximum field. It is therefore also suitable to assume for the first approximation such apex angles, at which the direct radiation field reaches its maximum value to be optimum. The direction of this maximum is roughly the diagonal of the rhombus from the feeding point to the terminating point.

The amplitude of the direct radiation field in the direction of the diagonal of the rhombus will be determined from equation (42):

$$E_{\perp} \quad K \sin^2 u \left] \frac{\sin\delta}{\cos\delta} \right. \tag{55}$$

where $u = \pi \frac{l}{\lambda} (1 - \cos\delta)$. K is a constant factor.

For determining the condition when the maximum of the direct radiation field is in the direction of the diagonal with varying δ we take

$$\frac{dE_{\perp}}{d\delta} \quad 0.$$

From this, half the apex angle, δ_m, for which the direct radiation field in the direction of the diagonal is maximum, will be computed from the relation:

$$\tan\left(\alpha l \sin^2 \frac{\delta_m}{2}\right) \quad \alpha l \sin^2\delta_m. \tag{56}$$

The optimum angles δ_m for different values of l/λ were computed from (56) and shown in Fig. 6. The angular elevations of these maxima of the direct radiation field, resulting from setting δ_m according to this curve, can be seen in Fig. 2, lower part.

For a more exact computation it is necessary to take into account the waves reflected from the ground near the antenna. For the antenna proposed in this paper, having the dimensions as indicated in paragraph 22 and in Fig. 2, and assuming approximately that $K_u = 1$, angles of the rhombus for different l/λ have been computed, at which the total direct as well as reflected wave fields in the vertical plane of symmetry are maximum. Fig. 6 includes these angles δ'_m, too. The respective elevations $90° - \Theta_m$ and the relative amplitudes E_{mr} of these maxima (compared to the amplitude at $l/\lambda = 1$, see the right scale) are comprised in the same figure.

From the fundamental theory of the horizontal rhombic antenna [14] we know the following conditions for the maximum field to be in the vertical plane of symmetry of the antenna assuming $K_u = 1$:

$$\alpha l \sin^2\delta = \pi, \quad \frac{H}{\lambda} = \frac{1}{\sin\delta},$$

where H is the elevation of the antenna above the ground surface and the angular elevation of the maximum lobe equals δ. The half-apex angle δ_{mh} for different l/λ computed herefrom is included in Fig. 6 as well.

The values of the optimum apex angles of the rhombus for the proposed antenna are between the values for which the direct radiation field is maximum, and the values stipulating the maximum field with the horizontal rhombic antenna. By adjusting these optimum angles for each wavelength used it is possible to obtain the maximum field throughout the entire waveband in which the antenna is used, e. g. throughout the short-wave band.

43. *Angular Elevation of the Maximum Field*

As mentioned above, the maximum field of the direct radiation in the direction of the diagonal of the rhombus from the feeding point to the terminating point of the antenna is attained by adjusting the apex angles of the rhombus according to the δ_m curve in Fig. 6. The angular elevations ϑ of these maxima with the antenna according to Fig. 2, as a function of δ may be interpreted from the bottom diagram of Fig. 2. For $l/\lambda = 2, \ldots, 6$ in this case, ϑ is between 16° to 13°, i. e. practically without any change.

With the horizontally suspended rhombic antenna the angular elevation of the maximum field is usually equal to δ, i. e. from 30° to 17° at $l/\lambda = 2, \ldots, 6$; see the curve δ_{mh} in Fig. 6.

However it is necessary to consider the ground-reflected radiation as well. With the antenna of Fig. 2, the optimum angles of the rhombus are then given by the δ'_m curve, and the angular elevations of the maximum field by the curve of $90° - \Theta_m$, both in Fig. 6. The angular elevation of the maximum field with the proposed antenna within the limits $l/\lambda = 2, \ldots, 6$ will, therefore, be from 15° to 4°, i. e. from one half to one quarter of the angular elevation obtainable with the horizontal antenna. Even when the proposed antenna is used with its dimensions reduced by one half, the angular elevation in the same waveband ($l/\lambda = 1, \ldots, 3$) is from 25° to 10°, i. e. about 5° lower than with the horizontal antenna. Some of the advantages of lower angular elevations have been mentioned previously in this paper. Besides, these low angular elevations suit actual communication better as they correspond to suitable angles of incidence of the transmitted waves on the ionosphere at the wavelength determined by its parameters and the distance to the receiving point. With the horizontal rhombic antenna the radiation at angles higher than that of the maximum lobe, and possibly most of the radiated energy about this angular elevation, will go through the ionosphere; with the proposed antenna the main lobe will be reflected by the ionosphere even for angles greater than that of the maximum field. This will improve the efficiency of transmission as well

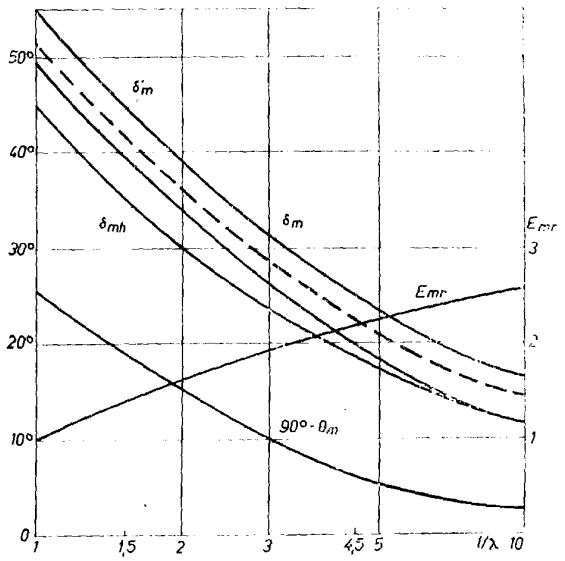

Fig. 6

as the regularity of reception, because with variations of the ionosphere the rays on both sides of the maximum field will still be of use.

It is necessary to suspend the horizontal rhombic antenna high enough so that the projection of twice the height of the masts in the direction of the maximum field will be roughly half the wavelength used. In that case the phase difference between direct and reflected waves in the direction of the maximum radiation is not too great and, therefore, the reflected wave substantially contributes to the total value of the field. It would, therefore, be necessary to suspend the horizontal rhombus higher than usual in order to diminish the angular elevations. With the proposed antenna, on the other hand, it is possible to lower the feeding point relative to the horizontal rhombus even with lower angular elevations, because of the contribution given by the difference $2u' - 2u$ to the phase angle of the reflected wave due to the sloping suspension. With the antenna dimensions of Fig. 2, the direct and reflected wave in

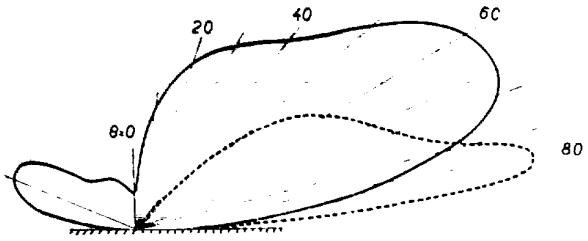

Fig. 7

all elevations of the maximum field will be approximately in phase throughout the entire range $l/\lambda = 1 \ldots 10$. That is because within these limits the projection of twice the height of the feeding point in the direction of the maximum field remains practically one quarter of the wavelength used, and $2u' - 2u$ is nearly $\frac{\pi}{2}$. Also, for this reason, the efficiency of the proposed antenna will be improved as against the horizontal rhombic antenna, mainly on the longest wavelengths used.

44. *Computed Field Patterns*

From the relations in paragraph 37 vertical field patterns have been computed for the proposed antenna of dimensions as indicated in paragraph 22 and Fig. 2; at apex angles adjusted according to the δ_m curve of Fig. 6, and at assumed ground constants $\sigma = 5 \times 10^7$ esu and $k_g = 15$. In Fig. 7, the most unfavourable of these field patterns, at $l/\lambda = 1$ ($\lambda = 50$ m), is marked in full line, and the main lobe of the pattern at $l/\lambda = 3$ (λ approx. 17 m) in dotted line. The sloping planes of the antenna for both of these cases are drawn in dot-dash line.

The azimuthal field patterns of the proposed antenna according to Fig. 2 at constant angular elevation equal to the angular elevation of the maximum

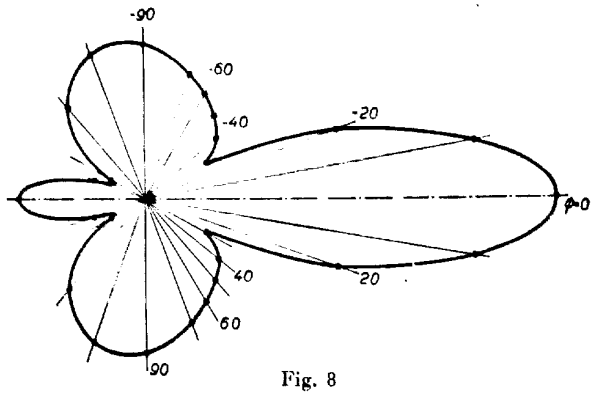

Fig. 8

lobe in the vertical field pattern and at apex angles adjustment and ground properties as mentioned above, have been computed by the method described in paragraph 38. Fig. 8 presents the most unfavourable directional diagram ($l/\lambda = 1$) at angular elevation of 23°. Fig. 9 gives the shape of the main lobe and of the secondary front lobes at l/λ 3 and at angular elevation of 10°.

45. *Suitable Angular Elevations of the Maximum Field in Traffic*

From the graphical predictions of the ionosphere conditions, as published by the National Bureau of Standards valid for a period approximately midway

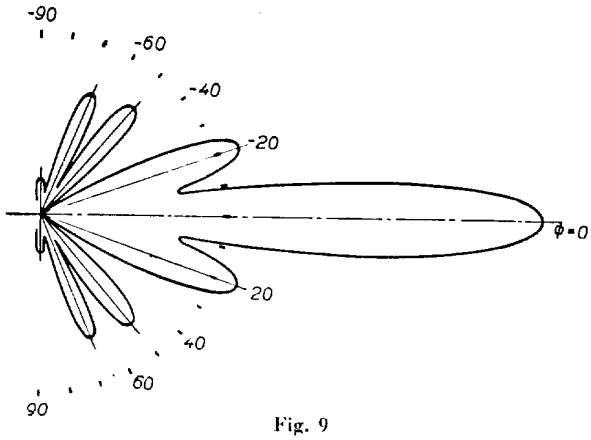

Fig. 9

between the maximum and the minimum of solar activity, virtual heights of the F (or F_2) layer were computed for angle of wave incidence on that layer of about 70° (angular elevation about 3°) and for waves slightly above the critical wavelength.

For communication over distances of from 1000 to 6000 km, i. e. also with lower angles of incidence in that range, the virtual heights thus determined were considered constant. Although the virtual height increases with diminishing angle of incidence, still in communication over shorter distances, where the angle of incidence diminishes, longer waves are used, which reduces the virtual height. With the use of these virtual heights, limiting angles of incidence on the F (F_2) layer were determined from the said graphs, and therefrom the limiting angular elevations of the radiated waves for four typical states of ionisation. The limiting angular elevations thus determined are drawn in Fig. 10 (left scale) in thick lines, as a function of wavelength. The symbols are: *DS* summer noon, *DW* winter noon, *NS* summer midnight, *NW* winter midnight. For these four states of ionisation, scales of distance of communi-

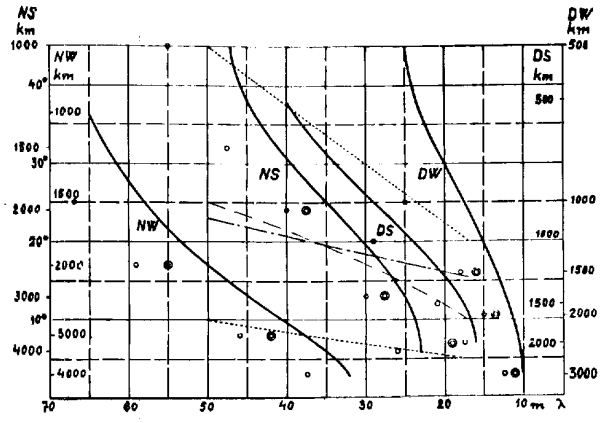

Fig. 10

cation (for one reflection of the wave from the layer F), corresponding to the scale of angular elevations, are at the sides of the graph. Circles to the left of each curve of limiting angular elevations indicate suitable wavelengths for communication (at the respective ionisation) over distances according to the corresponding distance scale at one F layer reflection; double circles indicate suitable wavelengths at two F layer reflections and one ground reflection. So, e. g., at summer midnight, for communication over 4000 km at one F layer reflection, the suitable wavelength was 26 m and its suitable angular elevation was 6° (limiting angular elevation 13°); at two F layer reflections, the suitable wavelength was 37·5 m and the angular elevation 24° (limit 27½°).

Furthermore, Fig. 10 contains, drawn in dot-dash line, the angles of inclination (for the waveband 17. .... 50 m) of the plane of the antenna; dotted lines indicate approximate angular elevations at which the field intensity of the antenna reaches 70% of the maximum field, as interpreted from diagrams of Fig. 7, for wavelengths of 50 m and 17 m only. The angular elevations of the maximum field for adjustment of angles according to the curves δ'_m in Fig. 6, are drawn in broken line. It is evident that the favourable angular elevations of almost all wavelengths suitable for communication over distances 1000. .... 6000 km in the considered waveband lie between both of the dotted lines, so that the field in the vertical plane of incidence in direction of the favourable angular elevation has at least 70% of the maximum lobe of the antenna. Only on winter nights the proposed antenna of dimensions quoted would be less convenient, because then longer waves and lower angular elevations would be more suitable.

From Fig. 10 is evident how important it is that the vertical field pattern of the proposed antenna be less sharp. So, e. g. the favourable angular elevation for wavelengths 46. .... 47·5 m for summer midnight was 32°, for winter midnight 8°. Fig. 10 shows at the same time how advantageous is the reduction of angular elevation of the maximum field of the proposed antenna with its adjustment for shorter wavelengths. The foregoing consideration principally explains the advantages of the proposed antenna concerning the favourable angular elevations of the radiated waves, even when the actual circumstances will be much more complex. So, e. g. vertical concentration of the radiation to lower angular elevations than about 15°. .... 20° can be reached only with very big and complicated directional arrays. But because the angular elevation of such concentration with these complicated arrays not only cannot be adjusted with wavelength, but can change itself to a great extent, in consequence of the differences of electrical properties of the ground near the antenna, due to meteorological changes, such concentration with these arrays is generally unfavourable to the security of traffic. On the other hand, the automatic control of the maximum lobe angular elevation with adjustment of the angles of the proposed antenna for different wavelengths approximately corresponds to actual requirements. The sloping suspension of the antenna diminishes the influence of the ground-reflected wave and thus also the influence of the mentioned uncontrollable changes of the ground properties.

5. CONTROLMEASUREMENT

51. Method of Measurement

The computation of directional properties of an antenna suspended aslant was controlled by measuring the vertical and azimuthal field patterns of a scale model of the antenna. Dimensions of the ori-

gnal antenna were chosen as follows: length of conductors l 50 m; height of the mast 23 m; elevation of the feed point 2·5 m; radius of rails 100 m; angles of the rhombus adjusted for wavelength λ 50 m ($l/\lambda = 1$, $\delta = 55°$, $\vartheta = 20°$), i. e. for the most unfavourable case considered. The scale model was constructed for $\lambda = 3$ m; i. e. all dimensions mentioned were reduced in the ratio of $\frac{\lambda}{50}$.

hauled by a rope to different elevations h above the ground, the distance r_0 between the center of the measuring antenna and the feed point O of the model being, within limits, about $4{\cdot}3 \ldots 5{\cdot}7\lambda$ (at angular elevation 40°). The values of field intensity measured at different r_0 were corrected for $r_0 = 13$ m. During this measurement, the measuring antenna was perpendicular to the vertical plane of symmetry

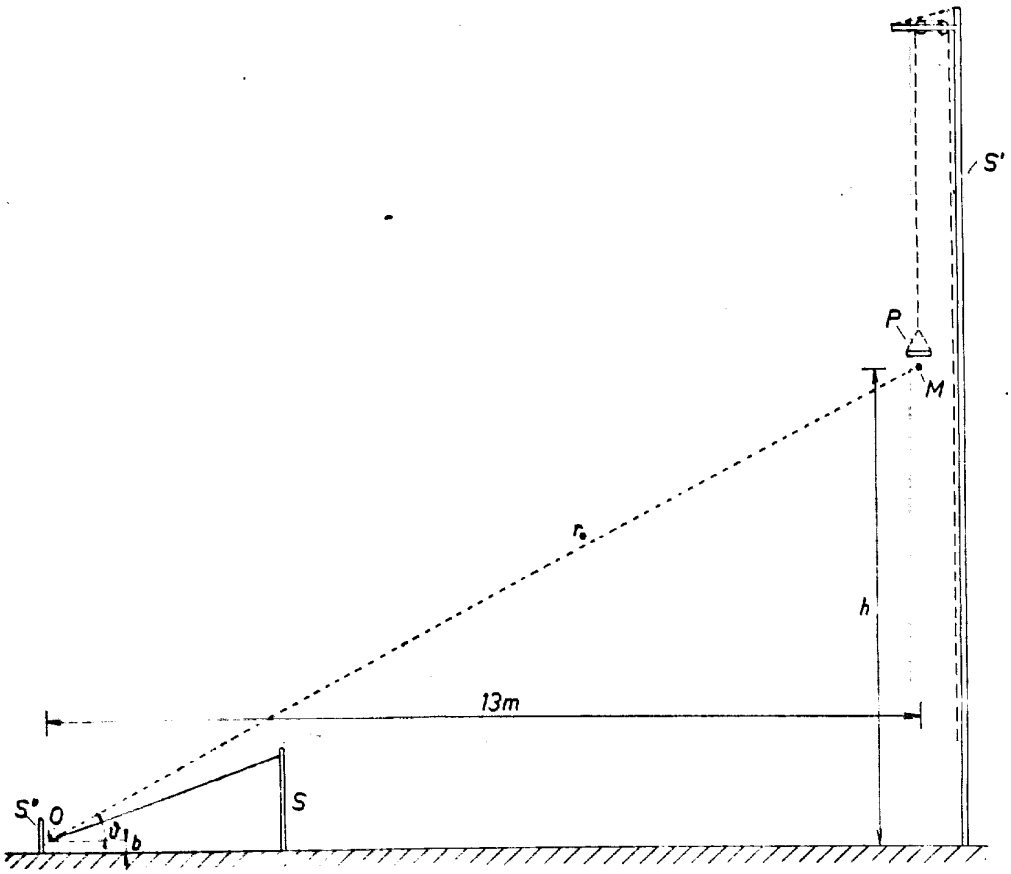

Fig. 11

The method of field measurement of this scale model is shown in Fig. 11. The model was suspended on a pole S, fastened with ropes to poles S'' and fed by an oscillator at the point O. In the vertical plane of symmetry of the model and at ground plane distance about 13·5 m from O was a 12 m high mast S' on which the field measuring apparatus was suspended by means of pulleys fixed on a horizontal beam at the top of the mast S'. The apparatus comprised a measuring antenna M and a meter P (a thermocouple and a galvanometer). The distance between the ground plane projection of the measuring antenna and the ground plane projection of O for the arrangement drawn in Fig. 11 (while measuring the vertical field pattern) was 13 m.

When measuring the vertical field pattern of the scale model antenna, the measurement setup was

of the model. Deflection of the meter was read by means of a mirror and a telescope.

The measurement of the azimuthal field pattern at constant angular elevation required turning the model antenna (together with the oscillator) around the pole S and hauling the measurement setup to such elevations that the line between the center of the antenna M and O be inclined to the ground at a constant angle of elevation. This method is opposite to the usual measurements of directional patterns of actual antennas, where a measuring setup is moved in a circle around the fixed antenna.

52. The Scale Model of the Antenna

The scale model of the antenna is a rhombus with legs 3 m long; one apex, non-conductively suspended

on a pole at an elevation 1·4 m above ground, is terminated by a resistance equal to the characteristic impedance of the conductors. The opposite apex, non-conductively suspended on a peg at a height of 15 cm, is connected to the output terminals of the

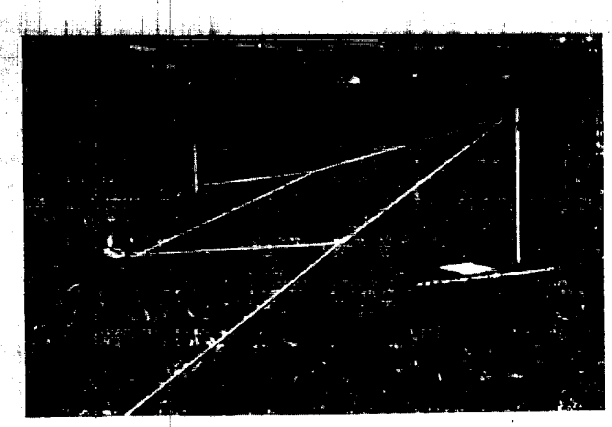

Fig. 12

oscillator. Both remaining apexes are stretched by means of ropes and pegs so that the apex angle of the rhombus at the pole be twice 55° and the antenna conductors lie in a plane inclined to the ground at an angle of 20°.

In Fig. 12 the scale model of the antenna can be seen, suspended on the pole and stretched by the ropes. The terminating resistance is seen at the top of the pole and the oscillator at the left-hand edge of the picture.

The value of the terminating resistor was found by measuring the real part of the input impedance of the antenna terminated by the chosen resistor,

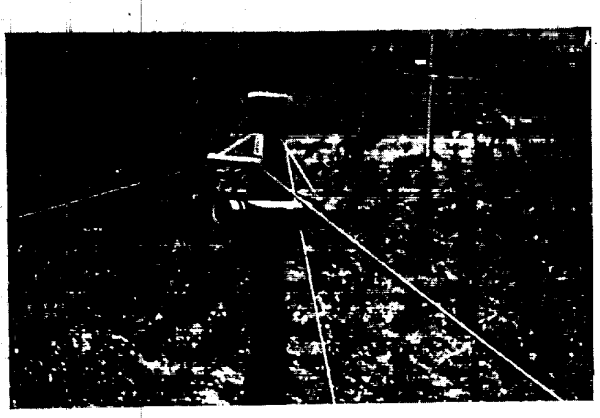

Fig. 13

using the substitution method, at different frequencies in a broad band around 100 Mc s. Then the value of the terminating resistance was changed and the measurement repeated, till the real part of the input impedance was practically constant. Fig. 13 shows the connection of the terminating resistor to the scale model of the antenna; the measuring setup can be seen in the background.

53. *The Oscillator*

The 100 Mc/s measuring oscillator was constructed to have adequate frequency stability and so that its output could be controlled and kept constant. A push-pull oscillator with two tubes TC04/10 was used. The grid circuit was a $\frac{1}{4}\lambda$ Lecher wire line consisting of two copper tubes, shorted at one end and connected to the cathodes by a 1500 Ohm resistor. At an appropriate distance from the shorted end the line was tapped and connected with the grids of the tubes through very short connecting strips. The

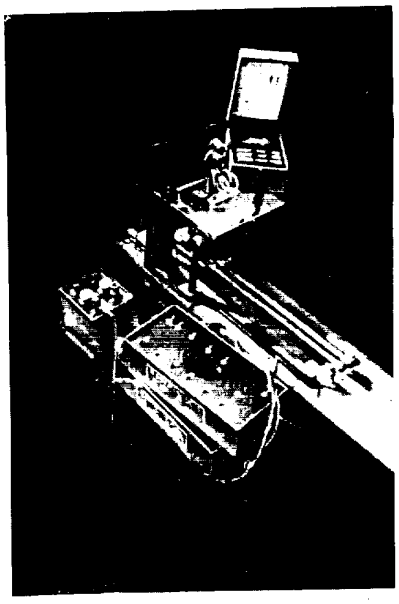

Fig. 14

lengths of the line and the grid taps were chosen so that the power output be maximum. The push-pull anode circuit, mounted on a polystyrene plate, was tuned by a condenser and inductively coupled to the antenna; the coupling was variable. The antenna current was measured by a R. F. ammeter and, during measuring, held constant by varying the coupling. The oscillator output at 100 Mc/s was about 1 W.

The oscillator can be seen in Fig. 14. On the wooden base are two porcelain insulators carrying the Lecher line, the length of which is read on a dial in the middle of the right-hand side of the base. Parallel to the Lecher line are wooden ledges supporting the wooden stand carrying the oscillator. The stand carries a horizontal polystyrene plate, in the middle of which can be seen two turns of the anode circuit

coil and between them the coupling link connected to the output terminals, which stand on insulators at the top right-hand side of the vertical board of the stand. The output coupling is changed by turning

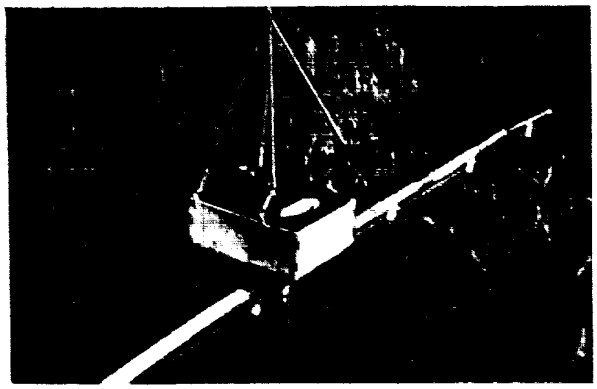

Fig. 15

the coupling coil by means of the knob at the left-hand corner of the polystyrene plate. Under its front corner is the dial knob of the anode tuning condenser. Right from this knob on the tubes can be seen the tapping rings with short copper strip connections to the grid terminals of the tubes, which are mounted under the polystyrene plate. When changing the tap positions on the quarter-wave resonant line the whole stand is moved on the wooden ledges

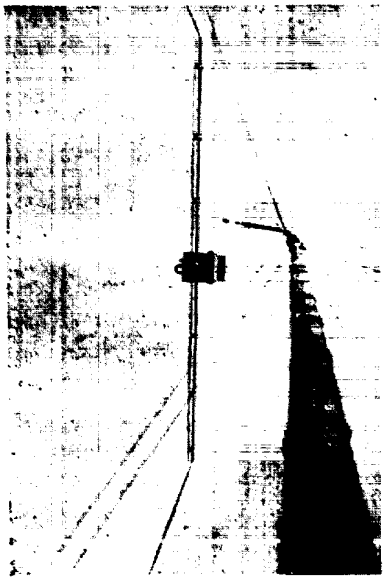

Fig. 16

and its position is read on a dial seen in the left-hand part of the front ledge. In the right side of the stand is the output current meter, at the front of the oscillator the filament battery and the anode battery.

54. The Measuring Setup

Figs. 15 17 show the setup used for measuring the electromagnetic field. On insulators under the bamboo stick, is the half-wave dipole, constructed of copper tubing; stiff copper wires, which tightly fit the ends of the tubing, provide for tuning the antenna to resonance at the oscillator frequency. In a stirrup fixed under the case carrying the galvanometer is the bamboo stick slipped on a bolt so that it can rotate (see Figs. 15 and 17); by pulling the ropes fastened to the ends of the stick, the antenna can be inclined in a vertical plane (see Figs. 16 and 17). To the center of the antenna a thermocouple element is connected by short leads, fastened to the bottom of the galvanometer case, to the terminals of which is connected the output from the thermo-

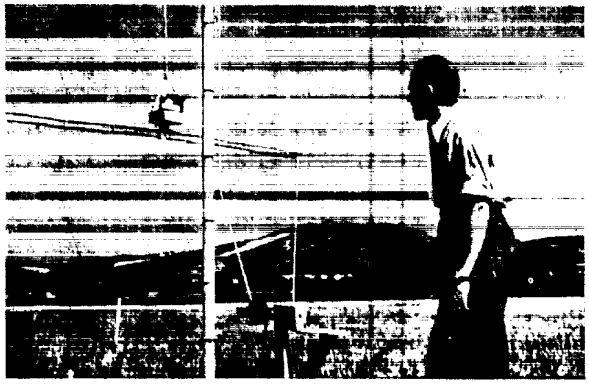

Fig. 17

couple. The terminals can be seen on the left-hand side of the case, Fig. 16.

The crystal detector on the one hand, and the diode detector on the other hand, were tried instead of the thermocouple element. The crystal detectors failed partly because of their instability, partly because in connection with the galvanometer used they were less sensitive than the thermocouple element. The diode detector was then tested. A KB2 diode was operated at the bend of its characteristic in order to keep its initial sensitivity as high as possible. The no-signal anode current flowing through the galvanometer was, by means of a potentiometer, exactly compensated by a bucking current from a battery. The filament, anode and compensating voltages were supplied by a tapped dry battery, fastened to the galvanometer case. This method has also been abandoned because the diode in connection with the galvanometer used was generally less sensitive than the considerably simpler combination with the thermocouple element; besides, the indication again was unstable. After this experience, for

all actual measurements the Western Electric 2·5 mA (maximum current) thermocouple element was used in connection with a sensitive unipivot galvanometer by the Cambridge Instrument Co. The thermocouple element with galvanometer was calibrated with D. C. current and it was found that its characteristic was square law, with sufficient precision. Because the galvanometer must be used in a horizontal position with its scale upwards, the meter needle deviation was read from below by means of a slanted mirror (see Figs. 15 and 17). At greater elevations of the measuring setup, an 8 times enlarging telescope was used for reading.

The measuring setup was suspended on a hempen rope, lead over pulleys on a horizontal beam at the top of the mast (one pulley at the center of the beam, the second at the end of the beam nearest to the mast, see Fig. 16) and back along the mast to the winch (Fig. 17), by means of which the elevation of the antenna center above the ground was changed. This elevation was indicated by means of metal marks fastened to the rope at 1 m intervals; if the antenna was horizontal during the measurement the elevation was also indicated by similar marks fitted to the ropes fastened to the ends of the bamboo stick. These ropes served to turn and fix the antenna in such a position, that the galvanometer reading was maximum, i. e. in the direction of the electric field vector when measuring the vertical pattern and in the direction of the major axis of the electric field polarisation ellipse when measuring the azimuthal pattern at constant angular elevation. All remaining ropes seen in Fig. 16 served as the mast anchors. The mast was made from two bamboo sticks 6 m long (the black connecting flange of which is seen in Fig. 16) and anchored by three ropes from the top and from the point of connection respectively. The pole for suspending the scale model of the antenna is seen in Fig. 17 in the left background, behind the mast.

55. *Results of Measurements*

After finishing the preparatory work (construction of the oscillator; construction of the scale model of the antenna and ascertaining the correct value of the terminating resistor; construction of the mast for supporting the measuring setup; testing the suitability of this setup) the rough orientation measurement of the scale model radiation field was carried out first, in the factory yard. Unevenness and unhomogenity of the ground and the proximity of factory buildings, of course, unfavourably influenced the results. Further exact measurements were then carried out in a large field in the broad flat valley of the river Berounka near Zbraslav. The nearest obstacles (trees) were about 100 m distant from the spot of measurement; a high tension line at a distance several times bigger. At that time there were heavy frequent rains and the ground was rather damp so that on days immediately following the rains it was sometimes impossible to carry the material in a car by the field road to the test location.

The following table contains results of measurements on the vertical field pattern of the scale model of the antenna. For different heights h of the center of the measuring antenna above ground and the distances r_0 from the feed point of the antenna model computed from them, and the angular elevations $\frac{\pi}{2} - \Theta$ of the rays r the galvanometer readings α are given. The amplitudes of the field are proportional to the square roots of these readings. These were reduced to the constant distance $r_0 = 13$ m and divided by such a factor that the field in the direction of the theoretical maximum of the vertical pattern ($\Theta = 60°$) be $E_{red} = 1{\cdot}12$ (the computed direct radiation field in the direction of the axis of the antenna was considered equal to 1).

Table I.

h (m)	r_0 (m)	$90° - \Theta°$	$\sqrt{\alpha}$	$\sqrt{\alpha} \cdot r_0/13$	E_{red}
1	13·05	4	0·3	0·55	0·26
2	13·15	7½	1·3	1·15	0·55
3	13·35	12½	2·1	1·48	0·71
4·2	13·65	17½	3·5	1·96	0·94
6·6	14·55	26½	4·1	2·26	1·08
8	15·2	31	4·0	2·34	1·12
9·6	16·1	36	3·6	2·35	1·12

The reduced amplitudes of the field were drawn in the corresponding directions Θ and indicated by circles in the upper part of Fig. 18, where the pattern computed for the model antenna is drawn in heavy line, assuming the average ground conductivity was $\sigma = 10^8$ esu and dielectric constant 20 at 100 Mc/s, and using the values of the reflection coefficient from Fig. 5. The consistent deviations of measured values compared with the computed ones in directions of low angular elevations indicate that the conductivity of the ground with the model antenna was somewhat greater than assumed. During this measurement it was ascertained by inclining the measuring antenna in a vertical plane and by rotating it in the horizontal plane that the galvanometer reading was greatest when the measuring antenna was perpendicular to the vertical plane of symmetry of the scale model, i. e. that the electric vector of the field was perpendicular to it.

Further the main lobe of the directional field pattern of the scale model antenna was measured at the constant angular elevation above ground, 30°, at

which the field in the vertical plane of symmetry of the model is roughly maximum.

The following table contains galvanometer readings α for different inclinations Φ of the vertical

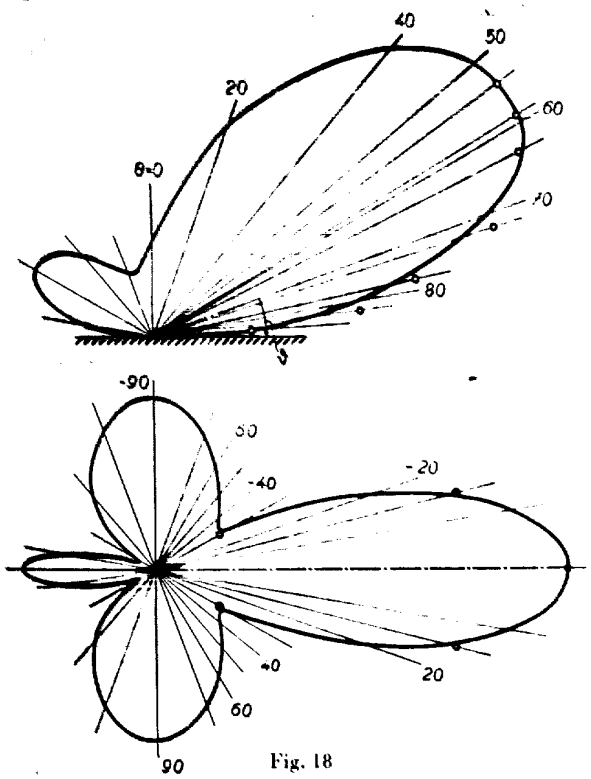

Fig. 18

plane of symmetry of the model with respect to the vertical plane containing the pole S and the mast S' (see Fig. 11). The values $\sqrt{\alpha}$ are proportional to the amplitude of the total field; all corrected for a constant distance r_0 = 15 m and reduced so that in the direction of the field maximum (Φ = 0) E_{red} be again equal to 1·12:

Table II.

Φ	r_0 (m)	α galv	$\sqrt{\alpha} \cdot r_0/15$	E_{red}
—30	14·8	0·2	0·44	0·195
—15	14·9	3·7	1·91	0·85
0	15	6·4	2·53	1·12
15	14·9	3·7	1·91	0·85
30	14·8	0·2	0·44	0·195

Here the distance r_0 was equal to 5λ. The measuring antenna was always inclined for maximum galvanometer reading.

The reduced measured values are marked on the respective rays Φ and indicated by circles in the lower part of Fig. 18, where the computed azimuthal pattern at constant angular elevation is drawn in heavy line.

Finally the control measurement was carried out; the apex angle adjustment for maximum field. The scale model antenna apex angle was adjusted to twice the three values δ mentioned below, the position of the feeding point of the antenna being adjusted accordingly, in the vertical plane containing the mast S' and the pole S (Fig. 11). Small changes of r_0 thus caused were taken into account. The current I_0 was always adjusted to a constant value. Slight changes of the characteristic impedance of the conductors at these small changes of apex angles were ignored, the terminating resistor was not necessarily readjusted. The measuring antenna remained at the height h = 7·5 m which, at δ = 55°, corresponds to the angular elevation 30°, in which direction the field is maximum. Slight changes of angular elevation connected with changes of r_0 were thereby ignored. In the same way as in the above tables, the corrected field amplitudes E_{red} were determined from the galvanometer readings α:

Table III.

δ	r_0 (m)	α galv	$\sqrt{\alpha} \cdot r_0/15$	E_{red}
45	15·8	1·0	2·1	0·93
55	15	6·4	2·53	1·12
60	14·75	3·6	1·87	0·83

By interpolating these three values of E_{red} we found that the field is maximum at δ adjusted to about 52°; i. e. at a value slightly higher than given by the curve δ'_m in Fig. 6 (calculated for the antenna suspended on a mast 35 m high), and lower than that given by the curve δ_m in the same figure valid only for direct radiation.

BIBLIOGRAPHY

[1] *Une antenne dirigée orientable pour la radiodiffusion sur ondes courtes, Nordlohne, Revue technique Philips, 1938, II, 3, No. 2.*

[2] *British patent No. 392201.*

[3] *French patent No. 785162.*

[4] *U. S. patent No. 2237765.*

[5] *British patent No. 485682.*

[6] *French patent No. 776575.*

[7] *Czechoslovak patent No. 77544.*

[8] *Radioélectricité générale, tome I, R. Mesny, ed. Chiron, Paris 1935.*

[9] *Elektromagnetické pole kosočtverečné anteny s ohledem na odraz vlnění od země (Electromagnetic Field of a Rhombic Antenna with Regard to the Reflection of Waves from the Ground), J. Bříza, Slaboproudý obzor 1940, 9 & 10, p. 5.*

[10] *Elektromagnetické pole vodiče s postupným vlněním a kosočtverečné anteny (Electromagnetic Field of a Conductor with Non-resonant Current Distribution and of a Rhombic Antenna), J. Bříza, Slaboproudý obzor 1940, 7 & 8, p. 5.*

[11] *Radiation from Rhombic Antennas, Foster, Proc. I. R. E. 1937, Vol. 25, No. 10.*

[12] *The Reflection Coefficient on the Earth's Surface for Radio Waves, McPetrie, Journal I. E. E., London, 1938, II, p. 82.*

[13] *Electrical Measurements on Soil with Alternating Currents, Smith-Rose, Journal I. E. E., 1934, VIII, p. 75.*

[14] *Rhombic Antenna Design, A. E. Harper, D. van Nostrand, New York 1941.*

Remote Control of the TESLA RU Rack and Panel Public Address System

Ladislav Pravenec

UDC 621.398:621.395.623.8

INTRODUCTION

With the growing popularity of public address installations in towns, industrial and business enterprises, offices, schools and other institutions, the problem of supplying vast areas with necessary electro-acoustical energy arises more and more often.

This problem can be fundamentally solved in two different ways:

1. By a centralised arrangement where the necessary equipment, including all power amplifiers, is placed at one point, preferably at the centre of the area to be supplied. The energy is distributed by means of high-tension, long distance lines and step-down transformers, placed at suitable nodal points of the network, from which it is fed directly to the speakers. The speaker voltage in Czechoslovakia is standardised at 100 Volts.

2. By a decentralised arrangement, where the nodal points are equipped with smaller P. A. stations, which are connected to the control station by means of a modulation and/or a control line. Both of these lines are of small cross-section and of very low voltage so that existing telephone lines can be used for that purpose.

The advantage of this system is not only lower cost of the feeding lines and elimination of high-tension transformers, but also the possibility of individual operation of substations independently of the main station. The main, central, programme is then

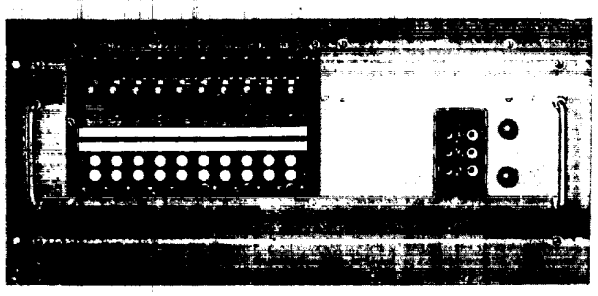

Fig. 1

connected to the whole system only on certain important occasions.

This kind of traffic is important mainly for big industrial enterprises and large towns. The various departments of big factories very often have different working hours and staggered rest periods, and provision must be made for their own individual programmes as well as the possibility of priority switching to the important central announcements. The same holds true for individual districts in big cities.

TESLA, in addition to the manufacture and design of a complete line of public address equipment, has developed a simple but efficient remote control

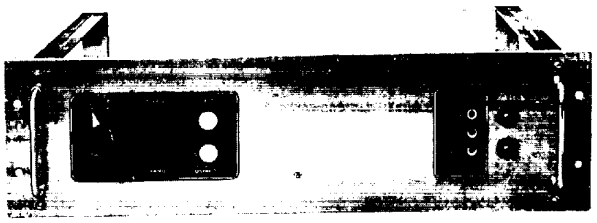

Fig. 2

system which should satisfy the needs of many customers. This system was developed for use with the rack-and-panel public address system RU, and consists of two panel units to be added to the existing RU system. These units are:

1. Remote control panel for the main station (see Fig. 1). This addition enables any RU station to control remotely as many as 10 substations. For the customer's convenience and economy this panel is manufactured in 3 types, for 3, 6 and 10 substations. However, stations equipped with the panel for 3 or 6 substations may be later extended for all 10 substations if future expansion calls for it.

2. Remote control panel for the substation (Fig. 2). By connecting this panel unit to any RU installation, it becomes a substation and can be remotely controlled by any type of main station. All possibilities for independent use are, of course, maintained.

The TESLA RU public address system enables any equipment to be "tailored" according to the customer's wishes while by means of suitable design of all units and efficiently organised production of interconnecting wiring, the price of custom-built stations is in reality not higher than that of standard types. Several types of arrangements have been standardised for convenience and quick delivery.

For remote control the three following types have been so far designed:

Type A3 (Fig. 3), the main station for remote control with the possibility of controlling as many as 10 substations. It can clearly be seen that only two units are added to the original standard set: the remote control panel (second from top) and— for better and easier operation the monitor speaker amplifier (fourth from bottom).

the use of a local microphone and gramophone is maintained. A special switch, placed on the remote control panel is furnished for switching over the microphone and gramophone channels of the local programme.

All three types can naturally be extended by adding more power amplifiers (supplementary cabinet type C1), if higher output is demanded. New standard types are being developed, using a universal

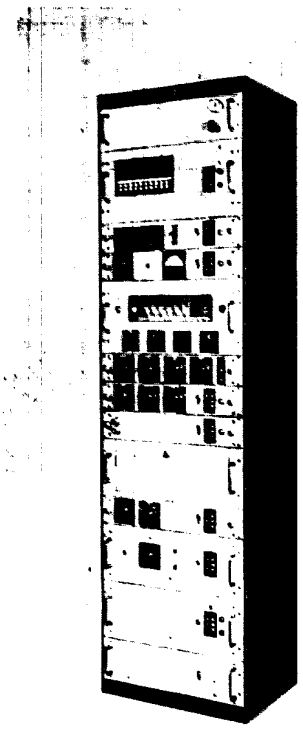

Fig. 3

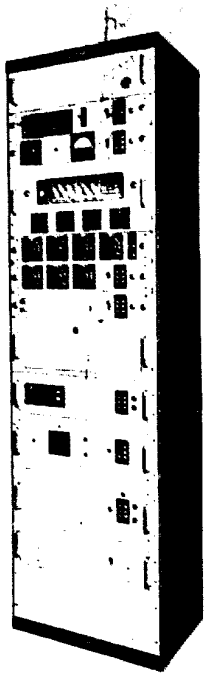

Fig. 4

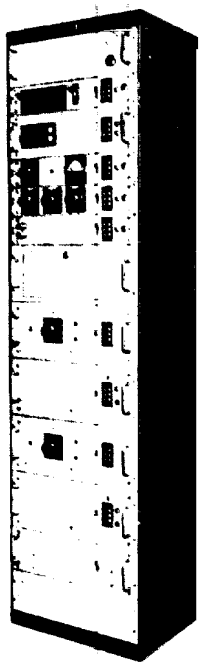

Fig. 5

Type B1 (Fig. 4), substation for remote control. This set-up has, in comparison with current types, only one additional panel - the remote control panel for substation (fifth from bottom). The arrangement of units remains exactly the same as for the current type A2. Type B1 is designed for larger installations and has all the possibilities for local programmes, which RU system has. It is used mainly for larger city districts and big departments of industrial enterprises.

Type B2 (Fig. 5), substation for remote control. This type is used usually for smaller installations where all possibilities of local programme are not necessary. We can see in the picture that the wireless receiver and mixer panel are missing, so that wireless reception and arbitrary mixing of different programme channels is not directly possible. However, control panel and 250 Watt power amplifiers. Most of the equipment manufactured so far, was provided with 75 Watt amplifiers.

PRINCIPLE OF OPERATION

The design of the system for remote control had to be carried out so as to fulfil the following requirements.

1. The necessary interconnection between the main station and the substation to be realised with a minimum number of wires to facilitate cheap installation of the whole equipment. Thus it should be possible to use only two wires plus earth (one telephone line). It is recommended, however, to use two telephone lines (four wires plus earth) for more reliable functioning and for monitoring.

2. The system must permit the stand-by condition of the substation. This condition, in which all valves are heated but the anode supplies are off, facilitates the instantaneous switching of the system into operation and results in great savings of electronic valves and consumed energy. It is used in all units of RU system.

3. Switching the substations on and off is accomplished by throwing a key in the same way as for connecting and disconnecting speaker loops. Throwing the key must bring the substation into accordance with the main station, i. e.

a) If the power is switched off at the main station, it is likewise switched off at the substation.

b) If the main station is in the stand-by position (heaters on), the substation is also in that position.

c) If the main station is switched to traffic, the substation is also switched on.

4. Disconnecting the substation by throwing off the key will cut off power from the substation, regardless of the condition of the main station.

5. When the substation is disconnected by throwing off the key in the main station, the substation is allowed to have its own local programme, quite independently of the main station.

6. This local programme must be maintained even when the connecting key of the substation in question is thrown into position, but the main station is switched off or is in the stand-by position. Only when the main station is switched on is the local programme of the substation interrupted and the main programme takes over.

7. The possibility of an extraordinary local programme (e. g. in case of alarm, etc.) in any position of the main station (totally independent traffic) is also required.

8. All positions of the substation are to be reliably indicated at the main station (i. e. switched-off, stand-by and traffic positions). Also the indication of the ordinary and extraordinary local programmes and acoustical monitoring are desired.

9. Functioning of the whole equipment must be reliable for normal line-voltage variations.

10. The possibility of transmission from any substation to the main station and consequently to the whole network is desirable.

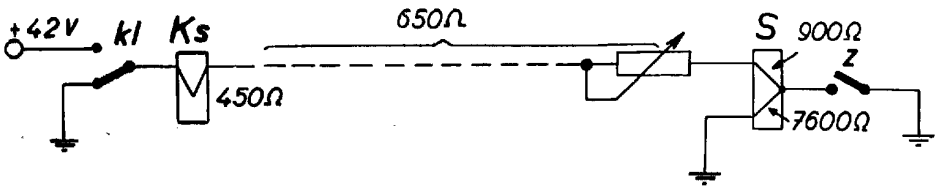

Fig. 6

11. The remote control of all substations must function even when the main station itself is remotely controlled from a microphone control box.

12. The switching over from the local to the main programme and vice versa should be executed by fading in and out rather than by sudden switching.

13. The cooperation with all other stations of the RU system should be assured.

All these conditions are fulfilled in the remote control system TESLA RU-D1, whose operation will be described in the following:

A) The switching of power at the substation and its indication.

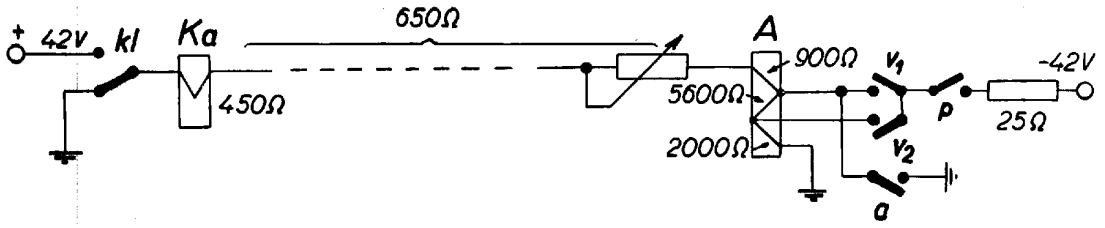

Fig. 7

The principle is obvious from Fig. 6. By throwing the key *kl*, the D.C. voltage of 42 Volts (from a dry rectifier) is applied to the line. The resistance of the whole circuit: earth—42 Volt rectifier—relay *Ks*—line—relay *S*—earth is approximately 9600 Ohms and the current is thus between 3.4 and 5.3 mA, depending on the mains-voltage variations and possible potential difference between the two points of earthing. The relay *S* operates (its reliable action starts with 3.1 mA) but the relay *Ks* is not affected (it needs a minimum of 16 mA for its action). The relay *S* will energise contactor *St* and this connects the substation to the mains. After the

voltage has built up on the auxiliary rectifier (for feeding stand-by relays), relay *Z* connected across it will energise and in the contact *z* will short the 7600 Ohm winding of *S*. The current in the line will increase to between 16.5– 25.5 mA and the signal relay *S* will operate and switch on the signal lamp.

B) The switching into traffic and its indication.

This function is achieved in essentially the same way. The schematic (Fig. 7), however, is complicated by the introduction of local programme signalling. When the substation has its local programme, the contacts *r1*, *r2* and also contact *p* are connected. Thus the 5600 Ohm section of relay *A* is shorted. The upper section (900 Ohms) together with line resistance and winding *Ka* makes a branch of about 2000 Ohm resistance, which is equal to the lower section of *A*. As both sections have equal number of turns and the current from the 42 Volt source (dry rectifier in the substation) flows through both sections in opposite directions, relay *A* will not operate, but the signal relay *Ka* operates and indicates the local programme.

From the law of superposition it is obvious that throwing off key *kl* connects the 42 Volt rectifier in the main station to the line and the additional current, produced by that, causes the relay *A* to operate and switch in the main programme.

Fig. 8 shows the whole switching circuit. Both wires *a* and *b* are connected into a two-wire line which is simultaneously utilised for acoustical monitoring. The A.C. circuit is closed over the two wires, primary windings of repeater transformers and condensers *C*. The windings of relays *Ks*, *S*, *Ka*, and *A* act simultaneously as chokes to isolate the A.C. circuit. Any small hum-voltage component of the control current caused by the rectifier is applied to the two wires in parallel and its effect on the A.C. circuit is thus essentially eliminated.

In this arrangement another two-wire line is needed for the modulation transmission. When it is not possible to provide two lines for remote control, the control line will be also used for the transmission of modulation to the substation. In that case the acoustical monitoring of the substation is not possible when the main programme is on. However, this monitoring is maintained for local programmes.

The function of the whole equipment will now be described in detail. Fig. 9 shows its wiring diagram, drawn in the usual way, i. e.:

All relays are marked with capital letters with small letter indices. Figures in brackets give the number of relay contacts. These contacts are indicated with corresponding small letters and are also

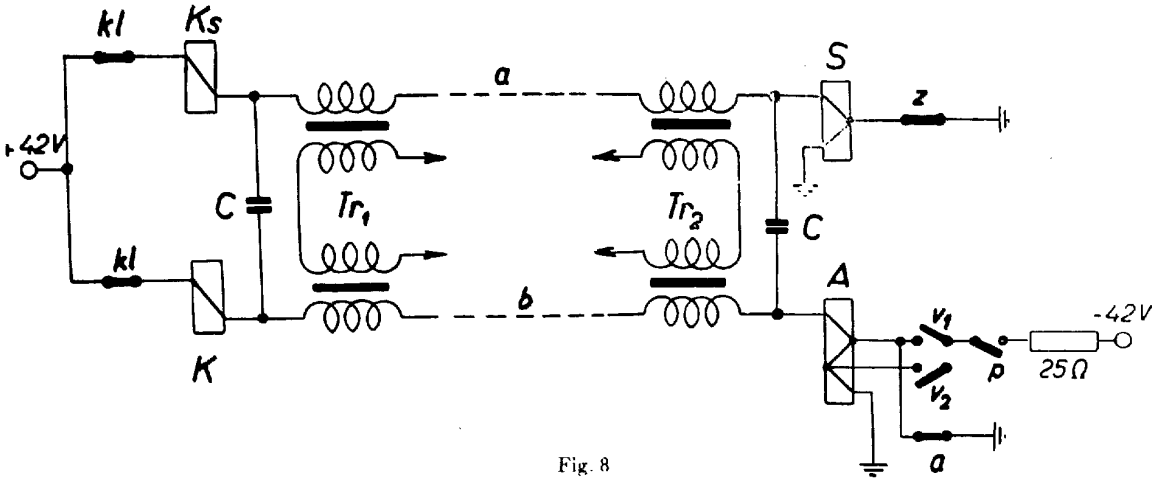

Fig. 8

numbered. Thus, e. g. relay *Ks*(3) has three contacts ks_1, ks_2, ks_3, etc.

All contacts are drawn in the rest position of relays, keys and push-buttons.

When a substation is to be remotely controlled, we throw its key on the remote control panel (main station). Supposing the main station to be in the stand-by position, the current will start in the circuit: 42 Volts 30 Ohm resistor—Kl_1—*Ks*—line – *S*—contacts z_1, p_2 –earth. In the manner described above relay *S* will operate and contactor *St* will connect the power line to the substation. Contactor *St* is energised by D.C. and, to comply with the safety regulations, only low voltage is used on the secondary of transformer Tr_3, because this voltage is present on the panel terminals and the cabinet wiring even when the main switch or contactor is off.

After starting the rectifier, relay *Z* energises and its contact z_1 short-circuits the 7600 Ohm winding of *S*. The current in the line steps up to the high value necessary for *Ks* to operate. Relay *Ks* connects the lamp Z_1 by contact ks_3. This lamp lights dimly, be-

cause of the 250 Ohm series resistor R_4, indicating in this way that power has been switched on.

In case the main station is switched off, no current will be delivered by the 42 Volt rectifier and the substation remains switched off in accordance with the main station. When the main station is switched off after the substation has been put in stand-by position, the current in the control line will cease and the substation will also be switched off.

When the main station is switched into traffic, the relay X will operate first. This relay is connected and a_2, current in wire b increases and the relay Ka in the main station operates. Its contact ka_2 shorts the 250 Ohm resistor R_4 and the lamp Z_1 lights up brightly, signalling in this way the traffic position of the substation. The lamp Z_2 has not been lit yet, as the contact x_3 is now disconnected and the contact ks_3 is thrown to the branch Z_1. If we now want to check the substation's programme acoustically, we press the push-button Tl. Its contact tl_2 causes relay P to operate (relay P is common to all 10 push-buttons) and contact tl_1 brings the desired

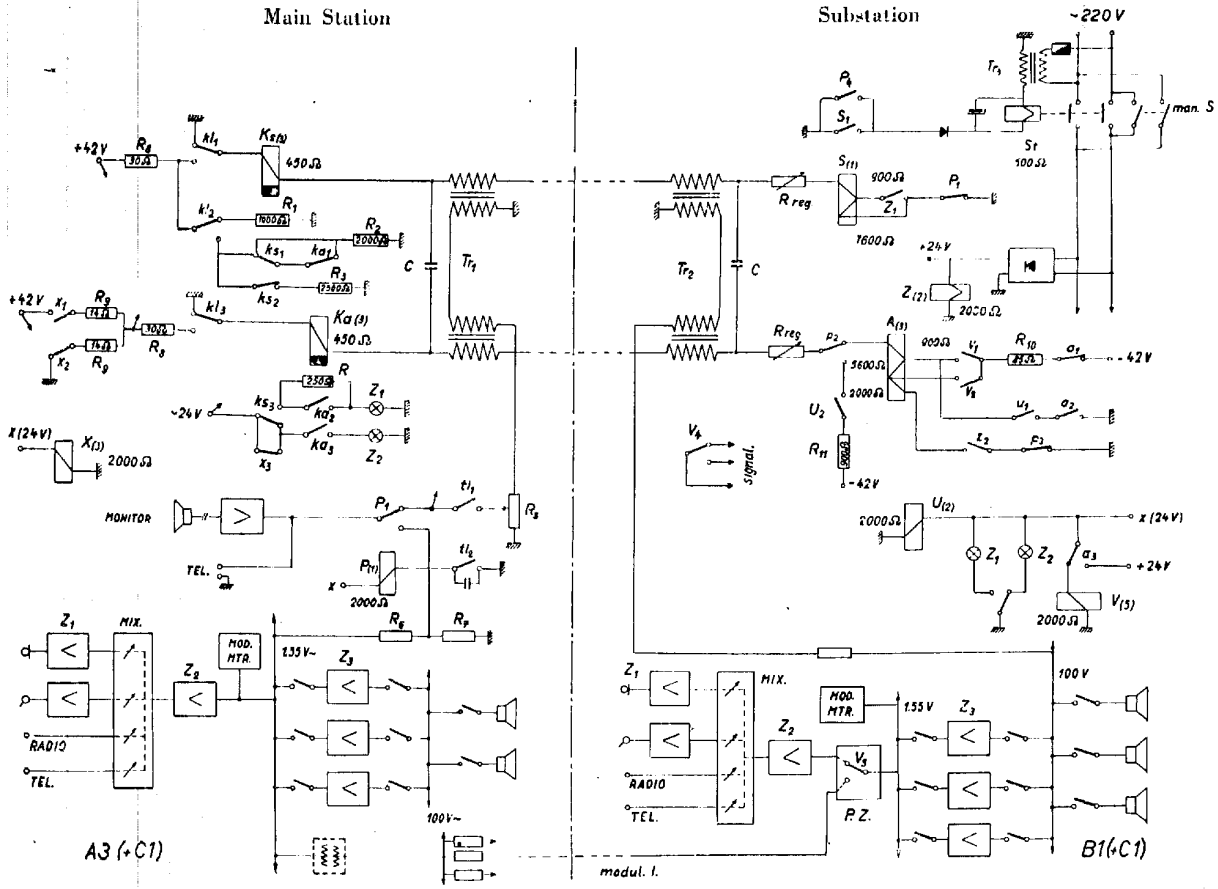

Fig. 9

to the auxiliary busbar X 24 Volts D.C. to which all the stand-by relays of all panel units are connected. Busbar X is connected either by means of a key, placed directly on the main station cabinet, or indirectly from the microphone control box. Relay X operates and its contact x_1 and key kl, already switched on, close the circuit: 42 Volts x_1 R_9 R_8 —kl_3 —Ka — line p_3 relay A contacts z_2, p_4— earth. Relay A operates, its contact a_3 connects 24 Volts D.C. to the auxiliary busbar of the substation and thus brings all its apparatus into traffic condition. The stand-by relay U of the substation remote control panel short-circuits by its operation the 5600 and 2000 Ohm sections of A by contacts u_1 substation's programme to p_1. The switch-over contact p_1 disconnects the main programme from the monitor amplifier and connects the substation's programme to it. The voltage dividers R_6—R_7 and R_5 are preset to equalise the programme levels so that loudness of the monitor speaker is the same for all substations and also for the main station, regardless of the different line attenuations, assuming the modulation of all stations to be the same and the stations to be in good order. When the main station is switched off, the programme monitoring is accomplished by plugging a head-set into the socket *Tel.*

As has already been mentioned, the substation can have its own local programme either when its

key *Kl* in the main station is thrown off or, if connected through that key, when the main station is in the off or the stand-by position. From the schematic it is obvious, that in either of these cases the wire *b* is connected to earth in the main station.

The substation can then be simply switched into stand-by position by the manual switch *man S*, connected in parallel to *St*. The traffic position will then be reached by connecting the auxiliary busbar *X* to the 24 Volt D.C. rectifier by means of the contact *Zap*. (drawn by a dashed line), which, similarly as in the main station, is either a direct switch on the cabinet or an auxiliary relay contact operated indirectly from the microphone box. This is a normal procedure in all types of RU stations.

Because the relay *A* is in its rest position, the relay *V* (switch-over relay for the local programme) operates and performs the following functions:

1. Contacts v_1 and v_2 short-circuit the 5600 Ohm section of relay *A* and so cause the current to flow through the wire *b* and to operate relay *Ka*. As described before, the relay *A* will not operate because the currents in its two sections counteract each other. The lamp Z_2 (in the main station) gets current over ka_3 and thus indicates the substation's local programme. If the substation was connected by means of its key *Kl* and the main station is in the stand-by position, lamp Z_1 will light up brightly (it was glowing dimly before). In all other cases only Z_2 glows. These lamps glow even when the main station is switched off as their feeding transformer is connected ahead of the main switch.

2. Contact v_3 connects lamp Z_1 in the substation which indicates the local programme. The Z_2 lamp is furnished in the substation to indicate that the main station programme is on.

3. Contact v_4 operates an auxiliary indicator for remotely controlled microphones. This signal informs the announcer of the local programme that he has been cut off by a more important central programme.

4. Ultimately the contact v_5 switches over the two programme channels in the switch-over amplifier (to be described later).

However, the main station may at any time, by getting into traffic position, interrupt the local programmes of all connected substations because operation of the relay *X* of the main station brings the 42 Volt control voltage to the wire *b*. The relay *A* operates (the current signalling the substation's local programme does not interfere with its action) and causes (by opening a_3) the relay *V* to fall off. In this way the substation is switched over to the main programme.

The function of the switch *P* in the substation is to ensure the local programme, i. e. entirely independent traffic of the substation. In that case the substation is separated by contacts p_2 and p_3 from the control line. Because the circuit of the wire *a* is then open, the signal lamp Z_1 in the main station cannot glow. However, the lamp Z_2 glows, because the wire *b* circuit is closed by p_3 and u_2 and connected over a 900 Ohm resistor to 42 Volts. In this way the main station is informed of the irregular local programme in the substation. Contact p_1 prevents the substation from being unintentionally switched off by the main station when it has been switched on remotely and later switched over for the independent traffic. For this purpose contact p_4 prevents the relay *A* from operating and thus interrupting the desired local programme.

The principal operation of the remote control has thus been described. It now remains to explain the purpose of some auxiliary parts.

Resistors R_8, R_9, R_{10} are safety resistors to limit short-circuit currents, caused by chance connection of all three poles of switch-over contacts.

Resistors R_1, R_2, R_3 with the appropriate relay and key contacts kl_2, ks_1, ka_1, ks_2 form a substitute load for the 42 Volt rectifier when the currents in the control line of some substation are switched off. The dry rectifier has poor voltage-regulation and its voltage would vary considerably with the number of substations switched on. By means of the said resistors and contacts the load of the rectifier and consequently its voltage is kept constant.

Resistors R_{reg} (in substation) serve for setting the resistance of the circuits of wires *a* and *b* to 2000 Ohms, regardless of the length and cross-section of the contol line wires.

For the sake of completeness the schematic (Fig. 9) contains also the block diagram of the main station and substation, where:

Z_1 represents a preamplifier,
Z_2 represents a line amplifier,
Z_3 represents a power amplifier.

This diagram is quite clear and does not need any detailed explanation. What will perhaps seem as rather unusual, is the parallel coupling of all power amplifiers on both the input and output sides, reminding one of a power plant schematic. Likewise, there are no substitute resistors to replace switched-off loudspeakers. The power amplifiers are equipped with a very strong feedback to ensure nearly constant output voltage independent of the loading. The danger of uneven distribution of load on such amplifiers working in parallel which could be caused by even small asymmetry is removed by a patented

equalizing circuit (differential feedback). It helps the regular distribution of load on individual amplifiers and minimizes the distortion.

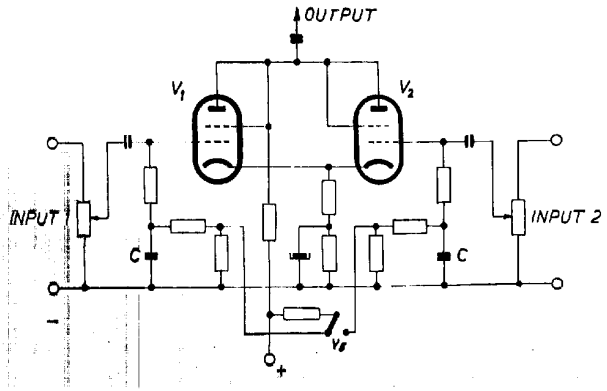

Fig. 10

Now a few details of the switch-over amplifier PZ will be added. This amplifier enables the two programmes to be switched over by slow fading in and out which lasts about four seconds. Its principle is easily understood from Fig. 10. The valves' cathodes are at a rather high potential, producing a bias much larger than that necessary for cut-off and making the valve in question non-conductive. By

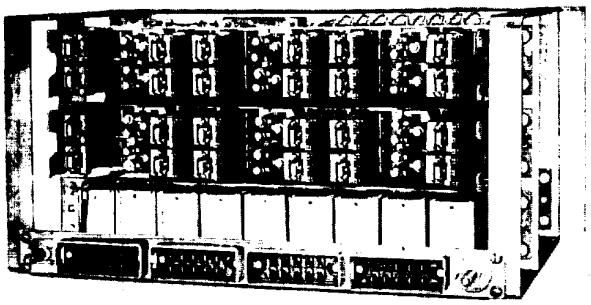

Fig. 11

applying a positive voltage of a certain magnitude to the grid of a valve, its bias is lowered to the value of optimum amplification. The other valve is blocked. By throwing the contact v_5 to the other side, the other valve will conduct. This switching-over is not instantaneous but takes a certain time for the charging and discharging of the condensers C, thus causing one programme to fade out while the other is fading in. Quick, unpleasant switching and broken words are thus eliminated.

As is obvious from the description, this system does not control the individual speaker loops of the substations. In most cases this control is not demanded. However, for certain large installations this central control and perhaps more simultaneous programmes are demanded. The described system is not adequate for such cases, and the equipment is assembled individually according to the customer's wishes. At present, a new system of universal units is being developed for installations of this kind, to speed up production and to facilitate the assembly of any equipment from prefabricated units.

To conclude let us add a few words of explanation to supplement Figs. 1, 2, 11—15, showing the actual forms of remote control panels.

Fig. 1 presents the front side of the remote control panel for main stations. On the left-hand control unit, starting from the top, we see the keys for con-

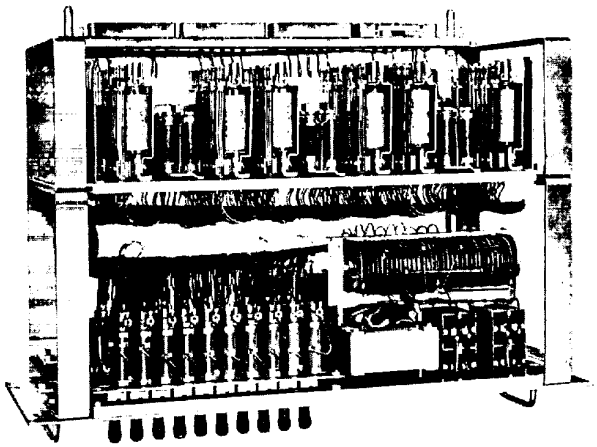

Fig. 12

necting the substations. Below them (and below the label strips) there are two rows of signal lamps, indicating the substation positions (the upper row) and substations' local programme (the lower row). The push-buttons for acoustic monitoring by means of the monitor speaker or a head set (sockets T in the right-hand part) are located under the lamps. By plugging a special meter (accessory to every RU station) into sockets E_1 or E_2 on the right-hand part of the panel, the auxiliary D.C. voltages 24 and 42 Volts may be checked. The two signal lamps on the

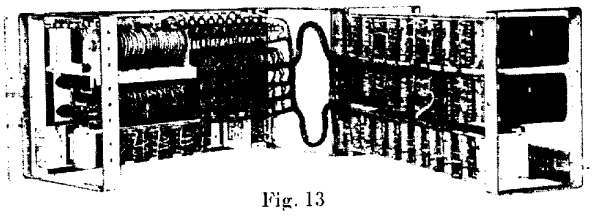

Fig. 13

right from the meter sockets indicate stand-by and traffic positions.

The back view of the panel with the relay covers removed is seen in Fig. 11. Fig. 12 is the panel seen from the top. The auxiliary 42 Volt rectifier is seen clearly on the right-hand side of the picture. On

the left are the voltage dividers R_8 for adjusting the monitor speaker levels. To facilitate easy manufacture and components replacement, the whole apparatus is divided into two parts that can be opened as seen in Fig. 13. In this position all parts are easily accessible.

The front view of the remote control panel for substations is seen in Fig. 2. From left to right we see there resistors R_{15} for adjusting line resistance and also the regulating resistors for adjusting the levels in the switch-over amplifier.

Fig. 15 shows the bottom view of this panel. All these pictures show the simple design of both units. Like all other units, they are easily connected by simple insertion in their proper places.

The description given in this article does not exhaust all possibilities which this system of remote control enables as, e. g. transmission from substations, cooperation with remote control microphone boxes, etc. It presents, however, a general exposition of the principal features. Of course, the present simple apparatus is not the last word and development in this branch goes on incessantly to keep TESLA equipment among the leading products of the best quality.

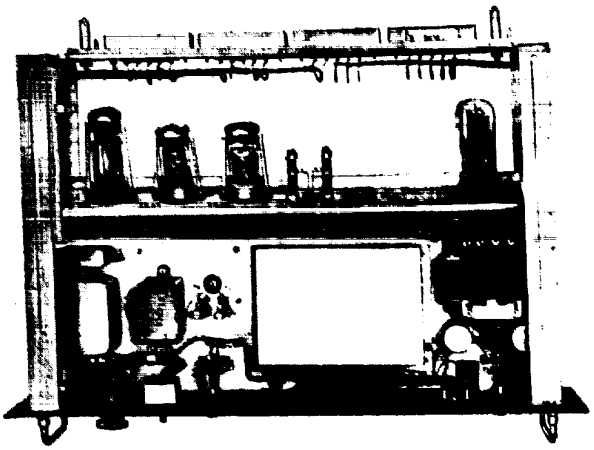

Fig. 14

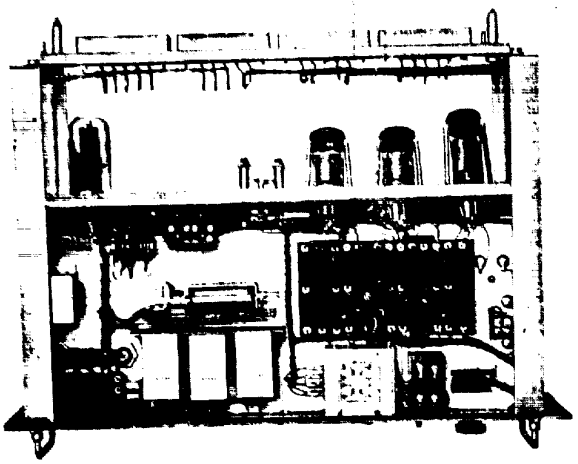

Fig. 15

see the switch P for special local programmes (entirely independent traffic). Next is the microphone-gramophone switch, used only in stations of type B2 (without mixing panel) for switching microphone or gramophone channels of the local programme. The signal lamps for local and central programmes are placed next. On the right-hand side are again the usual meter sockets for checking different voltages and two lamps indicating that heaters and anode voltages are on. The top view is in Fig. 14. We can

A Contribution to the Design of Horn Loudspeakers

Josef Merhaut

UDC 621.395.623.77

Loudspeakers are generally fitted with an exponential horn, the throats of which have a smaller cross-sectional area A_0 than the active area A_d of the diaphragm, thereby increasing the radiation resistance by the factor $\left(\frac{A_d}{A_0}\right)^2$. Owing to this difference in cross-sectional area there are phase differences in the acoustical waves coming from different parts of the diaphragm which cause a reduction in radiated power when large phase lags occur, e. g. at high frequencies. This effect can be greatly reduced by proper treatment of the throat as a transmission line. Examples of different constructions are given in Figs. 1 to 3. Fig. 1 shows a loudspeaker of the simplest type, Fig. 2 is Bostwick's design and Fig. 3 shows a speaker designed by Lansing-Shearer. This last design practically eliminates the above effect because all waves enter the sub-divided throat at nearly equal phase.

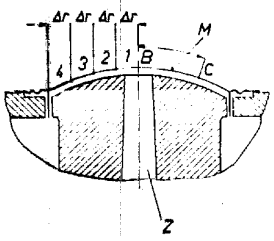

Fig. 1

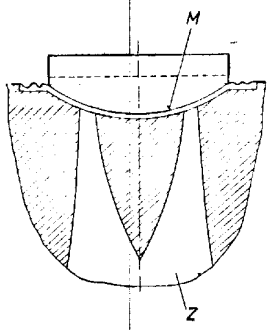

Fig. 2

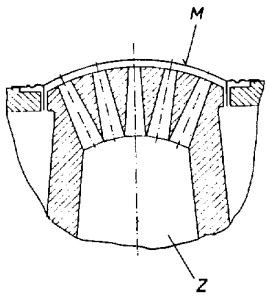

Fig. 3

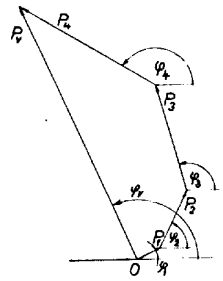

Fig. 4

The instantaneous acoustic pressure originating at an arbitrary point of the diaphragm C (Fig. 1) arrives at the centre of the throat B with a time delay

$$\Delta t = \frac{l}{c} \tag{1}$$

where l is the distance $\overline{CB}$ and c (Fig. 1) is the velocity of sound. The phase lag φ which corresponds to the time delay Δt is given by

$$\varphi = 2\pi f \Delta t \tag{2}$$

where f is the frequency.

If we let $l \approx r$ which, according to Fig. 1, is acceptable, then from equations (1) and (2) the phase lag φ equals

$$\varphi = 2\pi f \frac{r}{c}. \tag{3}$$

We now divide r into elements Δr of area $\Delta F = 2\pi r\, \Delta r$ (Fig. 1) and add all the forces originating in these elements vectorially, the result being the total pressure in the throat. Let us take the pressure p on the diaphragm as a harmonic function of time but independent of the radius r

$$p = p_0 \sin 2\pi f t.$$

We then obtain the force contribution from the element Δr at the point B by adding all the vectors of length $p_0\, \Delta F$ and angle φ, so that for $r = 0$, $\varphi = 0$. The vectors form a polygon (see Fig. 4), which was constructed for $f = 4000$ cps, $r = 4$ cm. The real force at the point B is equal to the vector P_r (Fig. 4), and the loss in decibels at the frequency f, for which the polygon was constructed, is given by

$$\mu = 20 \log \frac{P_r}{P_0} \tag{4}$$

where $P_0 = \pi r^2 p_0$. This solution is only approximate because we took φ to be constant over the element Δr. To satisfy this condition we must take Δr infinitesimal: $\lim \Delta r = \mathrm{d}r$. The polygon of Fig. 4 then becomes a continuous curve, which we can compute by introducing rectangular coordinates x and y from:

$$\left.\begin{aligned} x &= p_0 2\pi \int_0^r r \cos\varphi \, \mathrm{d}r \\ y &= p_0 2\pi \int_0^r r \sin\varphi \, \mathrm{d}r \end{aligned}\right\} \tag{5}$$

which, after substituting φ from equation (3), and integrating, give

$$\left.\begin{aligned} x &= \frac{p_0 r^2}{2\pi f^2}\left[\frac{2\pi f}{c} r \sin\left(\frac{2\pi fr}{c}\right) \cdot \cos\left(\frac{2\pi fr}{c}\right) - 1\right] \\ y &= \frac{p_0 r^2}{2\pi f^2}\left[\sin\left(\frac{2\pi fr}{c}\right) \cdot \frac{2\pi fr}{c} \cos\left(\frac{2\pi fr}{c}\right)\right]. \end{aligned}\right\} \quad (6)$$

The coordinates x, y from equation (6) express the curve which is the limit of the vector polygon for

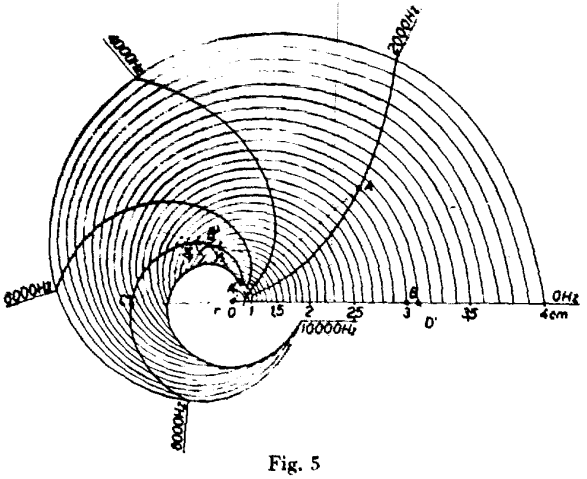

Fig. 5

$\Delta r \to 0$. Fig. 5 shows some of these curves for $f = 0$, 2000, 4000, 6000, 8000 and 10,000 cps; they are drawn for a radius of $r = 0$ to $r = 4$ cm. Points of equal radius are joined giving another set of curves. The resulting diagram can be used to find the magnitude and phase angle of the forces acting at the throat of the horn. The line connecting the origin (0) with the corresponding point on the vector curve for a given frequency and radius is the resultant vector of force at the centre of the diaphragm

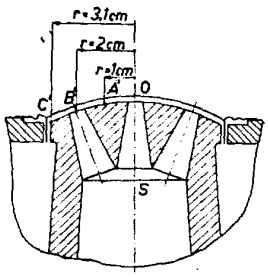

Fig. 6

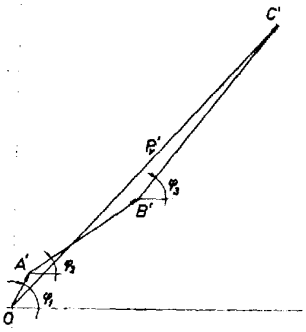

Fig. 7

given as the sum of the partial pressures on the diaphragm.

Example: At the centre of the throat of a simple speaker (Fig. 1), of radius 3 cm, the force vector is given (at 2000 cps) by the line $\overline{OA}$. The length of the line $\overline{OA}$ is proportional to the magnitude of the resultant force at the throat, the angle between $\overline{OA}$ and the x-axis (vector for $f = 0$ cps) being its phase-angle. From the diagram we can, therefore, determine the frequency distortion in magnitude and phase. The loss in db is obtained by taking the ratio of $\overline{OA}$ to the corresponding vector at $f = 0$ cps. In the given example, $r = 3$ cm, $f = 2000$ cps, and we obtain:

$$\mu_{2000} = 20 \log \frac{\overline{OA}}{\overline{OB}} = 0.1 \text{ db}.$$

Even though the diagram in Fig. 5 is constructed for forces at the centre of the diaphragm, it can be used with advantage for speakers with sub-divided throats placed off the axis of the speaker. The application is best illustrated by another example. A cinema high-frequency speaker was first fitted with a throat as in Fig. 1, and then as in Fig. 6. The radius of the diaphragm was in both cases 3.1 cm. According to Fig. 6, the force vectors for $f = 8000$ cps are evident from the broken lines in Fig. 5.

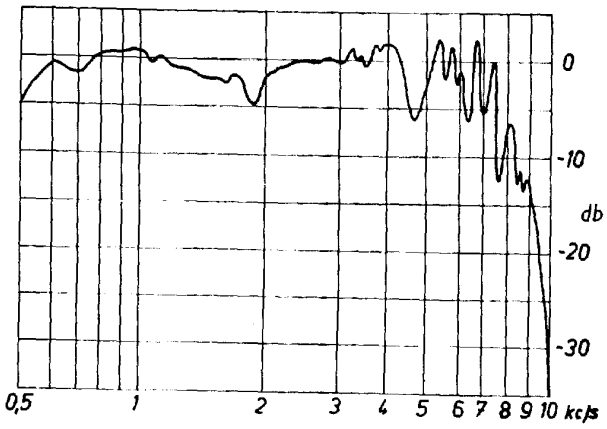

Fig. 8

Point B' corresponds to the second throat which collects acoustical energy between points A' and C' (edge of diaphragm). The forces $\overline{A'B'}$ and $\overline{B'C'}$ have to be added to the force $\overline{OA'}$ in such a way that the angle of vector $\overline{B'C'}(\varphi_3)$ is measured from the tangent to the vector curve at the point B' (Fig. 5). Similarly for the vector $\overline{A'B'}$ (φ_2), with the difference that the angle has to be taken with the opposite sign from that given in Fig. 5. This is so because Fig. 5 was constructed on the assumption that the sound travels from the edge of the diaphragm to the centre, whereas in the interval $A' - B'$ the direction of travel of sound is the opposite, e. g. from A' to B'.

The reason for taking the angles φ_2, φ_3 from the tangent at the point B' is that the sound channels $O - S$ and $B' - S$ are equal in length and do not contribute to any phase differences.

In Fig. 7 we have the sum of the vectors $\overline{A'B'}$, $\overline{B'C'}$ and $\overline{OA'}$ with the correct phase angles. It is evident that the angles of $\overline{A'B'}$, $\overline{B'C'}$ and $\overline{OA'}$ are nearly equal; it is, therefore, often possible to add

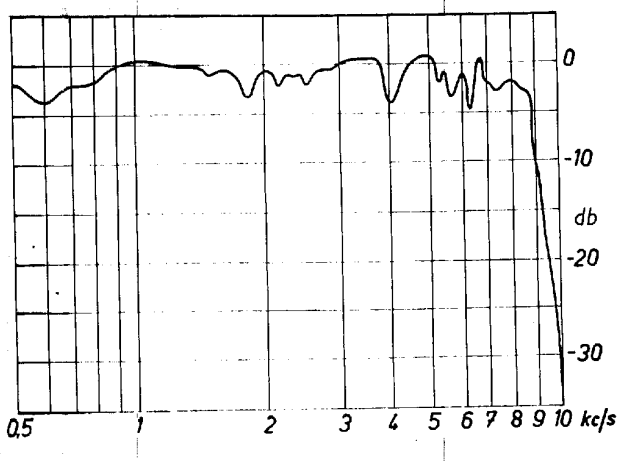

Fig. 9

the magnitudes of the vectors algebraically. The loss in decibels for f 8000 cps is

$$\mu_{8000} = 20 \log \frac{P'_v}{P'_{v0}} = 0.7 \text{ db.}$$

where P'_v is the magnitude of the resultant vector from Fig. 7 and P'_{v0} is the length $\overline{OD'}$ from Fig. 5 (P'_v for 0 cps).

The loss in db in the arrangement of Fig. 1 is much greater (broken horizontal line) in Fig. 5.

$$\mu''_{8000} = 20 \log \frac{\overline{OC'}}{\overline{OD'}} = 5.2 \text{ db.}$$

The difference in loss at this frequency is therefore

$$\mu'_{8000} - \mu_{8000} = 4.5 \text{ db.}$$

The above result is in good agreement with the experimental value. Figures 8 and 9 show the frequency responses actually measured. Fig. 8 gives the response of the speaker arranged as in Fig. 1; Fig. 9 is the response of the same speaker when arranged according to Fig. 6. The responses were measured in an acoustic chamber of about 80 m³, with irregular walls fitted with a thick absorbing layer (resultant coefficient of absorption 0.95). A measuring condenser microphone was placed at a distance of 1 m on the axis of the speaker. The curves were registered automatically.

The difference of the average responses at 8000 cps from Figs. 8 and 9 is 4.7 db, which agrees excellently with the calculated value of 4.5 db.

BIBLIOGRAPHY

Mac Lachlan: Loudspeakers, Oxford 1934.

Olson: Elements of Acoustical Engeneering. D. Van Nostrand, New York.

An AC Potentiometer for Low Frequencies

Bohdan Carniol

UDC 621.317.727.083.5

1. APPLICATION OF A.C. POTENTIOMETERS

Potentiometer methods have been used up to now mainly for D.C. measurements. The reason for this is that A.C. potentiometers and potentiometer measurements are more complicated. It is not sufficient to balance the amplitudes as in D.C. methods; the phase difference has also to be compensated, as well as using voltages of exactly the same frequency. From these facts follow the difficulties encountered in the construction of A.C. potentiometers.

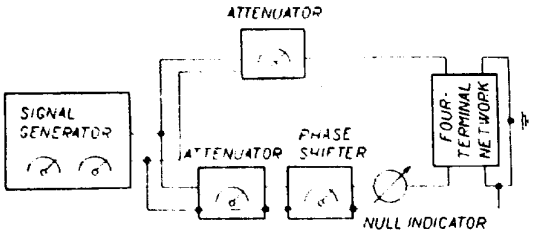

Fig. 1

A.C. potentiometer methods are however of advantage in certain applications, especially when using suitable potentiometers. They can be used to make quick, convenient and relatively accurate measurements of the real and imaginary components of an arbitrary impedance (reactance), the frequency dependence and characteristic constants of four-terminal networks, etc. Detailed information of these possibilities can be found in the literature cited at the end [1], [2], [3].

The A.C. potentiometer offers unusual possibilities for measuring low powers, e. g. measuring the losses in small samples of iron, the losses in electrolytic condensers, etc. [4]. It can similarly be used where the measuring equipment has to have a very great input impedance. Special simplicity is achieved when using the A.C. potentiometer for the measurement of audio-frequency amplifiers with negative feedback, where, according to Nyquist, we must determine the frequency and phase response of the feedback loop for frequencies far exceeding the useful band of the amplifier in question [5].

2. DETAILS OF EXISTING POTENTIOMETERS

2.1. The oldest A.C. potentiometer is probably Franke's machine with two single-phase generators mounted on a single shaft, one of them having a movable stator.

The voltage of the fixed stator generator is fed into the network to be measured (two-pole, four-pole, amplifier, etc.) while the voltage from the other generator is used for the actual balancing. The frequency can be adjusted by a change of speed, the single shaft-mounting guaranteeing the same frequency from both sources. The phase can be adjusted by rotating the stator of the second generator, the voltage of which can also be varied for balance.

The disadvantage of the whole equipment is its size, unwieldiness and limited frequency range, given by the maximum speed of rotation.

2.2. For some measurements a single frequency potentiometer is sufficient. This permits a considerable simplification of the equipment. This type of potentiometer was described in *Slaboproudý Obzor*, 1946, Nos. 3—4 [4].

2.3. Variable frequency potentiometers and phase shifters with frequency dependent calibration.

In case a single frequency is not sufficient, an audio frequency signal generator can be used, which feeds through an attenuator into the component to be measured; the balancing voltage being obtained

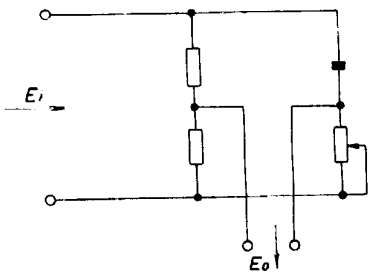

Fig. 2

through an attenuator, phase-shifter and null-indicator (see Fig. 1).

The phase-shifter is a difficult problem.

A frequently used phase-shifter is shown in Fig. 2. It can be easily shown that the output voltage is constant for all phase-shifts φ

$$E_{out} \quad \frac{E_{in}}{2} \underline{/\varphi},$$

The required phase shift can be obtained by a change in the variable resistance R which can be calibrated directly in degrees. Let us put $\frac{1}{RC} \quad \omega_0$:

then the phase angle φ of the output voltage depends on the angular frequency ω according to the relation

$$\tan \varphi = 2 \frac{\omega \omega_0}{\omega^2 - \omega_0^2}.$$

The phase calibration is frequency-dependent and valid for one frequency only.

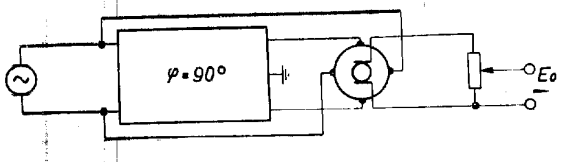

Fig. 3

There is a simple method—the use of a booster—for phase change, if a poly-phase generator is available. When the source is single phase—and this is generally the case—then we can obtain a second phase shifted by 90° by connecting a phase-shifter permanently adjusted to 90° between the source and the booster (Fig. 3). A great advantage of this method is the linear calibration of phase angle from 0° to 360°.

Instead of a booster we can also use a circular potentiometer as shown in Fig. 4. The phase can again be adjusted from 0° to 360°. The calibration, however, is not quite linear when a linear potentiometer is used. The output voltage varies between E_2 (when the sliding contact is in the positions where the two-phase generators are connected) and $E_2/\sqrt{2}$ (at the points 45° away). At these 8 points the phase angle and the sliding contact angle agree, at intermediate points this agreement is not complete.

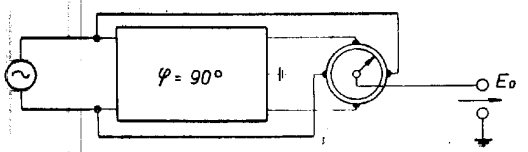

Fig. 4

A quadrant condenser especially for the higher frequencies can also be used. The stator consists of four quadrants, each of which is connected to one lead of the two-phase generator (Fig. 5). Here we get a linear calibration by choosing the eccentricity of the rotor so that the axis is halfway between the centre of the disc and its edge [6].

The calibration of the last three phase-shifters (Figs. 3 to 5) is independent of frequency. This, of course, is only an apparent advantage over the connection in Fig. 2, because the four-terminal networks with constant phase-shift of 90° connected between generator and phase-shifter are generally frequency dependent. At each change of frequency it is necessary to re-adjust either the phase angle of 90° or the magnitude of the two-phase voltage, or both.

2.4. Variable frequency potentiometers with constant phase calibration (frequency changers).

The disadvantage of the frequency dependent phase calibration can be eliminated by the use of an A.F. beat-frequency generator, with the phase-shifter included in the branch of constant high frequency [2], [3]. The high frequency phase-shift appears as a phase shift of the difference (audio) frequency (Fig. 6).

This type of potentiometer is well adapted for quick and convenient measurements over wide frequency bands.

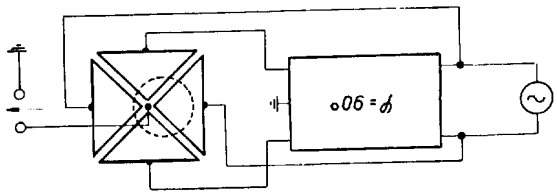

Fig. 5

Its disadvantage is the disadvantage common to all beat-frequency generators, i. e. relative complexity of equipment and poor frequency stability on low frequencies, which cannot be improved, for the frequency stability of high frequency oscillators cannot be increased without limit. If, for example, the stability of the high frequency oscillators is of the order of 10^{-4} (at 100 kc/s) then the low frequency stability will be $\perp 10$ c/s. In the range up to a hundred cycles these generators can only be used for certain applications. Another point against the beat-frequency generator at low frequencies in the non-linear distortion caused by "pulling in".

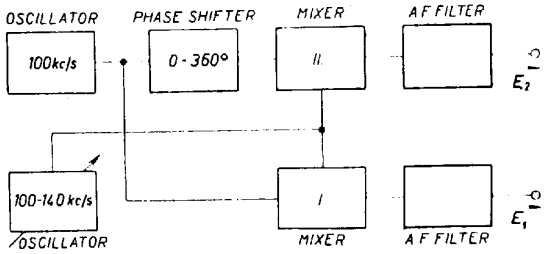

Fig. 6

When investigating low frequency amplifiers with negative feedback it is often necessary to measure the Nyquist diagram for frequencies far exceeding

the frequency range usually handled by the amplifier under test [5]. This leads to the need for an A.C. potentiometer for very low frequencies, of the order of a few c/s.

3. THE PRINCIPLE OF A NEW LOW FREQUENCY POTENTIOMETER

(Czechoslovak patent No. 76650)

For the new potentiometer we abandoned the principle of the beat-frequency oscillator for the simpler and now widely used *R-C* generator, without losing the chief advantage of the former, the frequency independent phase calibration.

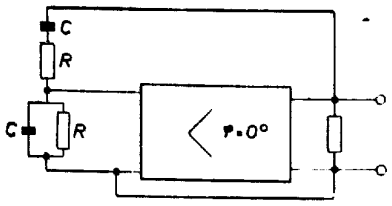

Fig. 7

The potentiometer consists basically of the well-known generator shown in Fig. 7, the frequency of such an oscillator being given by

$$\omega_0 = \frac{1}{RC}.$$

Oscillation occurs for amplification real and greater than or equal to 3. If we interchange the parallel and series branches an amplification of 1.5 is sufficient. The frequency of this oscillator can be changed by changing the resistances R or the condensers C. The voltages on R and C in the series branch will, however, always be equal in magnitude and different by 90°, just as is needed for a two-phase voltage source in a potentiometer.

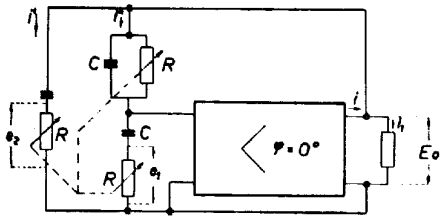

Fig. 8

These two voltages are, however, practically unusable as a two-phase voltage source, because their reference potential is different from ground potential and added parasitic capacities would unbalance phase conditions, thereby complicating the whole equipment.

We can however improve the circuit shown in Fig. 7, e. g. as shown in Fig. 8. On condition that $R_1 \ll R$ we can neglect i' and i'' as against i_1 and write

$$\mathfrak{E} = i_1 R_1 = E e^{j\omega}$$

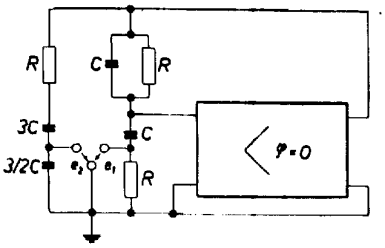

Fig. 9

calculating e_1

$$e_1 = i'' \frac{1}{j\omega_0 C} = i'' R e^{j\frac{\pi}{2}}$$

and substituting for i''

$$i'' = \frac{\mathfrak{E}}{\frac{R}{2}(1-j) + R(1-j) + \frac{3}{2}R} = \frac{\mathfrak{E}}{R\sqrt{2}} e^{-j\frac{\pi}{4}}$$

$$i'' = \frac{2\mathfrak{E}}{R3\sqrt{2}} e^{-j\frac{\pi}{4}}$$

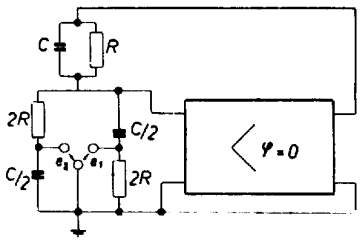

Fig. 10

we obtain

$$e_1 = \mathfrak{E}\frac{\sqrt{2}}{3} e^{-j\frac{\pi}{4}} \qquad (1)$$

Further,

$$e_2 = i' R$$

substituting for i':

$$i' = \frac{\mathfrak{E}}{R(1-j)}$$

$$e_2 = \mathfrak{E}\frac{\sqrt{2}}{2} e^{-j\frac{\pi}{4}}. \qquad (2)$$

From equations (1) and (2):

$$\frac{e_2}{e_1} = \frac{3}{2} e^{-j\frac{\pi}{2}}.$$

We can take off two voltages in relation to ground potential, having a constant amplitude ratio and

a constant phase difference of 90° independent of frequency. So that the amplitude ratio should not only be constant but equal to 1, the additional R-C branch can be connected to a tap on R or the feedback loop can be arranged as shown in Figs. 9 or 10.

By this means we obtain a simple R-C generator with a two-phase output independent of frequency setting, which can be used for very low frequencies. One of the above-described phase-shifters can now be used to obtain an arbitrary phase-shift independent of frequency. The frequency can be adjusted by the simultaneous adjustment of 3 resistors (ganged potentiometers) or three condensers (3-gang condenser) in steps or continuously.

Both methods can be combined; for example the condensers can be changed in steps, thereby changing the frequency band in wide steps, at the same time adjusting the frequency continuously with a triple potentiometer. This last method is of advantage when subdividing a large frequency range into smaller bands, thereby requiring only a small change in R. The main part of the resistors can then be fixed values, which increases accuracy, as the tracking of 3-gang potentiometers is always connected with certain manufacturing difficulties.

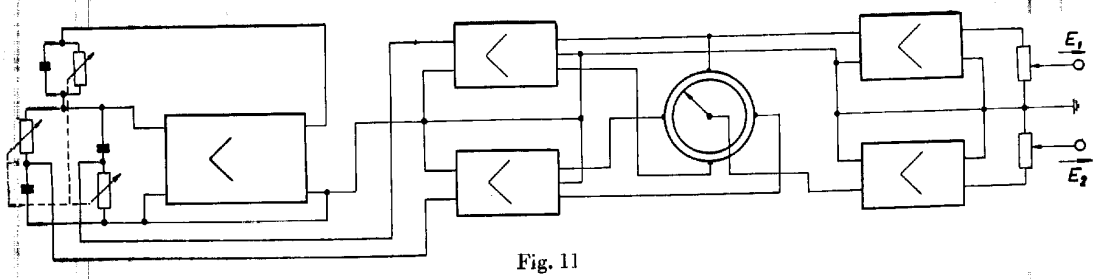

Fig. 11

4. EXAMPLE OF EXECUTION OF THE NEW POTENTIOMETER

The complete block-diagram is shown in Fig. 11. When designing the oscillator it is necessary to take care that the condition of zero phase-shift in the amplifier be fulfilled down to extremely low frequencies and further that its output impedance be low ($R_1 \ll R$). This leads to a few peculiarities in the design. Even though the required amplification is only 1.5 we have to use, for reasons of phase-shift, a two-stage amplifier. To obtain a low output impedance, a cathode-follower can be added making it a three-stage amplifier. The first two stages of the amplifier will easily give an amplification of $\geq$ 200, so that we can take the output from a tap at a point which is a small fraction of the cathode load impedance to fulfil the feedback condition. This solution is also of advantage for the first valve, as the feedback loop does not give an appreciable positive bias, allowing the valve to operate without grid current.

For extremely low frequencies it is disadvantageous to use grid coupling condensers. The amplifier was, therefore, designed as a D.C. amplifier. To avoid complicated circuits (Loftin-White, etc.) connected with the above condition, a D.C. amplifier with EF8 valves driven on the third grid was developed [7].

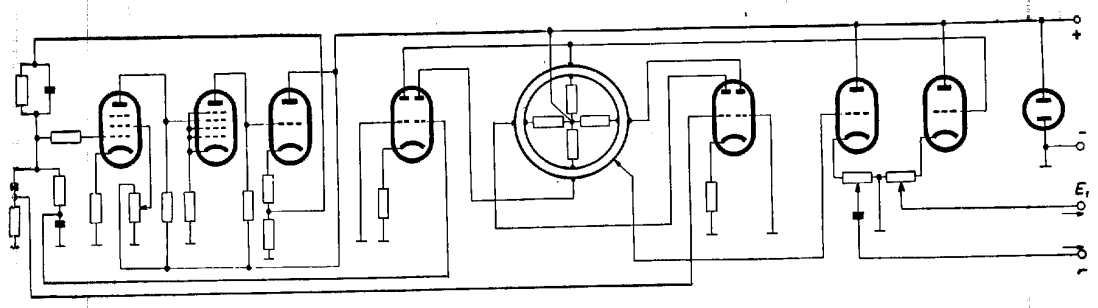

Fig. 12

Double-triode cathode coupled buffer stages mag be used for connecting the ring potentiometers to the oscillator as is evident from Fig. 12 [8], [9]. The conditions can be so adjusted that on both anodes there is an A.C. component of equal amplitude and 180° phase-difference while the D.C. components are equal.

A double-triode cathode coupled amplifier, coupled with an ordinary amplifier if necessary, can be

used in the output stage. Here a phase-shift does not harm: it is sufficient if both halves have equal phase-shifts. The variable phase output, can be taken through a condenser as this voltage serves for balancing: on balancing, the output voltage is exactly equal to the voltage being balanced, and the circuit behaves as if the output were open circuited. No phase-shift can therefore occur. At the direct output, which is loaded, this condenser should be omitted, so as not to introduce phase-shift errors.

An example of such a potentiometer is shown in the simplified diagram of Fig. 12.

Even though the purpose of the described instrument was to fill a gap in the range of low and extremely low frequencies, it is not necessarily restricted to this domain. Potentiometers on the same principle can be built for the whole range of audio and ultrasonic frequencies. At higher frequencies the present instrument loses some of the advantages over conventional potentiometers: at the same time many constructional difficulties are eliminated and the instrument for these frequencies becomes very simple.

BIBLIOGRAPHY

[1] *Wechselstrom-Kompensatoren; ATM, J 91-1, J 91-9, J 91-10, J 911-2.*

[2] *Nüsslein-Rupp: Wechselspannungskompensatoren mit veränderbarer Frequenz: Funktechnische Monatshefte, 1943, Nos. 2-3, pp. 17-22.*

[3] *Vladimír Hlavsa: Compensator-a Device for Measurement of Alternating Currents Within a Broad Frequency Range; Tesla Technical Reports, March 1949, pp. 1-10.*

[4] *Vladimír Hlavsa: Měření malých výkonu střídavého proudu (Measuring Low Powers of A.C.): Slab. Obzor, 1946, Nos. 3-4, p. 36.*

[5] *B. Carniol: Stabilita zesilovačů se zpětnou vazbou (Stability of Amplifiers with Feedback); Slab. Obzor, 1946, Nos. 7-8, p. 111.*

[6] *F. E. Terman: Radio Engineering Handbook, 1943.*

[7] *B. Carniol: Zesilovač pro velmi nízké kmitočty (Amplifier for Very Low Frequencies); Slab. Obzor, 1946, Nos. 3-4, p. 51.*

[8] *Clare: The Twin Triode Phase-Splitting Amplifier; Electronic Engineering, 1947, No. 2, p. 62.*

[9] *Szikloi-Schroeder: Cathode-Coupled Wide-Band Amplifiers, Proc. IRE, 1945, X, p. 701.*

TESLA TECHNICAL REPORTS

Edited and distributed by KOVO LTD.,
Metal & Engineering Products and Raw Materials
Trading Company, Publicity Dept., 5, Mezibranská,
Praha II, Czechoslovakia.
Published by the Printing Enterprise of the Central
Union of Czechoslovak Industry.
Printed at Prometheus, Praha.

CONTENTS

III T 668a - 5002